

SEP 28 1964

GEAP-4504  
EURAC

JOINT U.S.-EURATOM RESEARCH  
AND DEVELOPMENT PROGRAM  
APRIL 15, 1964

1193

MASTER



**SPECIFIC ZIRCONIUM ALLOY  
DESIGN PROGRAM  
SUMMARY REPORT**

H. H. KLEPFER

U.S. ATOMIC ENERGY COMMISSION  
CONTRACT AT(04-3)-189  
PROJECT AGREEMENT 24

VALLECITOS ATOMIC LABORATORY

**GENERAL  ELECTRIC**

ATOMIC POWER EQUIPMENT DEPARTMENT  
SAN JOSE, CALIFORNIA

11/3

## **DISCLAIMER**

**This report was prepared as an account of work sponsored by an agency of the United States Government. Neither the United States Government nor any agency Thereof, nor any of their employees, makes any warranty, express or implied, or assumes any legal liability or responsibility for the accuracy, completeness, or usefulness of any information, apparatus, product, or process disclosed, or represents that its use would not infringe privately owned rights. Reference herein to any specific commercial product, process, or service by trade name, trademark, manufacturer, or otherwise does not necessarily constitute or imply its endorsement, recommendation, or favoring by the United States Government or any agency thereof. The views and opinions of authors expressed herein do not necessarily state or reflect those of the United States Government or any agency thereof.**

## **DISCLAIMER**

**Portions of this document may be illegible in electronic image products. Images are produced from the best available original document.**

EURAE  
GEAP-4504  
Joint U.S.-EURATOM  
Research and Development  
Program


SPECIFIC ZIRCONIUM ALLOY DESIGN PROGRAM

SUMMARY REPORT

H. H. Klepfer

May 19, 1964

APPROVED BY:

  
A. N. Holden, Manager  
Metallurgy and Ceramics

Prepared Under AEC Contract AT(04-3)-189, P.A. No. 24  
for the  
Joint US-EURATOM Research and Development Program

Printed in the U.S.A. ~~Price \$2.25~~ Available from  
the Office of Technical Information Department  
of Commerce, Washington 25, D.C.

VALLECITOS ATOMIC LABORATORY

GENERAL  ELECTRIC

ATOMIC POWER EQUIPMENT DEPARTMENT  
SAN JOSE, CALIFORNIA

LEGAL NOTICE

THIS DOCUMENT WAS PREPARED UNDER THE SPONSORSHIP OF THE ATOMIC ENERGY COMMISSION PURSUANT TO THE JOINT RESEARCH AND DEVELOPMENT PROGRAM ESTABLISHED BY THE AGREEMENT FOR COOPERATION SIGNED NOVEMBER 8, 1958, BETWEEN THE GOVERNMENT OF THE UNITED STATES OF AMERICA AND THE EUROPEAN ATOMIC ENERGY COMMUNITY (EURATOM). NEITHER THE UNITED STATES, THE U.S. ATOMIC ENERGY COMMISSION, THE EUROPEAN ATOMIC ENERGY COMMUNITY, THE EURATOM COMMISSION, NOR ANY PERSON ACTING ON BEHALF OF EITHER COMMISSION:

- A. MAKES ANY WARRANTY OR REPRESENTATION, EXPRESS OR IMPLIED, WITH RESPECT TO THE ACCURACY, COMPLETENESS, OR USEFULNESS OF THE INFORMATION CONTAINED IN THIS DOCUMENT, OR THAT THE USE OF ANY INFORMATION, APPARATUS, METHOD, OR PROCESS DISCLOSED IN THIS DOCUMENT MAY NOT INFRINGE PRIVATELY OWNED RIGHTS; OR
- B. ASSUMES ANY LIABILITIES WITH RESPECT TO THE USE OF, OR FOR DAMAGES RESULTING FROM THE USE OF ANY INFORMATION, APPARATUS, METHOD OR PROCESS DISCLOSED IN THIS DOCUMENT.

AS USED IN THE ABOVE, "PERSON ACTING ON BEHALF OF EITHER COMMISSION" INCLUDES ANY EMPLOYEE OR CONTRACTOR OF EITHER COMMISSION OR EMPLOYEE OF SUCH CONTRACTOR TO THE EXTENT THAT SUCH EMPLOYEE OR CONTRACTOR OR EMPLOYEE OF SUCH CONTRACTOR PREPARES, HANDLES, DISSEMINATES, OR PROVIDES ACCESS TO, ANY INFORMATION PURSUANT TO HIS EMPLOYMENT OR CONTRACT WITH EITHER COMMISSION OR HIS EMPLOYMENT WITH SUCH CONTRACTOR.

## FOREWORD

"The United States and the European Atomic Energy Community (EURATOM), on May 27, 1958 and June 18, 1958, signed an agreement which provides a basis for cooperation in programs for the advancement of peaceful applications of atomic energy. This agreement, in part, provides for the establishment of a Joint US-EURATOM research and development program which is aimed at reactors to be constructed in Europe under the Joint Program.

The work described in this report represents the Joint US-EURATOM effort which is in keeping with the spirit of cooperation in contributing to the common good by the sharing of scientific and technical information and minimizing the duplication of effort by the limited pool of technical talent available in western Europe and United States."

PAGES iv to v  
WERE INTENTIONALLY  
LEFT BLANK

## CONTENTS

	<u>Page</u>
ABSTRACT . . . . .	1
INTRODUCTION . . . . .	3
I. TASK A - CORROSION MECHANISMS . . . . .	5
A. Solute Distribution Between Corrosion Films and Zirconium Alloy Substrates . . . . .	5
B. Diffusion of Oxygen in Bulk Zirconium Dioxide . . . . .	6
C. Oxide Plasticity . . . . .	7
D. Corrosion Hydriding . . . . .	8
E. Summary . . . . .	10
II. TASK B - ALLOY DESIGN . . . . .	11
A. Design Requirements . . . . .	11
B. Selection of Alloy Field . . . . .	12
C. Experiment Design and Procedures . . . . .	13
1. Alloy and Sample Fabrication . . . . .	14
2. Corrosion Testing . . . . .	17
3. Mechanical Testing . . . . .	18
4. Hydrogen Analyses . . . . .	19
D. Corrosion Results . . . . .	19
E. Hydriding Results . . . . .	22
F. Mechanical Properties . . . . .	25
1. As-Fabricated Tensile Properties and Fabricability . . . . .	27
2. Post-Corrosion Mechanical Properties . . . . .	29



	<u>Page</u>
G. Additional Investigations . . . . .	37
1. Nickel and Beryllium Additions . . . . .	38
2. Fabrication Schedules . . . . .	39
III. RECOMMENDATION OF FUEL CLADDING ALLOY . . . . .	45
A. Application for Superheat Cladding . . . . .	45
B. Application for Water Reactor Cladding . . . . .	46
1. Problems with Commercial Zircaloy-2 Cladding . . . . .	46
2. Possible Solutions for Zircaloy-2 Cladding Problems . . . . .	47
C. Analysis of Results . . . . .	52
REFERENCES . . . . .	57
APPENDIX . . . . .	61

ILLUSTRATIONS

<u>No.</u>	<u>Title</u>	<u>Page</u>
1	Alloy Mechanical Properties as a Function of Composition . . . . .	28
2	Resistance to Hydrogen versus Total Alloy Content . . . . .	33
3	Resistance to Hydrogen versus Niobium . . . . .	34
4	Resistance to Hydrogen versus Total Nb + Fe . . . . .	35
5	Post-Transition Corrosion Rate of Zircaloy-2 as a Function of Reciprocal Absolute Temperature . . . . .	49
6	Regions of Composition for an Arbitrary Level of Performance at Various Temperatures . . . . .	54

SPECIFIC ZIRCONIUM ALLOY DESIGN PROGRAM  
Summary Report

H. H. Klepfer

ABSTRACT

The results of selected basic experiments gave strong indications that the corrosion and corrosion hydriding of zirconium alloys is dependent on the chemical, mechanical, and electrical properties of the oxide film. The composition of corrosion films was found to be directly proportional to the alloy content of the substrate even in complex alloys. Excellent agreement was found between the activation energy for oxygen diffusion in  $ZrO_{1.994}$  and the activation energies for parabolic or cubic oxidation of zirconium in both air and water. Iron, chromium, and nickel had no significant effect on oxygen ion diffusion, but the addition of 1 mole %  $Y_2O_3$  to monoclinic zirconia increased the rate of oxygen diffusion by about 1 order of magnitude. Yttrium decreased the plasticity of zirconium oxide while chromium and iron increased plasticity, and thus accounted for the early spalling of oxide observed for Zr-Y alloys and the good adherence of films on Zr-Cr and Zr-Fe alloys. Corrosion hydriding of zirconium alloys could not be directly related to the electro-chemical properties of the matrix and the inter-metallic phases in an alloy. Corrosion hydriding may be controlled by whether electronic, or protonic, charge transport is promoted by the addition of a given alloying element to the zirconium oxide film.

Corrosion rates, hydriding rates, and mechanical properties of 31 alloys containing selected additions of Nb, Cr, Fe, or Cu were measured at 300, 400, and 500°C. Selection of the 31 experimental compositions from the pre-determined range of additions was treated as a statistical problem. A near-orthogonal design ensured computer analysis of the results to give polynomial expressions of the alloy response surfaces. None of the better alloys will be applicable as fuel cladding for superheat reactors. The experimental results were analyzed for the best alloy for service as water reactor fuel cladding and the optimum alloy was computed to be one containing

2.0 at. % Cr + 0.16 at. % Fe. Special experiments showed that neither Ni nor Be additions to Zr + 2.0 at. % Cr gave better over-all performance than did the Fe addition. An increase in performance did result from increasing the final annealing temperature for corrosion samples to 788°C from the reference temperature of 565°C. The Zr-Cr-Fe alloy has about the same fabricability and tensile properties as does Zircaloy-2; it is superior to Zircaloy-2, particularly in resisting the adverse effect of over-temperature on the rates of corrosion and corrosion hydriding. The alloy has been recommended for evaluation as fuel element cladding.

## INTRODUCTION

The demands on reactor materials have become more severe as nuclear power development has progressed. Longer life, improved neutron economy, and higher operating temperatures have been specified in each new generation of reactors. Meeting these requirements will demand the development of several Zr alloys designed to meet specific requirements. The requirements for coolant channels and pressure tubes may well be best met by an alloy not suited for thin-section cladding. Certain requirements have been stressed above others in different reactor designs. The compromises necessary in designing any alloy may be decidedly different and depend on the critical properties in a particular application. The well-known development of special steels for special service requirements will be paralleled for Zr as it was for Al and for Ti.

Recognizing the need to develop a number of Zr alloys for reactors, it is important to consider the most economic approach to solving the general problem of Zr alloy design. The resources for design are precise metallurgical analysis of needed properties, empirical data, fruitful mechanistic theories, and full understanding of the pertinent basic metallurgy of Zr. These resources are not sufficiently complete to allow direct economic design of specific compositions. The most powerful approach available to the metallurgist is a statistically designed empirical screening of Zr alloy compositions. Concurrent investigations of basic alloy phenomena in selected areas provides an improved context for judging the empirical results and increases the precision in the statistical design of Zr alloys.

The Specific Zirconium Alloy Design Program (Contract AT(04-3)-189, Project Agreement 24) was initiated on January 29, 1962 as a 2-year program. Design of a Zr base alloy for specific application as a fuel cladding in a high-temperature steam environment was studied. The total program consisted of basic corrosion mechanism studies (Task A) and a statistically designed alloy development program (Task B).

Work under Task A included experiments contributing to a better understanding of corrosion and hydrogen uptake mechanisms, with particular emphasis on the role of alloying additions.

Under Task B, target properties for a Zr alloy suitable for steam service were derived. A restricted field of alloy compositions was established and 31 alloys in this field were melted and fabricated for study. Statistical evaluation of the results of steam exposures up to 6750 hours at 300, 400, and 500°C was performed. The results were analyzed for applicability for superheat reactor fuel cladding and for water reactor fuel cladding. An optimum alloy composition was selected for engineering evaluation as a fuel cladding alloy.

## I. TASK A. CORROSION MECHANISMS

The mechanism of corrosion in zirconium alloys in high-temperature water and steam has been extensively studied during the last decade, but the knowledge of the fundamental properties of the alloys and oxide films is still not adequate for the design of alloys. This program was intended to provide additional understanding of the over-all corrosion process; and although the extent of the corrosion mechanism program was insufficient to enable a complete understanding to be obtained, the work did help explain why some alloying additions are beneficial and others are not.

The approach taken was to explore certain specific questions about whether (and what) oxide film properties control the corrosion and hydriding mechanisms. It had never been established that the oxide film compositions were directly related to the alloy compositions. It was not clear whether the corrosion and hydriding processes were controlled by transport and/or deformation in the alloy substrate or in the oxide. If the oxide properties were the most important, and simply related to the alloy composition, then the properties of pure and alloyed bulk  $ZrO_2$  are of interest.

A. SOLUTE DISTRIBUTION BETWEEN CORROSION FILMS AND ZIRCONIUM ALLOY SUBSTRATES

Douglass<sup>1</sup> analyzed stripped corrosion films by wet chemical methods, neutron activation and microprobe analysis. It was found that the amount of Sn, Nb, and Cr in post-transition oxide films was directly proportional to the amount in the alloy. There was no measurable difference in film composition of a given alloy as a function of film thickness, and the combination of alloying elements in ternary alloys had no effect on the amount of a given element in the corrosion film.

Analyses of a pre-transition film on a Zr + 2 at. % Cr binary alloy were made by using a tracer,  $Cr^{51}$ . No concentration differences in Cr were found in corrosion films 7,000 to 18,000 Å thick, formed in

+00°C steam. It was concluded that this alloy did not exhibit concentration changes in the substrate adjacent to the oxide film such as those known for Ni-Pt alloys, and that diffusion of Cr in the metal was unimportant in controlling the oxidation of the Zr-Cr alloy.

The beneficial effect of Cr and the harmful effect of both Sn and Nb on post-transition corrosion rates can be associated with the amount of these solutes in the corrosion film. The oxide compositions are directly related to alloy compositions, therefore, the composition (and perhaps properties) of bulk oxides can be related to alloy compositions.

#### B. DIFFUSION OF OXYGEN IN BULK ZIRCONIUM DIOXIDE

Although  $ZrO_2$  is white in the stoichiometric condition, the oxide films which form on the metal during oxidation during the early stages of the process are usually black. The blackness is due to non-stoichiometry, specifically caused by anion vacancies, and may be attributed to the high solubility of oxygen in the metal substrate. The pure metal (or alloy) is thermodynamically unstable in contact with the oxide, and solution of the oxide occurs in the metal substrate until saturation is achieved. Thus, the metal represents an oxygen sink, and as long as it exists the color of the oxide should remain dark from the anion deficiency. In some cases white spots are observed; these spots may be attributed to cracks in the oxide film parallel to the surface, the cracks serve as a diffusion barrier to oxygen. It is this marked color change in the oxides which has provided a basis for measuring the diffusion coefficient of oxygen.

Douglass<sup>2</sup> prepared black, anion-deficient  $ZrO_2$  by vacuum hot pressing in graphite dies. Rectangular slabs of the oxide were exposed to either high-purity oxygen or steam for various times, sectioned, and the rate of thickening of the white stoichiometric layer was measured. The diffusion coefficient was computed directly from these data.

The diffusion rate of oxygen in anion-deficient,  $ZrO_{1.994}$  is represented by  $D = 0.055 \exp(-33,400 \pm 3100/RT)$ .

A comparison of this activation energy with that of diffusion in the metal substrate showed no agreement. Excellent agreement was noted between the activation energy for oxygen diffusion in  $ZrO_{1.994}$  and activation energies for parabolic or cubic oxidation of Zr in both air and water. It appears that oxygen diffusion in the oxide is rate-controlling during oxidation of the metal.

Measurements were also made to determine the diffusion of oxygen in non-stoichiometric  $ZrO_2$  doped with  $Y_2O_3$  (Y alloy additions are known to be harmful with respect to corrosion resistance),  $Cr_2O_3$ , and NiO (Cr and Ni are generally considered good alloy additions). The results of these studies are summarized by:

<u>Oxide</u>	<u>Diffusion Rate Equation</u>
$ZrO_{1.994}$	$D = 0.055 \exp(-33,400/RT)$
$(Zr_{0.999}, Ni_{0.001}) O_{1.965}$	$D = 0.024 \exp(-30,600/RT)$
$(Zr_{0.997}, Cr_{0.003}) O_{1.975}$	$D = 0.005 \exp(-29,400/RT)$
$(Zr_{0.981}, Y_{0.019}) O_{1.980}$	$D = 0.27 \exp(-27,200/RT)$

Iron, Cr, and Ni had no significant effect on oxygen ion diffusion, but the addition of 1 mole %  $Y_2O_3$  to monoclinic zirconia increased the rate of oxygen diffusion by about 1 order of magnitude.

### C. OXIDE PLASTICITY

The plasticity was also studied by Douglass<sup>3</sup> on the same doped, non-stoichiometric  $ZrO_2$  used for oxygen diffusion work. The results of the solute segregation experiments and the oxygen diffusion studies gave a consistent picture of the early parabolic or cubic corrosion kinetics of Zr alloys, but did not indicate any reason for the known



transition to approximately linear kinetics at some critical film thickness (the critical thickness increases from about 1.7 to about 3.3  $\mu$  as the corrosion temperature is increased from 360 to 500°C).

The oxide films which form on Zr and its alloys during the early stages of oxidation are protective and exhibit no spalling or cracking. In fact, the lack of spalling is surprising because of the high ratio of molar volume of oxide to molar volume of metal. Elastic stresses which would exist at the coherent metal-oxide interface would be on the order of millions of pounds per square inch based on the lattice mismatch for the most favorable epitaxial relationship. The usual manifestation of such gross mismatch is violent spalling of the oxide or extensive cracking. In the absence of oxide exfoliation, it is necessary to propose some method by which the very high stresses can be relieved. The obvious possibilities are plastic deformation of either the metal substrate or of the oxide film itself.

Hot hardness measurements (0 to 700°C) showed that doping monoclinic zirconia with Fe, Ni, or Cr resulted in softer (more plastic) structures and that Y additions slightly reduce the plasticity. The behavior of white, anion-deficient oxides indicated that they were more plastic than stoichiometric oxides even though the hardness values were identical at 23°C. The former were free from cracks at the indentations, whereas, stoichiometric oxides exhibited cracking around and between the indentations.

The behavior of actual, thick (72  $\mu$ ) oxide films during tensile deformation of oxidized metal samples indicated that considerable plasticity occurs in the oxide at 500°C but that the films are brittle at 23°C. It was concluded that the plasticity of the oxide may be greater than that of the oxygen-contaminated substrate at elevated temperatures and may be the means by which epitaxial strains are minimized.

D. CORROSION HYDRIDING

Armijo<sup>4</sup> considered the hypothesis that the difference between corrosion hydrogen uptake in various alloys is related to the electrochemical properties of the intermetallic compounds in the alloys. He made hydrogen overvoltage measurements of Zr, Zr<sub>2</sub>Ni, Zr<sub>2</sub>Cu, ZrV<sub>2</sub>, and Zr - 90 wt % Nb in 1M H<sub>2</sub>SO<sub>4</sub> over a large current density range. Electrochemical potentials as a function of time were measured for the following galvanic cells: Zr-Zr<sub>2</sub>Ni, Zr-Zr<sub>2</sub>Cu, Zr-ZrV<sub>2</sub>, Zr-ZrFe<sub>2</sub>, Zr-ZrCr<sub>2</sub>, and Zr-(Zr - 90 wt % Nb).

Armijo pointed out, on the basis of the electrochemical potential measurements, that only some of the intermetallic compounds would even be expected to be hydrogen discharge sites. Furthermore, any relationship between hydrogen overvoltage on the intermetallics and the hydrogen uptake of the corresponding alloy is at best an inverse relationship.

The intermetallics are, in fact, not in contact with the corrosion medium. The results obtained by Douglass<sup>1</sup> on solute segregation require that the intermetallics be taken into the oxide in toto by either direct oxidation or by oxidation of the matrix around the particles.

Klepfer<sup>5</sup> studied Zr-Cr, Zr-V, and Zr-Fe binary alloys of varying composition. The composition change in the Zr-Cr and Zr-V systems results only in a change in amount of intermetallic phase, as the solubility is very limited. In these systems, increasing the intermetallic phase affected the oxygen weight gain (and thus, the hydrogen weight gain) but increasing intermetallics did not grossly alter the percentage of corrosion-produced hydrogen passing through the oxide film.

But the effect of the volume fraction intermetallic phase could not be generalized. For Zr-Fe alloys, where solid solubility is again limited, increasing the intermetallic phase did not grossly affect

oxygen weight gain, but the percentage hydrogen uptake varied from 25 to 100% as iron content increased from 0.26 to 3.90 wt % Fe.

Thus, the intermetallics do not appear to play a direct role in determining hydrogen uptake, but rather the effect of their oxidation on the corrosion film properties must be most important. Klepfer has explained his uptake data by proposing that the alloy effect is an effect on the electrical transport properties of the  $ZrO_2$  corrosion film. Alloy additions which increase the electronic conductivity of the oxide are predicted to lower hydrogen uptake.

#### E. SUMMARY

The results of the mechanism studies strongly indicate that corrosion and hydriding of Zr alloys is dependent on the solid-state properties of the oxide film. The composition of the film is directly proportional to the alloy content even in complex alloys. Alloy additions may affect the corrosion and hydriding kinetics by their effect on the chemical properties (diffusion of oxygen), electrical properties (charge transport), and mechanical properties (plasticity) of the oxide.

One example in support of this general proposal was determined directly. Yttrium decreased the plasticity of the oxides and accounted for the early spalling of oxide observed for Zr-Y alloys. Chromium and iron increased the plasticity of the oxides and the adherence of films on Zr-Cr and Zr-Fe alloys.

When alloys are designed on the basis of fundamental understanding, more knowledge of the detailed structure of  $ZrO_2$  corrosion films will be required. Generalizations about the effects of alloy additions on the chemical, electrical, and mechanical behavior of non-stoichiometric  $ZrO_2$  will be required.

## II. TASK B. ALLOY DESIGN

A. DESIGN REQUIREMENTS

The application considered was that of thin sections, such as those in fuel element cladding. Resistance to steam corrosion and to degradation of mechanical properties were the critical requirements. Good fabricability and high ductility were required, but high strength was not a prime requisite. The target alloy was to be useful as cladding material for unbonded  $UO_2$  fuel elements, perhaps even those designed to rely on the  $UO_2$  in the fuel tubes for support of the cladding against the reactor coolant pressure.

The alloy requirements to be met by the alloy design were categorized:

1. Neutron economy,
2. Low cost,
3. Low susceptibility to hydrogen embrittlement,
4. Usable corrosion resistance,
5. Usable ductility, and
6. Strength

Each of these requirements was studied in detail and quantitative targets developed.<sup>6,7</sup> The approach to assigning quantitative specifications for each of these requirements involved making the specific engineering assumptions, e.g., thin wall non-self-supporting cladding. The entire alloy design effort was distinguished from that required for reactor pressure tube alloys by these assumptions. A summary of the specifications for the alloy design under this program is:

1. The alloy shall have no alloying additions which would lead to a calculated increase in required U-235 enrichment of more than 0.05% over that for a pure zirconium core with the general nuclear parameters of the Dresden Nuclear Power Station core.

2. The alloy shall have no alloying elements, and no inherent problems with fabrication, which would lead to a calculated increase in cost of more than 5% over the cost of Zircaloy-2 tubing.
3. The alloy shall show less than 1500 ppm hydrogen in excess of the solubility limit (at the service temperature) after a calculated service life of 3 years for a 25-mil tube corroded on one side. In lieu of this requirement, the alloy would be acceptable if it could be extrapolated that the alloy after 3 years service would have a reduction in area of 10% or better at the service temperature.
4. The alloy shall have a corrosion rate when tested in out-of-pile steam tests of  $1 \text{ mg/dm}^2/\text{day}$  or less (as a steady-state, post-transition corrosion rate).
5. The alloy shall have an initial room temperature ductility defined by the values 20% elongation to fracture or 35% reduction in area (or better).
6. The alloy shall be as strong as sponge Zr or stronger.

The specifications for the structure-insensitive properties of neutron economy and cost and for the less critical strength and ductility factors were written in a straightforward way. In writing the specifications for susceptibility to hydrogen embrittlement and for corrosion behavior, it was necessary to rely heavily on judgement. The design approach was found productive not only in bringing forth new alloys but also by focusing attention on the most critical problems requiring research emphasis.

B. SELECTION OF ALLOY FIELD

Alloying elements and their composition limits were determined which would not be excluded by the alloy design specifications. The alloy field finally selected after a detailed review process included additions of 0 to 4.0 at. % Nb, 0 or 0.8 to 2.5 at. % Cr, 0 or 0.25 to 0.48 at. % Fe, 0 or 0.70 to 2.1 at. % Cu.<sup>6,7</sup> The review process

involved an element-by-element calculation or literature review for values pertinent to the six alloy design specifications.

The major deficiency in the background information necessary to make a more precise selection of alloy additions was found to be the lack of a theory which is fruitful in predicting alloy effects. It would have been very desirable to have been able to state what the combined effects of two different alloying elements would be. Because this was not possible theoretically, it was necessary to make the conservative assumption that the effect of the alloying elements which are harmful by themselves, would be to lead to poor corrosion resistance when in combination with other elements.

#### C. EXPERIMENT DESIGN AND PROCEDURES

Experimental data on corrosion rates, hydriding rates, and mechanical properties were obtained to find the optimum alloy in the alloy field selected. Corrosion exposures of over 3000 hours were performed in high-pressure, flowing, refreshed steam (containing controlled amounts of oxygen and hydrogen) at 300, 400, and 500°C. Weight gains, mechanical properties, and hydrogen contents were determined on samples removed from test at selected intervals.

The problem of determining which particular alloy combinations would be run was treated by Gaylor<sup>8</sup> and by Jaech<sup>9</sup> as a problem in statistical design. Since the effects of the four alloying elements (Nb, Cr, Fe, Cu) could not be presumed to be linear, it was necessary to include at least three levels of each alloy. In addition, combinations of the alloying elements taken one, two, and three at a time also required investigation; this meant the zero level (no addition) for each element had to be included. A complete investigation of all possible combinations of alloys would have meant preparing 255 alloys in a 4-factor, 4-level factorial experiment (exclusive of the 0,0,0,0 point which was not admissible). Clearly, a complete factorial experiment was not required. It was assumed that the response surface was

not so complex, it could not be represented by a quadratic polynomial within the experimental region. (This assumption was proved valid by the excellent correlation factor between the final test results and the corresponding values calculated from the final quadratic polynomial equations). An assumed quadratic response meant that only about 30 alloys had to be tested to determine all the necessary parameters and to assure enough "degrees of freedom" to estimate the random error variance and hence the uncertainty associated with each parameter estimate.

Thirty-one alloys were actually selected (Table 1) in such a way that a near-orthogonal design was ensured. A near-orthogonal design meant that terms could be removed from the response surface equations without changing the other parameter estimates, which allows examination of not only any quinary alloy in the alloy field, but also all quaternary, ternary, and binary alloys. Actually, the chemical analysis of the 31 alloys investigated deviated slightly from the make-up targets; near-orthogonality was maintained in spite of these deviations.

(A very limited second series of tests was also performed to extend the results from this first series of tests on the 31 alloys. The objectives of these additional investigations were to determine if (a) Ni or Be additions to the best alloys found in the first series and (b) if a selected change in heat-treating schedules would lead to further improvement in performance of the best compositions. These additional investigations will be discussed in Section II-G after the discussion of the statistical experiments on the first 31 alloys).

#### 1. Alloy and Sample Fabrication

Because it was planned to develop an alloy for direct application, the fabrication methods chosen closely paralleled those standard in the Zr industry. A summary of the details reported by Antony and Jones<sup>10</sup>

follows:

Each alloy composition was consumably arc-melted and remelted in 1.8-kg heats from sponge-base Zr and high-purity alloying materials. Ingots were forged at 788°C to billets 6.3 x 7.6 cm wide by 2.5 cm thick. Billets were hot rolled at 788°C to 0.178-cm sheets. Care was taken in hot working to remove surface defects and surface gaseous contamination. Hot-rolled sheets were solution treated for 6 hours at 950°C under vacuum and water quenched (hot zone to water in 30 seconds).

The beta-quenched sheets were cleaned, etched, and cold rolled to a final thickness 0.127 cm (15 to 20% cold work). Cold fabricability was found to be directly proportional to total alloy content. Excellent fabricability was observed for all alloys containing less than 1.5 at. % alloy addition. Difficulty with cold fabricability was experienced above 2.5 at. % total alloy content and these alloys required modification (less reduction per pass or even intermediate annealing for the alloys of highest alloy content) of the cold-rolling procedure. After the final cold-rolling operation, all sheets received a stabilization and precipitation anneal for 24 hours at 565°C. (It will be shown that complete stabilization was not achieved for all alloys; further precipitation occurred in some alloys after long times in corrosion test at 500°C).

The reason<sup>6</sup> for using this heat treatment schedule was because beta treating followed by 565°C annealing is optimum for promoting the corrosion resistance of Nb-containing alloys.<sup>11</sup> (Later results showed that, for alloys containing only Cr or Cu, improvement in corrosion resistance was realized with a slightly higher final annealing temperature).

Nitrogen check analyses, chemical analyses, and corrosion check tests on each alloy, showed them to have good homogeneity. Nitrogen contents for various ingots varied from 10 to 40 ppm with an average of  $19 \pm 5$  ppm. Oxygen contents ranged from 770 to 910 ppm with an average of  $825 \pm 75$  ppm. Hydrogen analyses ranged from 3 to 34 ppm with an average of  $13 \pm 6$  ppm.<sup>10</sup>

Chemical analysis for each alloy addition were made by the methods reported by Perrine and by Urata.<sup>12</sup> The resulting values were those given in Table 1.



TABLE 1. Zr Alloy Composition Analyses (at.%)

Alloy	<u>Nb</u> <u>Analyzed</u>	<u>Cr</u> <u>Analyzed</u>	<u>Fe</u> <u>Analyzed</u>	<u>Cu</u> <u>Analyzed</u>	<u>Total</u> <u>Analyzed</u>
001	0.49	0.91	0.23	0.68	2.31
002	0.50	0.92	0.50	1.34	3.25
003	0.48	1.85	0.23	1.28	3.83
004	0.50	1.75	0.52	0.61	3.38
005	2.19	0.64	0.08	1.41	4.33
006	1.90	0.93	0.47	0.71	4.02
007	1.92	1.56	0.23	0.58	4.49
008	2.25	1.87	0.48	1.33	5.93
009	2.33	1.32	0.52	1.07	5.23
010	0.91	2.69	0.23	1.03	4.86
011	0.87	1.37	0.58	1.16	4.00
012	1.06	1.40	0.34	1.83	4.54
013	-	1.27	0.36	1.04	2.66
014	0.99	0.01	0.34	1.03	2.36
015	1.05	1.22	0.32	1.08	3.67
016	1.05	1.36	0.52	-	2.93
017	-	0.01	0.34	1.09	1.44
018	-	1.27	0.05	1.04	2.36
019	-	1.34	0.54	-	1.87
020	0.84	0.01	0.03	1.02	1.90
021	0.56	0.01	0.34	-	0.90
022	0.98	1.18	0.24	-	2.41
023	0.83	0.01	0.05	-	0.90
024	-	1.46	0.20	-	1.66
025	-	0.01	0.33	-	0.34
026	-	0.01	0.05	1.20	1.26
027	0.27	0.01	0.34	-	0.63
028	0.20	1.38	0.36	-	1.94
029	0.19	0.01	0.36	1.02	1.57
030	0.25	1.35	0.37	1.25	3.23
031	0.88	1.42	0.19	1.10	3.59
032*					

\*(Zr-2 Sn = 1.2 wt %; Fe = 0.16 wt %; Cr = 0.08 wt %; Ni = 0.04 wt %) by analysis

Test specimens, sufficient in number and description, to satisfy the statistical design were sheared or punched out of the annealed alloy sheets of each composition with reproducing dies.<sup>13</sup> All corrosion test specimens were used also as mechanical test specimens and the broken halves of each mechanical test specimen were analyzed for hydrogen. Two types of test specimens, a sheet tensile specimen, and a sheet impact specimen were used for each alloy composition.

### 3. Corrosion Testing

A special high-pressure, low-flow, refreshed-steam corrosion system consisting of three 145-liter stainless steel autoclaves and associated equipment was developed<sup>14</sup> for corrosion tests at 300, 400, and 500°C. The important corrosion system parameters were

1. Pressure. A constant specific steam volume of 48.7 cc/gm which is equivalent to pressures of 46 atm at 300°C, 58 atm at 400°C, and 68 atm at 500°C was chosen.
2. Flow Rate. A steam flow of 3 cm/sec was maintained in the sample section.
3. Oxygen and Hydrogen. Controlled additions of  $25 \pm 7$  ppm O<sub>2</sub> and  $3 \pm 2$  ppm hydrogen were made to simulate radiolytic decomposition of steam.
4. Water. Deionized water of 1 megohm resistance was heated to provide the test steam.
5. Temperature. Temperature variations across the sample section were measured to be less than 2°C and control was  $\pm 5^\circ\text{C}$ .

Steps were taken to ensure that departures from a homogeneous environment would not affect the alloy comparisons. The autoclave was divided into 16 regions within each of which, one coupon of each alloy was tested. In addition, the coupon placement within each region was deliberately made random. (Evidence for a minor lack of homogeneous autoclave environment was, in fact, detected in the test data; the

precautions taken permitted the effect to be removed in data analysis without bias in the alloy comparisons).

The exposure schedule for each of the 1565 coupons tested required periodic weighing of all samples and removing certain coupons at time intervals to 3000 hours. Actually, extra coupons of all alloys were run to 7812 hours at 300°C and to 3578 hours at 400°C. At 500°C, extra coupons of those alloys which showed low corrosion rates and negligible corrosion hydrogen embrittlement were run as long as 6792 hours.

Since the corrosion testing involved almost 2000 coupons and 20,000 weighings, weight gains were calculated by computer from the weighing data. The computer output cards for weight gains were then re-used as input cards for analysis of steady-state corrosion rates for each alloy at each test temperature. Finally, the steady-state rates were used to determine linear quadratic equations relating corrosion rate to alloy composition. These computations have been reported in detail by Jaech.<sup>9</sup>

### 3. Mechanical Testing

Duplicate tensile tests on uncorroded specimens were performed on each alloy at 300, 400, and 500°C. Triplicate tests were performed at room temperature. Sample dimensions and test apparatus have been described elsewhere.<sup>13</sup>

Each corrosion coupon removed for test was tested to fracture. Sheet tensile coupons were removed in pairs; one was tested at room temperature and the other held for test at the corrosion exposure temperature. (Only tests for 300 and 500°C exposures were actually performed. Since no embrittlement was observed at these test temperatures, the specimens exposed at 400°C were not tested at 400°C.) Sheet impact coupons were all tested at 300°C to detect embrittlement as a function of exposure.<sup>8,13</sup>

#### 4. Hydrogen Analyses

The specimens for hydrogen analysis were cut from one-half of each broken post-corrosion impact coupon. These specimens were analyzed for hydrogen by inductively heating at  $1200 \pm 50^{\circ}\text{C}$  in a high vacuum system. The apparatus and procedure were reported by Perrine.<sup>12</sup> The U.S. Bureau of Standards values for hydrogen in Ti standard samples 352 and 353 were reproduced well within the 95% confidence limit.

The precision of the hydrogen analysis expressed as over-all coefficients of variation was determined to be 5.6% in the range 12 to 30 ppm hydrogen and 2.4% at 100 ppm hydrogen. These measures of precision have a 95% confidence level.

#### D. CORROSION RESULTS

The weight gain data for each of the 32 alloys tested are summarized in the Appendix: Table A-1, for  $300^{\circ}\text{C}$  exposures, Table A-2, for  $400^{\circ}\text{C}$  exposures, and Table A-3 for  $500^{\circ}\text{C}$  exposures.

A summary of the steady-state corrosion rates for each alloy at the three exposure temperatures is given in Table 2. An analysis was also made for rates for the best alloys exposed for longer times at  $500^{\circ}\text{C}$ . This second analysis showed that the steady-state condition had not been reached at 3000 hours. All alloys showed lower rates at longer times; an analysis made with data for exposures up to 6792 hours showed rates 29% lower than those computed after 3000 hours. Therefore, the long-term corrosion rates are predicted to be at least as low as those given in Table 2. A comparison of alloy effects on rate did not change with longer exposure.

The dependence of steady-state corrosion rate on alloy content was computed from the data shown in Table 2; the following polynomial equations resulted:

$$\begin{aligned} \text{At } 500^{\circ}\text{C: } \ln y = & 1.392 + 0.802 \text{ Nb} - 0.212 \text{ Cr} + 1.426 \text{ Fe} - 0.77 \text{ Cu} \\ & - 0.327 \text{ Nb}^2 - 0.047 \text{ Cr}^2 - 1.084 \text{ Fe}^2 + 0.182 \text{ Cu}^2 \\ & + 0.264 \text{ CrCu} - 0.125 \text{ FeCu} \end{aligned}$$

$$\begin{aligned} \text{At } 400^{\circ}\text{C: } \ln y = & 0.539 + 1.050 \text{ Nb} - 0.217 \text{ Cr} + 0.065 \text{ Fe} - 0.419 \text{ Cu} \\ & - 0.535 \text{ Nb}^2 - 0.043 \text{ Cr}^2 - 2.137 \text{ Fe}^2 - 0.217 \text{ Cu}^2 \\ & + 0.042 \text{ NbCr} + 0.464 \text{ NbFe} + 0.389 \text{ NbCu} + 0.417 \text{ CrFe} \\ & + 0.023 \text{ CrCu} + 0.316 \text{ FeCu} \end{aligned}$$

$$\begin{aligned} \text{At } 300^{\circ}\text{C: } \ln y = & 1.987 + 0.944 \text{ Nb} - 0.949 \text{ Cr} - 0.964 \text{ Fe} - 0.270 \text{ Cu} \\ & + 0.074 \text{ Nb}^2 + 0.279 \text{ Cr}^2 - 3.489 \text{ Fe}^2 + 0.031 \text{ Cu}^2 \\ & - 0.452 \text{ NbCr} + 0.378 \text{ NbFe} - 0.425 \text{ NbCu} + 1.415 \text{ CrFe} \\ & + 0.076 \text{ CrCu} + 0.800 \text{ CrFe} \end{aligned}$$

where

$y$  = Corrosion rate in  $\text{mg}/\text{dm}^2/\text{day}$ ,

Nb = Niobium content in atomic percent,

Cr = Chromium content in atomic percent

Fe = Iron content in atomic percent, and

Cu = Copper content in atomic percent.

The correlation coefficient between experimental data and values calculated by using these equations was found to be 0.89. Corrosion rate data for selected binary and ternary alloys included in the experiment permit direct illustration of the implications of these equations. The ability to make such direct illustrations demonstrates the near orthogonality of the data, and permits confident analytical examination of any composition in the total field.

Niobium additions are generally detrimental to alloys containing any or all of the other elements: Cr, Cu, and Fe. The Cr-Cu interaction is strongly positive especially at the higher test temperatures; there are binary alloys containing just Cr or just Cu which are better than any ternary Cr-Cu alloy; any alloy with both Cr and Cu will show relatively poor performance.

TABLE 2. Long-Term Corrosion Rates (mg/dm<sup>2</sup>/day) for First 31 Alloys as Determined by Statistical Analysis

Alloy	300°C		400°C		750-3000 h	3000-6792 h
	300°C	400°C	500°C	500°C	500°C	500°C
001	0.073 ± 0.014	1.09 ± 0.29	4.64 ± 0.31	3.91 ± 0.18		
002	0.061 ± 0.014	0.41 ± 0.06	5.82 ± 0.32	-	-	
003	0.069 ± 0.014	0.34 ± 0.04	5.57 ± 0.27	-	-	
004	0.075 ± 0.014	0.46 ± 0.06	5.56 ± 0.53	-	-	
005	0.132 ± 0.026	0.58 ± 0.03	3.14 ± 0.26	2.16 ± 1.02		
006	0.115 ± 0.014	0.65 ± 0.04	4.65 ± 0.18	-	-	
007	0.089 ± 0.014	0.63 ± 0.04	5.72 ± 0.47	-	-	
008	0.084 ± 0.014	0.76 ± 0.04	6.56 ± 0.61	-	-	
009	0.086 ± 0.014	0.74 ± 0.09	6.61 ± 0.58	-	-	
010	0.077 ± 0.014	0.52 ± 0.04	5.35 ± 0.44	-	-	
011	0.051 ± 0.014	0.47 ± 0.05	4.98 ± 0.42	-	-	
012	0.059 ± 0.014	1.73 ± 0.14	6.05 ± 0.32	-	-	
013	0.068 ± 0.014	0.32 ± 0.03	3.30 ± 0.18	2.32 ± 0.02		
014	0.163 ± 0.024	0.87 ± 0.09	4.09 ± 0.49	3.58 ± 0.54		
015	0.070 ± 0.014	0.44 ± 0.06	5.58 ± 0.40	-	-	
016	0.081 ± 0.014	1.21 ± 0.08	9.41 ± 0.84	-	-	
017	0.065 ± 0.015	0.26 ± 0.03	2.49 ± 0.35	2.05 ± 0.36		
018	0.056 ± 0.014	0.24 ± 0.04	2.09 ± 0.44	1.92 ± 0.24		
019	0.071 ± 0.014	0.27 ± 0.03	3.75 ± 0.37	2.42 ± 0.48		
020	0.149 ± 0.026	0.76 ± 0.07	4.23 ± 0.29	3.54 ± 0.34		
021	0.212 ± 0.041	1.39 ± 0.15	6.88 ± 0.34	-	-	
022	0.113 ± 0.024	1.20 ± 0.32	8.09 ± 1.43	-	-	
023	0.466 ± 0.126	1.03 ± 0.12	6.00 ± 0.31	-	-	
024	0.079 ± 0.022	0.32 ± 0.03	3.37 ± 0.48	2.60 ± 1.16		
025	0.061 ± 0.014	0.29 ± 0.03	-	-	-	
026	0.113 ± 0.014	0.22 ± 0.03	1.89 ± 0.22	1.53 ± 0.08		
027	0.070 ± 0.014	0.62 ± 0.05	7.23 ± 0.50	5.25 ± 0.80		
028	0.040 ± 0.014	0.60 ± 0.08	5.16 ± 0.29	3.07 ± 0.74		
029	0.072 ± 0.014	0.35 ± 0.03	4.23 ± 0.33	3.62 ± 0.22		
030	0.061 ± 0.014	0.31 ± 0.03	4.00 ± 0.22	3.11 ± 0.88		
031	0.088 ± 0.014	0.49 ± 0.03	4.53 ± 0.43	-	-	
032*	0.074 ± 0.014	1.36 ± 0.13	9.56 ± 2.01	-	-	

\* Zr-2

The remaining combinations, Cu-Fe and Cr-Fe, demonstrate beneficial additive effects. Particularly, if it is desirable to have good corrosion resistance at both 300 and 500°C, alloys containing both Cu and Fe are much better than Zr-Cu or Zr-Fe binaries. At 300 and 400°C, Fe may be a beneficial addition to certain compositions of Zr-Cr alloys; at 500°C, Fe additions are generally detrimental.

E. HYDRIDING RESULTS

Hydrogen contents determined after various exposures are given in the Appendix (Tables A-4, A-5, and A-6) for all 32 alloys exposed at 300, 400, and 500°C, respectively. At the time the statistical analysis was made of the 500°C results, data were available for exposure times of 75, 175, 375, 750, 1125, 1500, and 3000 hours, respectively. For 17 alloys, data were also available at 3792 hours. Similar data for 3578 hours of exposure were used in the analysis of the 400°C results. Initially, plots were made of hydrogen pickup in parts per million versus time for all alloys to determine when the steady-state condition was reached. It became apparent in making these plots that biases may have existed between the different exposure groups of specimens. In particular, the 500°C specimens exposed to 1500 hours, seemed to give results lower than those expected when considering the results for the other specimens. In several instances, the total hydrogen pickup was actually lower at 1500 hours than that observed at 1125 hours. Chemical re-analyses disclosed that this bias was not due to instrument bias.

Since only a very few points were available for each alloy in determining the rate of hydrogen pickup, if one point were consistently biased for some reason, it was important to allow for this in the analysis. For this reason, before proceeding with the analysis of the hydrogen data, the weight gain data were examined more closely. These data were more extensive than the hydrogen data, and if real biases existed in the weight gain sample groups, they could be determined more precisely. Variations in alloy content could scarcely be responsible if a given specimen group is biased for all alloys since, if there were a certain lack of homogeneity in the original sheets of metal, this would scarcely give rise to a bias in the same sample group for all alloys. Causes of possible sample group biases must be tied up with factors common to the same sample group for all alloys.

In the analysis of weight gain data previously reported, corrosion rates were estimated for each sample for a given specimen, and a weight average was taken to obtain the over-all corrosion rate for the alloy. These individual sample data for weight gain were re-examined. The 1500-hour samples, suspected to have low hydriding rates, were found to be remarkably consistent in having the smallest weight gain of all the samples. In fact, for 14 of the 30 alloys, the corrosion rate of the 1500-hour samples was the lowest of the 12 sample groups, which is clearly a significant result.

A more thorough analysis was made of all the weight gain data to detect any other biases that may exist. Tests were made which separated the samples into groups, between which real biases exist, but within which the samples were not significantly different. Although the 1500-hour group had the most obvious bias, there were other real differences between various groups. This was not due to the type of specimen (tensile versus impact). One possible explanation is the position within the test autoclave. Using the sample loading schematic diagram<sup>13</sup> the sample group loading disposition was checked against the sample group weight gain biases. If there were a temperature gradient in the autoclave, this would explain the observed differences between groups. The gradient would have to be on the order of 10 to 15°C, with the higher temperature at the bottom of the autoclave, to explain all the bias.

(The weight gain data for 400°C exposures were also re-examined. There was no apparent bias caused by a temperature gradient).

It should be pointed out that the chosen loading pattern for the sample group was purposely designed for removing any possible biases from the average values reported for corrosion rates. The biases would have no relative effect on composition comparisons. The biases do have to be considered, however, in determining hydriding rates where the data are less extensive.



With the results of these analyses in mind, the hydrogen data could be analyzed by taking steps to remove the bias at the expense of a loss in precision. Hydridding rates at 500°C, therefore, were estimated from data after 1125 and 3000 hours for 14 alloys and after 1125, 3000, and 3792 hours for the remaining 17 alloys. These data were analyzed by estimating the slopes of the straight lines fit through the data points. The usual least squares techniques was used, which is legitimate in this case because the sample points are mutually independent. The estimated slopes, or hydridding rates are given in Table 3. Based on the differences between the fitted points and the observed points, the uncertainty (95% confidence interval) associated with a given estimated hydridding rate at 500°C is  $\pm 1.2$  ppm/day for the values marked with an asterisk and  $\pm 0.8$  ppm/day for the remaining values.

For the 400°C data, hydrogen contents at 1125, 1500, 2250, 3000, and 3570 hours were included in estimating their hydridding rates. The 400°C hydridding rates are also given in Table 3. For 400°C data, the standard deviation is  $\pm 0.05$  ppm. It is emphasized that the limits are on precision and do not include all possible un-removed biases.

For 300°C exposures, the increase in hydrogen content even after 6750 hours was generally so small that analysis of hydridding rates was not performed. It was generally true that the majority of the corrosion hydrogen uptake occurred in the first 2250 hours. In some cases, the data show a decrease in hydrogen content with increasing exposure time after 2250 hours.

The dependence of steady-state hydridding rate on alloy composition was determined from the data given in Table 3 for 400 and 500°C exposures. The resulting polynomial expressions were:

$$\begin{aligned} \text{At } 500^{\circ}\text{C: } \ln y &= 1.835 - 0.115 \text{ Nb} - 0.060 \text{ Cr} - 0.368 \text{ Fe} - 1.097 \text{ Cu} \\ &\quad - 0.097 \text{ Nb}^2 - 0.148 \text{ Cr}^2 + 1.049 \text{ Fe}^2 + 0.242 \text{ Cu}^2 \\ &\quad + 0.072 \text{ NbCr} + 0.043 \text{ NbFe} + 0.069 \text{ NbCu} - 0.160 \text{ CrFe} \\ &\quad + 0.634 \text{ CrCu} - 0.619 \text{ FeCu} \end{aligned}$$

$$\begin{aligned} \text{At } 400^{\circ}\text{C: } Z &= 0.777 + 0.815 \text{ Nb} - 1.108 \text{ Cr} + 0.619 \text{ Fe} - 0.834 \text{ Cu} \\ &\quad - 0.192 \text{ Nb}^2 + 0.191 \text{ Cr}^2 - 7.898 \text{ Fe}^2 + 0.842 \text{ Cu}^2 \\ &\quad + 0.015 \text{ NbCr} + 1.157 \text{ NbFe} - 0.432 \text{ NbCu} + 2.556 \text{ CrFe} \\ &\quad - 0.048 \text{ CrCu} - 0.432 \text{ FeCu} \end{aligned}$$

where

$y$  = Hydriding rate in ppm/day,

$\text{Nb}$  = Niobium content in atomic percent,

$\text{Cr}$  = Chromium content in atomic percent,

$\text{Fe}$  = Iron content in atomic percent,

$\text{Cu}$  = Copper content in atomic percent, and

$$Z = \ln \frac{(y + \sqrt{y^2 + 0.2})}{2}, \text{ to permit use of negative estimates.}$$

The coefficient of variation for these expressions was also about 0.9; orthogonality was again confirmed.

In some instances, the alloy dependence of hydriding rate differs from the alloy dependence of corrosion rate, e.g., the dependence on Fe and Nb content at  $500^{\circ}\text{C}$  and the dependence on Cu content at  $400^{\circ}\text{C}$ . These differences arise since hydriding involves not only corrosion hydrogen production, but also the fraction of the corrosion hydrogen picked up by the underlying metal. Both the rate of corrosion hydrogen production and the pickup fraction vary with alloy content.<sup>5</sup>

#### F. MECHANICAL PROPERTIES

There are three requirements for a successful Zr alloy cladding which relate to mechanical behavior: good fabricability, high ductility, and resistance to corrosion hydrogen embrittlement. Consistent with the over-all program design, it was desirable to express each of the

TABLE 3. Estimated Hydriding Rates

Alloy	Hydriding Rate (ppm/day)	
	400°C	500°C
001	0.06	4.8*
002	-0.15	3.2
003	0.05	4.2
004	0.30	3.8
005	0.15	2.2*
006	0.10	2.0
007	0.34	2.3
008	0.71	2.4
009	0.27	3.0
010	0.23	4.2
011	0.25	2.5
012	2.1 ( $\hat{\sigma} = 0.4$ )	4.0
013	-0.02	3.2*
014	0.40	1.3*
015	0.22	3.3
016	0.62	5.2
017	0.09	1.7*
018	0.02	3.7*
019	0.06	2.4*
020	0.65	2.4*
021	0.49	6.6
022	0.44	3.4
023	0.73	5.8
024	0.02	4.4*
025	-0.04	-
026	0.23	2.6*
027	0.12	4.8*
028	0.03	3.6*
029	-0.07	2.8*
030	0.06	3.4*
031	0.09	3.3*
032	0.54	10.6*

\* $\hat{\sigma} = 1.2$  ppm/day; for all others  $\hat{\sigma} = 0.8$  ppm/day.

alloy properties which relate to these requirements in terms of alloy composition. It was possible to do this for as-fabricated tensile properties and to relate these tensile results to qualitative observations on fabricability. Post-corrosion mechanical behavior was also observed to be dependent on alloy composition; crystallographic and microstructural factors were also found to have an effect on mechanical behavior.

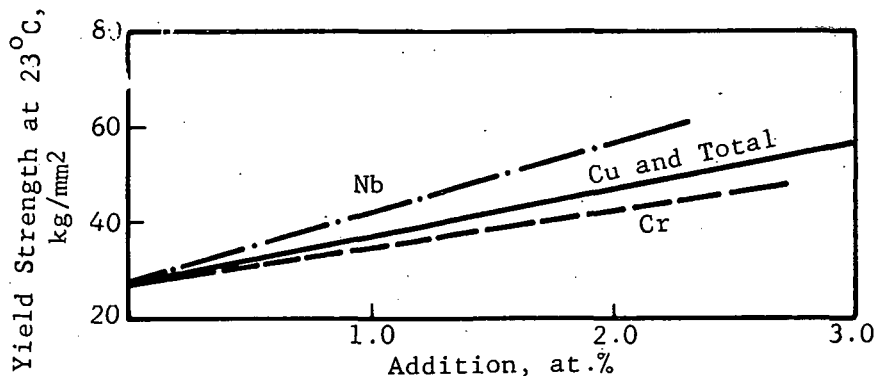
#### 1. As-Fabricated Tensile Properties and Fabricability

The tensile properties of all alloys after fabrication and final heat treatment are included in the Appendix, Tables A-7 through A-10. Data are given for tests at room temperature, 300, 400, and 500°C.

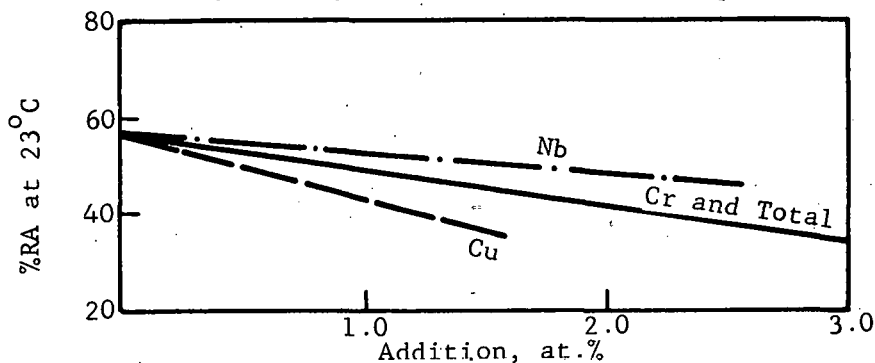
Room temperature data were analyzed. The most important factor in determining the as-fabricated mechanical properties was the total atomic percent alloy addition. Linear bands ( $\pm 10\%$  of values) which increased with an increase in total alloy content describe the yield and tensile strength data quite well; linear bands ( $\pm 20\%$  of values) which decrease with an increase in total alloy content describe the reduction-in-area and elongation data quite well.<sup>8</sup> Certain trends for the effects of individual alloying elements could be detected (Figure 1).

The dependence of mechanical behavior on alloy content is not unexpected. All the binary alloy systems involved (Zr-Nb, Zr-Cr, Zr-Fe, Zr-Cu) show limited solid solubility and increased volume percent second phase with increased alloy addition. Only Nb additions might give significant solid solution strengthening.<sup>15</sup> The role of intermetallic dispersions in increasing strength and decreasing ductility was reported by Keeler<sup>16,17</sup> early in the history of Zr alloy development.

A correlation was made between qualitative fabricability observations<sup>10</sup> and the reduction-in-area and elongation data. Alloys with less than 1.9 at. % total alloy content showed good fabricability.



a. Alloy Strength as a Function of Composition



b. Alloy Ductility as a Function of Composition

FIGURE 1. ALLOY MECHANICAL PROPERTIES AS A FUNCTION OF COMPOSITION.

Alloys with a total elongation greater than 19% or a reduction in area greater than 41% had good fabricability. For alloys with greater than about 4 at. % alloy content, that is, those showing less than 28% reduction in area or less than 11% elongation, poor fabricability was reported.

The fabricability observations were based on edge cracking and crack propagation tendencies during cold rolling. Only 20% cold work was required in our schedule, compared to 40 to 60% cold work in commercial mill product fabrication. All of the alloys could be fabricated by making changes in the reference fabrication schedule; however, it is clear that any alloy meeting the economic targets of this Alloy Design Program cannot grossly exceed 1.9 at. % total alloy content because of fabricability.

The upper limit on alloy content means (from the tensile data) that the target alloy will not have a yield strength greater than about  $45 \text{ kg/mm}^2$  at room temperature (compare  $39 \text{ kg/mm}^2$  for Zircaloy-2 in the same tests).

## 2. Post-Corrosion Mechanical Properties

Post-corrosion tensile properties at the exposure temperature are given in the Appendix, Tables A-11 and A-12.

Tensile coupons exposed at  $500^\circ\text{C}$  (for as long as 3792 hours) and tested at  $500^\circ\text{C}$  showed no brittle behavior. A Zircaloy-2 coupon contained the most hydrogen, 1756 ppm, of any tested; for Zircaloy-2 the solubility for hydrogen at  $500^\circ\text{C}$  is about 600 ppm hydrogen.<sup>18</sup> The Zircaloy-2 coupons (and those of all other alloys) showed a significant drop in tensile yield strength and a loss in elongation to fracture as exposure times and hydrogen content increased. However, for the longest exposure and highest hydrogen content, the tensile coupon did not show brittle fracture.

Tensile coupons exposed at  $300^\circ\text{C}$  and tested at  $300^\circ\text{C}$  contained relatively little hydrogen (80 ppm maximum compared to a hydrogen solubility limit in Zircaloy-2 of about 120 ppm at  $300^\circ\text{C}$ ). No significant changes in tensile properties at  $300^\circ\text{C}$  were observed after corrosion exposure at  $300^\circ\text{C}$  for exposure times up to 3000 hours. (The same was true for impact tests at  $300^\circ\text{C}$  after exposures to 3570 hours at  $300^\circ\text{C}$ , Appendix, Table A-13.)

Because of the 300 and  $500^\circ\text{C}$  results, the tensile coupons exposed at  $400^\circ\text{C}$  were not tested at  $400^\circ\text{C}$ .

The results of tensile tests at the exposure temperature are consistent with our earlier assumptions<sup>6</sup> that brittle fracture at elevated temperatures would occur only when a complete grain boundary network of hydride was present (estimated to occur at the solubility limit plus 1500 ppm hydrogen). Even the poorer alloys did not absorb this critical amount of hydrogen during the longest exposures. Some of the better alloys, therefore, would not be expected to be brittle until after 38,000 hours (over 4 years) even at 500°C (see the hydriding rates in Table 3). Thus, it appears that there are alloys meeting the corrosion and fabricability requirements which can also be expected to meet the design target for resistance to corrosion hydrogen embrittlement at service temperatures between 300 to 500°C.

Data for tensile coupons tested at room temperature after exposures at 300, 400, and 500°C are given in the Appendix, Tables A-14, A-15, and A-16. It was found that the resistance to hydrogen embrittlement at room temperature was lower than that at the exposure temperature and varied from alloy to alloy.

Tensile coupons exposed at 300°C (6570 hours maximum time, 80 ppm hydrogen maximum) and tested at room temperature did not show brittle fracture. Somewhat erratic results were observed for some of the highly alloyed compositions, e.g., alloys 002, 006, 008, 009, 011, 012, and 022. These alloys had 2.4 to 5.9 at. % total alloy addition, yield strengths on the order of 70 kg/mm<sup>2</sup> (100,000 psi), and were among those with only fair to poor fabricability.

Tensile coupons exposed at 400°C (3578 hours maximum, 574 ppm hydrogen maximum) and tested at room temperature also exhibited some erratic behavior for the more highly alloyed samples. Alloy 012 (1.1 Nb - 1.4 Cr - 0.3 Fe - 1.8 Cu) contained 559 ppm hydrogen after 3000 hours at 400°C and was brittle in the room temperature tensile

test. (This alloy also exhibited brittle behavior in the 300°C impact tests [Appendix, Table A-17] after 2250 hours, 462 ppm H<sub>2</sub>, but when tested in tension at 400°C showed 15% elongation and 57% reduction in area after an exposure of 3578 hours, 574 ppm).

There is some evidence that recovery (alloy 008 and 011) and aging (alloy 014 and 017) reactions also occurred at 400°C for some alloys. Tensile data for alloys exposed at 500°C and metallographic evidence further revealed that the stabilization anneal given all coupons at 565°C (24 hours) before corrosion exposure was not completely effective for every alloy.

Coupons exposed at 500°C and tested at room temperature in tension (Appendix, Table A-16) or at 300°C in impact (Appendix, Table A-18) contained the most hydrogen and provided the most information on resistance to hydrogen embrittlement. The data (Appendix, Tables A-16 and A-18) were analyzed to estimate the hydrogen content required to cause low-temperature brittle behavior as shown in Table 4.

When the embrittlement data were plotted as a function of total alloy content (Figure 2), a general trend was revealed, but four alloys did not fit the trend band at all. Except for these four alloys, it appeared that a total alloy content of less than 0.8 at. % would be required for resistance to 1000 ppm or more hydrogen. When the data were grouped by increasing Nb content and replotted (Figure 3), it was clear that Nb was responsible for much of the loss in resistance to hydrogen and that if Nb content were kept below 0.4 at. %, a high resistance to hydrogen was possible. In fact, alloy 030 (with 1.4 at. % Cr and 1.2 at. % Cu but only 0.3 at. % Nb) was not brittle until it contained 1000 ppm hydrogen. A tentative plot was made of Fe content versus amount of hydrogen to make the alloys brittle. For fixed Nb contents, this tentative plot shows Fe to be an undesirable addition. This result suggested the plot (Figure 4) which shows that good resistance to hydrogen can be obtained if total atom percent Nb + Fe is kept below 0.7 at. %. Alloy 003 has 0.7 at. % Nb + Fe but 3.2 total at. % Cr and Cu; this alloy required 900 ppm to cause brittle behavior.



TABLE 4. Estimates of Hydrogen Content to Cause Brittle Behavior at Low Temperatures

Alloy	Estimated H <sub>2</sub> (ppm) to Make Brittle	Analyzed Hydrogen Content (ppm)		
		Definitely Ductile	First Indication Brittle	Definitely Brittle
001	800	392	752	1064
002	600	327	-	601
003	900	440	-	910
004	600	440	-	780
005	300	165	246	420
006	300	231	247	429
007	300	176	316	557
008	300	138	327	591
009	200	98	212	345
010	400	247	324	875
011	300	116	271	513
012	400	261	406	734
013	>600	637	*	*
014	550	522	*	*
015	500	348	-	463
016	500	355	511	646
017	>600	575	*	*
018	>500	497	*	*
019	>400	415	*	*
020	1000	626	969	1069
021	1000	526	963	-
022	600	490	500	841
023	1100	623	1051	1196
024	>600	625	*	*
025	-	-	-	-
026	>800	844	*	*
027	1300	1159	-	1348
028	>700	744	*	*
029	>600	632	*	*
030	>800	791	*	*
031	400	231	415	647
032	1600	644	1563	1726

\* Alloy not brittle after longest exposure.

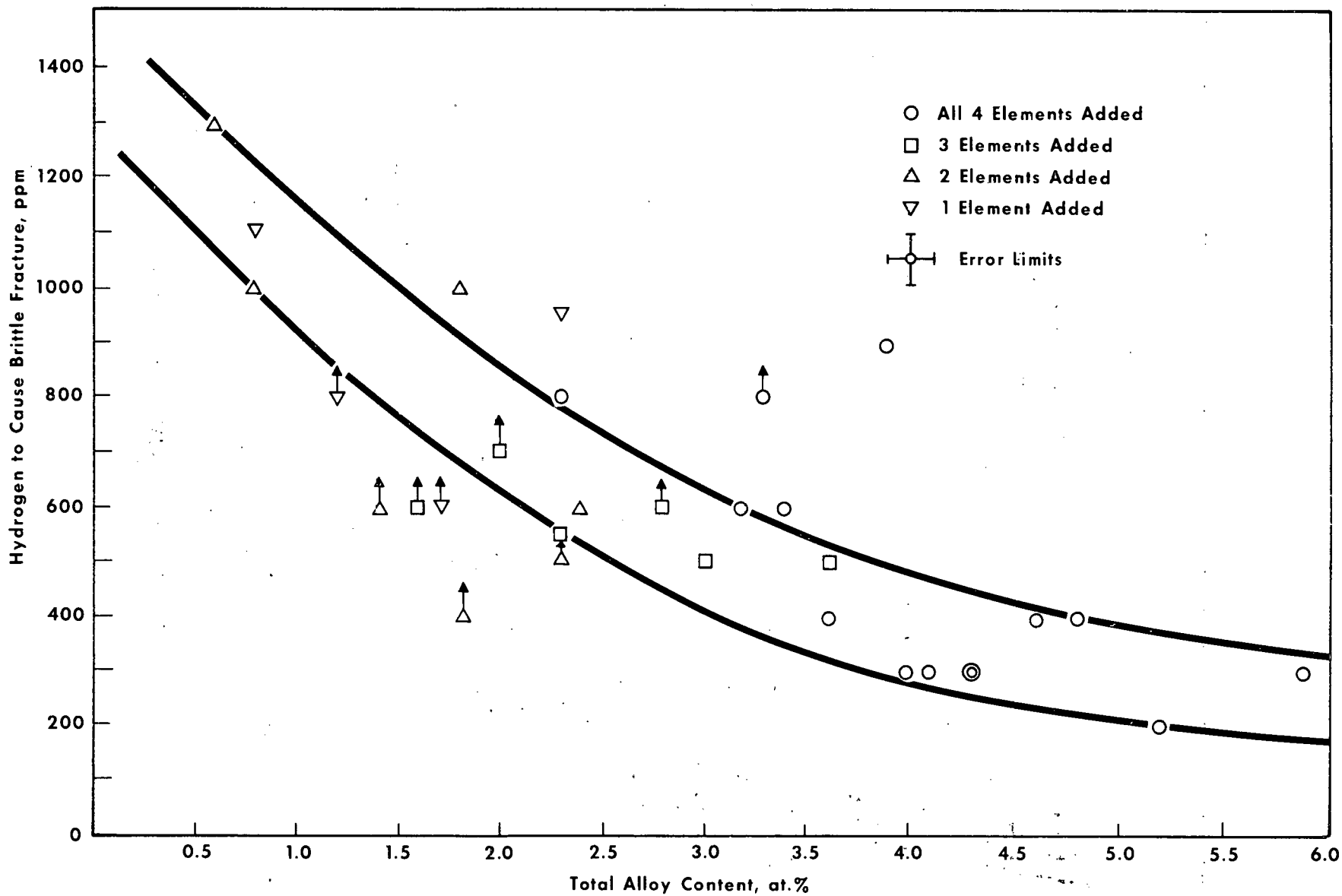


FIGURE 2. RESISTANCE TO HYDROGEN VERSUS TOTAL ALLOY CONTENT

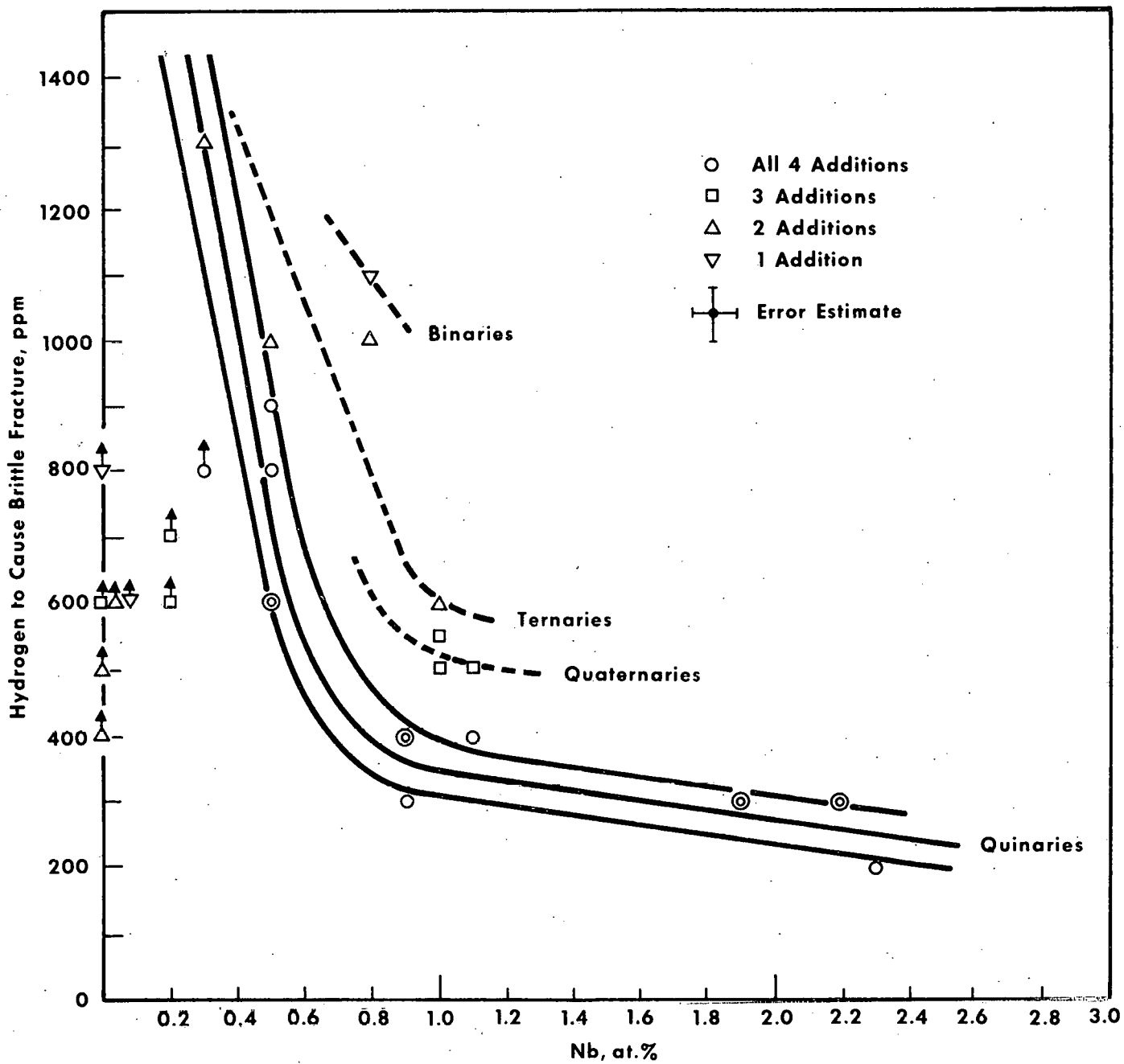


FIGURE 3. RESISTANCE TO HYDROGEN VERSUS Nb

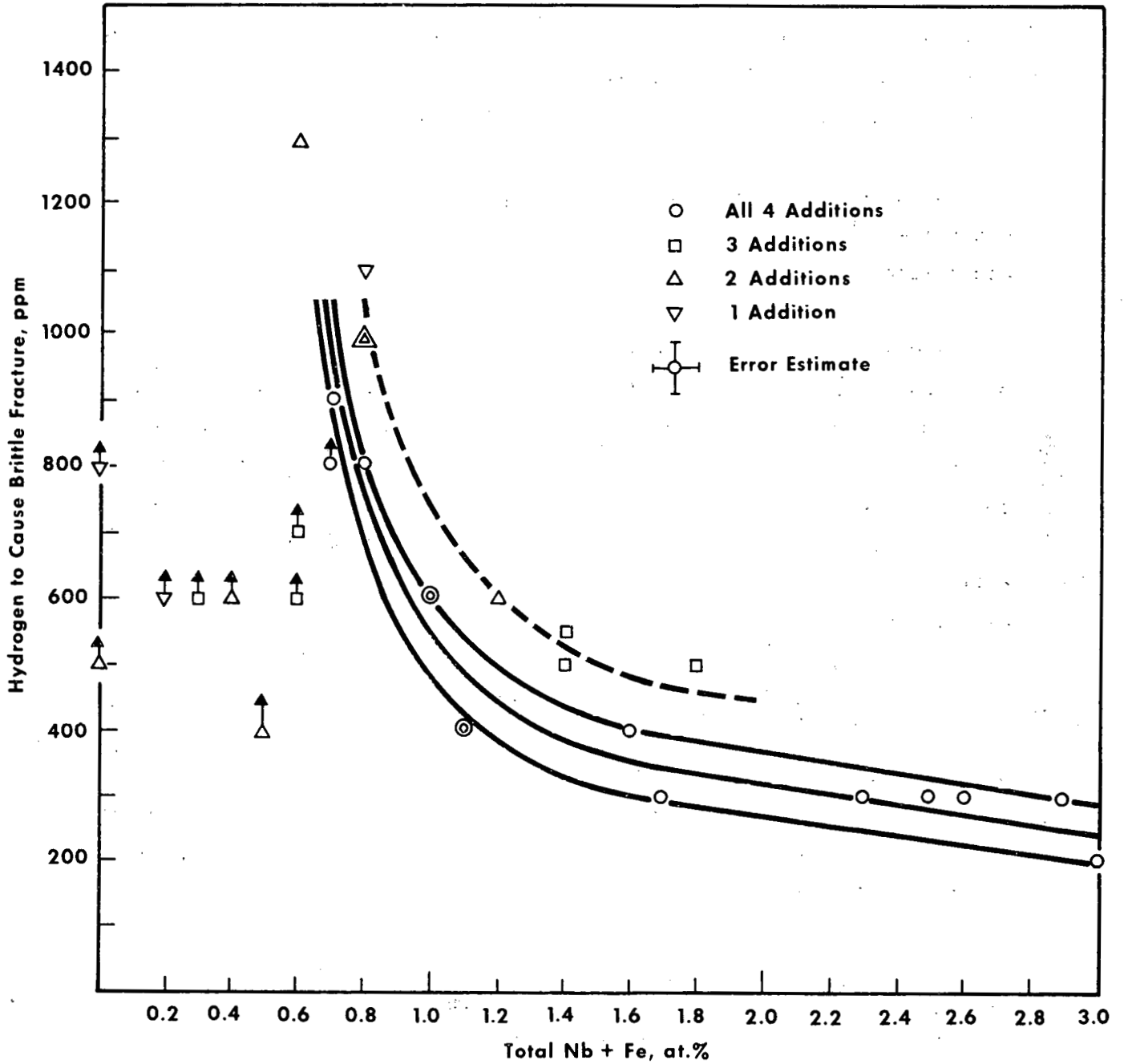


FIGURE 4. RESISTANCE TO HYDROGEN VERSUS TOTAL Nb+Fe

It is to be emphasized that the low Nb, low Fe alloys which have good resistance to a given hydrogen content are also among those which have low corrosion rates and low hydriding rates. Some of these alloys were exposed for over 6700 hours at 500°C without becoming brittle either at elevated temperatures or at room temperature.

Sheet texture and hydride platelet orientation were checked to determine how microstructural features were related to the alloy composition effects noted above.

Samples of each alloy were examined on the sheet, rolling surface by x-ray diffraction.<sup>19</sup> The recorded peak intensities were compared to the expected random intensities. Evidence for several distinctly different textures were revealed. Complete pole figures were run for coupons from an alloy in each of the three major texture groups; these detailed texture studies confirmed the orientations deduced from the diffractometer data. It was at first surprising to find distinctly different textures, since all the alloys were fabricated in the same way. However, slight modifications in the procedure were required to avoid cracking in the highly alloyed compositions. Furthermore, the weaker, less highly alloyed sheets might be expected to deform differently from the stronger sheets in cold rolling; different textures would result. Therefore, texture and alloy content are not independent variables. In fact, the embrittlement data are most directly explained by alloy composition rather than by sheet texture.

No preferred hydride platelet orientation was observed for the alloys tested. Hydride platelet orientations are known to affect resistance to hydrogen,<sup>20</sup> but this complication was not a factor in our tests. It was found, however, that the hydride phase precipitates on pre-existing intermetallic phases (either for the same reasons the intermetallic nucleated at that site, or because the intermetallic acted as a nuclei). Thus, the brittle intermetallics were progressively

connected with brittle hydride as exposure continued. The brittle samples were observed to show a preponderance of grain boundary fracture. Those high-Nb alloys with the lowest resistance to hydrogen were characterized by heavy grain boundary intermetallic precipitation before exposure; a small amount of hydride was required to connect these precipitates and provide a brittle grain boundary. The more resistant alloys (low in Nb) exhibited more uniformly dispersed intermetallics; more hydride was required to provide a continuous path of brittle phase.

These metallographic observations suggest that alloys high in Nb content might be improved with respect to resistance to hydrogen by using an appropriate heat treatment. (However, since the heat treatment used is optimum for corrosion resistance,<sup>11</sup> a net gain in performance might not accrue.) Conversely, the more attractive alloys containing Cr or Cu might be less resistant to hydrogen if care is not taken to ensure a finely dispersed, second-phase distribution.

#### G. ADDITIONAL INVESTIGATIONS

The results reported in the three preceding sections lead to the following conclusions:

1. Total alloy content should be less than about 1.9 at. % for good fabricability by the schedule followed.
2. Cu-Fe and Cr-Fe additions showed the more promise with respect to corrosion and hydriding over the total temperature range of interest. Copper at about 1.2 at. % and Cr at about 2.3 at. % appeared optimum.
3. Total Nb and Fe content should be less than 0.7 at. % for good resistance to hydrogen embrittlement.

The original fabrication schedule was chosen to produce optimum corrosion performance for additions of Nb. The final anneal did not produce a completely stable structure for all alloys, e.g., Cr-Cu alloy 018. With Nb of little interest, a final annealing temperature closer to the peritectic temperature for Zr-Cr, Zr-Cu, and Zr-Fe (about 800°C) was feasible and might be expected to give a more stable structure.

In the initial selection of the alloy field for study, several elements were listed for future consideration.<sup>6</sup> Of these, Ni and Be appeared worthy of further study.

#### 1. Nickel and Beryllium Additions

The first objective of the additional evaluations was to see if minor additions of Ni or Be to Zr + 1.9 at. % Cr or to 1.2 at. % Cu led to improved performance. The total corrosion exposure was 3000 hours at 300 and 500°C in steam. The final mechanical property, corrosion and hydriding data are presented in the Appendix, Tables A-19 through A-24. The data on the effect of Fe additions are included in these tables.

The mechanical properties of the as-fabricated alloys (Appendix, Tables A-19 and A-20) were generally consistent with the first results: strength and ductility were nearly linear functions of total alloy content. A notable exception to this generalization is found for the 0.8 at. % Be addition to Zr-Cr. The Be additions caused a significant decrease in strength with a corresponding increase in ductility. The additions of Be were chosen after calculating that 0.4 at. % Be would be less than enough to combine with the oxygen known to be in the sponge Zr; 0.8 at. % Be was calculated to be more than enough to combine with all the oxygen in the sponge. Oxygen is known to be a potent alpha strengthener. It is likely that the increase in ductility and decrease in strength noted with Be additions is caused by the formation of BeO, which reduces the amount of oxygen in the Zr matrix.

At the levels tested, none of the minor additions (Fe, Ni, or Be) to Zr-Cr are beneficial at both 300 and 500°C in improving both corrosion resistance and hydrogen pickup. Nickel additions give high hydrogen at 300°C; Be additions give high hydrogen at 500°C. Iron is the best of the three, but is not beneficial to corrosion resistance at 500°C. For particular temperatures, there were alloys better than the Zr-Cr binaries. The Zr + 1.9 at. % Cr + 0.8 at. % Be alloy is very interesting at 300°C; the addition of 0.1 to 0.4 at. % Ni gives alloys which perform best at 500°C.

None of the Zr-Cu base alloys are better than Zircaloy-2 at 300°C. Iron is the best addition for 300°C service. At 500°C, all of the Zr-Cu alloys are good. Nickel is the best addition at 500°C; Be is the worst. The Zr-Cu-Fe alloys show the best performance at both 300 and 500°C.

In comparing the Zr-Cu-Fe alloys with the Zr-Cr binaries, it is apparent that Zr-Cu-Fe would be preferred at higher service temperatures; Zr-Cr would be preferred at lower service temperatures. (Unfortunately, the simultaneous addition of Cr and Cu leads to a performance less desirable than for either addition alone.<sup>21)</sup>)

## 2. Fabrication Schedules

The second objective of the additional experiments was to determine the effects of two alternate fabrication schedules on the performance of a Zr + 2.3 at. % Cr alloy and a Zr + 1.2 at. % Cu alloy. The Zr-Cu alloy was a duplicate of alloy 026 of the first experiments. The three fabrication schedules for the 1.8-kg ingots were:

- A. The reference treatment: double arc-melted, forged at 788°C, hot-rolled at 788°C, cold-rolled within 20% of final thickness, beta solution treated 6 hours at 950°C, quenched into water, cold-rolled 20%, alpha annealed 24 hours at 565°C.



- B. The same as A. Except alpha annealed for 8 hours at 788°C.
- C. Double arc-melted (ingot cooling rate was  $> 50^{\circ}\text{C}/\text{min}$  in all three cases), forged at 788°C, hot-rolled at 788°C, cold-rolled 20% to final size, alpha annealed at 788°C.

The resulting microstructures were fine, uniform intermetallic dispersions for Schedule C and to a lesser extent for Schedule B. A less uniform and more cellular distribution of intermetallics resulted from Schedule A.

The effect of fabrication schedule on mechanical properties of the two alloys can be seen from the data in the Appendix, Table A-25. For both alloys, strength decreased and ductility increased significantly with the increase in alpha annealing temperature from 565 to 788°C. For the Zr-Cr alloy annealed at 788°C, the beta treatment resulted in both lower strength and lower ductility than did the all-alpha treatment. For the Zr-Cu alloy, the all-alpha treatment gave lower strength and higher ductility. (It should be emphasized that the "all-alpha" treatment include a rapid cooling rate from the beta during ingot cooling for the small ingots used here. Large production ingots cool more slowly.) Final annealing at temperatures above 565°C are clearly beneficial in improving the ductility of Zr-Cr and Zr-Cu alloys. This improvement in initial ductility is to be expected to increase resistance to hydrogen embrittlement.

The effect of fabrication schedule on the corrosion resistance and hydrogen content of the two alloys can be assessed from the data in Tables 5 and 6. The most significant conclusion is the excellent performance of the Zr + 2.3 at. % Cr alloy when alpha annealed at 788°C (Schedule C). With this heat treatment, this alloy clearly shows the best performance of any alloy tested in the entire program - both at 300°C and also at 500°C. The higher alpha annealing treatment is also beneficial for the Zr-Cu alloy, but even in this heat treatment the alloy is not as good as the Zr-Cr-Fe alloys are with less favorable heat treatment.

TABLE 5. Effect of Fabrication Schedule on Weight Gain  
(Weight Gain, mg/dm<sup>2</sup>)

<u>Alloy Composition</u>	<u>Fabrication Schedule*</u>	<u>175 h</u>	<u>750 h</u>	<u>1125 h</u>	<u>1875 h</u>	<u>2250 h</u>	<u>3000 h</u>
<u>300°C Exposure</u>							
Zr + 2.3 at.% Cr	A	-	13.8	15.0	-	16.9	19.3
	B	-	13.7	14.3	-	16.5	18.8
	C	-	11.3	11.9	-	13.9	15.8
<u>500°C Exposure</u>							
	A	50	123	188	313	-	439
	B	50	99	115	144	-	181
	C	48	95	110	138	-	168
<u>300°C Exposure</u>							
Zr + 1.2 at.% Cu	A**	-	15.7	18.8	-	25.4	26.9
	A	-	17.4	18.3	-	20.1	22.5
	B	-	19.5	20.3	-	23.0	25.5
	C	-	19.5	19.7	-	23.4	25.8
<u>500°C Exposure</u>							
	A**	125	187	214	-	-	360
	A	86	195	213	257	-	323
	B	82	173	187	220	-	294
	C	87	172	188	203	-	238

\* A and B were beta treated. Final anneal: A = 565°C, B and C = 783°C.

\*\* First experiment data for alloy 026 which is also Zr + 1.2 at.% Cu.  
Sponge Zr contained 0.05 at.% Fe.

TABLE 6. Effect of Fabrication Schedule on Hydrogen Content

<u>Alloy Composition</u>	<u>Fabrication Schedule*</u>	<u>0 h</u>	<u>750 h</u>	<u>1125 h</u>	<u>2250 h</u>	<u>3000 h</u>
<u>300°C Exposure</u>						
Zr + 2.3 at.% Cr	A	11	-	16	21	21
	B	9	-	8	10	10
	C	5	-	6	7	7
<u>500°C Exposure</u>						
	A	11	150	251	-	961
	B	9	107	117	-	246
	C	5	105	122	-	227
<u>300°C Exposure</u>						
Zr + 1.2 at.% Cu	A**	(13)	-	-	63	60
	A	14	-	67	64	65
	B	6	-	38	43	41
	C	5	-	38	41	40
<u>500°C Exposure</u>						
	A**	(13)	-	293	-	494
	A	14	291	319	-	490
	B	6	262	262	-	417
	C	5	264	275	-	294

\* A and B were beta treated. Final anneal: A = 565°C, B and C = 788°C.

\*\* First experiment data for alloy 026 which is also Zr + 1.2 at.% Cu.

Sponge Zr contained 0.05 at.% Fe.

Post-corrosion sheet impact tests at 300°C were performed on all coupons before hydrogen analyses were made. Only the Zr + 2.3 at. % Cr alloy coupon with the least favorable heat treatment (A) exposed 3000 hours at 500°C showed any significant loss of ductility. This coupon contained 961 ppm H<sub>2</sub>. The more ductile (B) and (C) coupons with only 227 to 246 ppm hydrogen after 3000 hours would be expected to go at least 15,000 hours at 500°C before becoming brittle in the 300°C impact test.



### III. RECOMMENDATION OF FUEL CLADDING ALLOY

The work performed was examined with respect to applying the results to water reactor fuel technology. Two separate service temperature ranges, 280 to 340°C and 500 to 700°C were considered. These temperature ranges correspond to those for water reactor fuel cladding and superheat reactor fuel cladding, respectively. To permit this examination of the applicability of the results to either fuel service temperature range, the corrosion experiments were purposely performed between 300 and 500°C.

#### A. APPLICATION FOR SUPERHEAT CLADDING

The factors that limit the utilization of Zr alloys in superheated steam were examined by Klepfer and Douglass.<sup>22</sup> Considering all available alloy data from all sites, it was concluded that there is little promise of using any Zr base alloy as superheat cladding.

The limiting factor is the acceleration of corrosion of a heat transfer surface caused by the growth of a thick, adherent ZrO<sub>2</sub> insulating film. Service would be terminated by loss of wall thickness, loss of strength with increasing metal temperature, and spalling of radioactive oxide to the reactor coolant. For the engineering assumptions taken by Klepfer and Douglass, this requirement (even without considering transient conditions) limits cladding surface temperatures to less than 540°C.

The results of this same analysis indicated that there is good promise for developing Zr alloys for a high, heat-flux, fuel cladding with a service life of over 4 years at 475°C. For non-heat transfer structural components the better potential alloys might be acceptable up to 670°C.

## B. APPLICATION FOR WATER REACTOR CLADDING

The performance of the commercial zirconium base alloy, Zircaloy-2, as a fuel cladding material for water reactors has generally been quite good. Several problems have, however, been revealed by extended fuel testing.

### 1. Problems With Commercial Zircaloy-2 Cladding

Early testing of fuel elements clad with Zircaloy-2 in the Vallecitos Boiling Water Reactor revealed a sensitivity to catastrophic failure if the cladding leaked steam. This was only true when the  $UO_2$  fuel contained fluoride impurities.<sup>23</sup> Fluorides in the  $UO_2$  are now held below 30 ppm and, in some instances, the vulnerable internal cladding surface is protected by a  $ZrO_2$  pre-service corrosion film. The fluoride problem is no longer considered to be the critical limit on clad lifetime.

Fuel element testing also revealed fuel rod bowing due to in-service recovery of fabrication cold work and residual stresses. All cladding material is now stress relieved at temperatures above  $400^\circ C$  before fuel element fabrication to ensure dimensional stability during autoclaving and during service. The research on which this heat treatment is based has been reported;<sup>24</sup> the full-life testing of fuel has confirmed this procedure. This problem is no longer considered the most critical.

Fuel element tests so far, have not resulted in failures directly attributed to radiation effects on the mechanical properties. Radiation does increase strength and decrease ductility; the extent of this damage both with coupon tests and with samples cut from fuel cladding has been determined. The problem of neutron damage to the cladding is considered to require continued surveillance, but is not judged to be the most critical problem revealed.

Failures of intact dimensionally stable rods caused by hydriding have not yet been experienced. However, massive hydride embrittlement was observed in conjunction with both the fluoride-accelerated corrosion failures<sup>23</sup> and the rod-bowing failures. The embrittlement of Zr alloys by corrosion hydrogen has been known for some years and has been the subject of considerable research. Hydrogen embrittlement of Zr alloys may set an ultimate technical limit for these materials. The exact limits depend on fuel design, service temperature distributions, cladding manufacturing process, alloy composition, and, very importantly, on in-service alloy corrosion rates (hydrogen production rates). This problem is considered important.

The problem considered the most critical at this time is that of in-service corrosion. From preliminary data, it is suggested that the corrosion rate in-reactor is perhaps 4 to 5 times faster than might be predicted from the standard Zircaloy-2 ex-reactor data.<sup>25</sup> The in-reactor corrosion is that expected at significantly higher temperatures. The growth of thick in-reactor corrosion films must be expected to result in the acceleration of corrosion caused by the attendant temperature increase of the oxide-insulated heat transfer surface. Furthermore, local over-heating caused by flow restriction or rod bowing could lead to extremely high local temperatures. Local corrosion has restricted the life of entire fuel bundles which were otherwise performing quite well. The direct and indirect (hydriding) effects of the corrosion of Zircaloy-2 at higher than expected local and general temperatures are considered the immediate factors which determine the life of fuel clad with Zircaloy-2.

## 2. Possible Solutions for Zircaloy-2 Cladding Problems

The most immediate problem with commercial Zircaloy-2 appears to be its low resistance to over-temperature. Three possible metallurgical approaches have been considered in improving this situation: heat treatment, minor changes in composition, and major changes in composition. It was concluded that improvement in the resistance to



over-temperature of water reactor fuel cladding should be explored by including a major compositional change from Zircaloy-2 as fuel test cladding material.

a. Heat Treatment

The data in the literature on the experimental determination of post-transition (long-time) corrosion rates for commercial Zircaloy-2 are given in Figure 5. The normal commercial heat treatment for tubing consists of forging or extruding at 790°C or below, cold working (with intermediate anneals at 760 to 815°C, if necessary) and stress relief or full annealing at temperatures between 455 and 815°C. Pemsler<sup>26</sup> has shown for Zr alloys containing Fe, Cr, and Ni (additions that are present in Zircaloy-2) that quenching from the beta (above 900°C) followed by annealing in the alpha range is beneficial for high-temperature corrosion resistance. Beta quenching alone causes warping and leads to low tensile ductility. Beta quenching is not desirable as a finishing treatment for thin-walled mill products. Zircaloy-2 with the following heat treatment was included in the Alloy Design Study: forge at 790°C, hot work at 790°C, cold work to within 20% of final dimensions, beta quench after a 24-hour solution treatment at 950°C, cold roll to final dimensions, anneal 8 hours at 565°C. The results for the post-transition corrosion rate of Zircaloy-2 in this condition also are shown in Figure 5. Below 400°C there is little difference between the commercial and the beta solution plus alpha anneal material. However, above 400°C there is a marked improvement over the present commercial heat treatment. When tested at 500°C the beta solution plus alpha anneal treated material shows a post-transition rate of about 9 mdd ( $\text{mg}/\text{dm}^2/\text{day}$ ) compared to a high of about 48 mdd for commercial material. The beta-solution plus alpha-anneal treatment for Zircaloy-2 is consistent with the desirability of a fine structure and with another treatment developed for increasing corrosion resistance above 400°C and for removing susceptibility to stringer corrosion.<sup>27</sup>

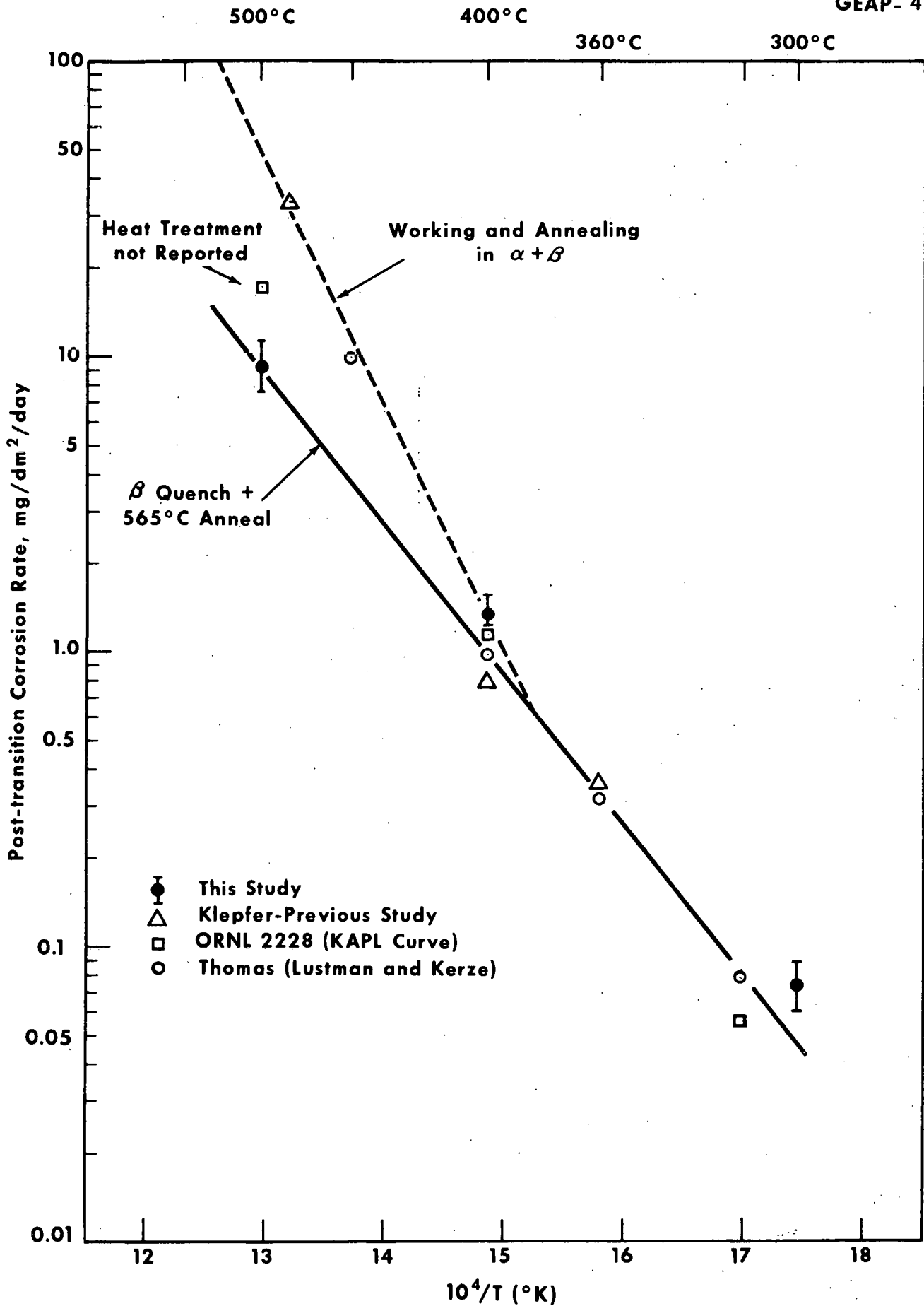


FIGURE 5. POST-TRANSITION CORROSION RATE OF ZIRCALOY-2 AS A FUNCTION OF RECIPROCAL ABSOLUTE TEMPERATURE

For alloys other than Zircaloy-2, other heat treatments are optimum. A final anneal of 24 hours at 565°C was best for Zr-Nb alloys.<sup>28</sup> For a Zr + 2.3 wt. % Cr alloy, the test data show that increasing the final alpha annealing temperature from 565 to 788°C lowers the long-term corrosion and hydriding rates, e.g., the 500°C corrosion rate decreases from 2.5 to 0.8 mdd.

b. Minor Composition Changes

Following the observation at Bettis Atomic Power Department that high Ni content in Zircaloy-2 leads to abnormally high hydrogen pickup, Ni-free compositions were developed.<sup>29</sup> One of these compositions, Zircaloy-4,\* is already being tested as fuel cladding in several programs. However, it has been our experience that Zircaloy-4 has less resistance to over-temperature than has Zircaloy-2. All available data on the corrosion rates of Zircaloy-4 at temperatures above 400°C were reviewed and these data support our experience with this alloy.

Some improvement in the high-temperature corrosion of Zircaloy-4 is to be realized by the beta solution plus alpha anneal heat treatment. Zircaloy-4 contains more Ni and less Fe than Zircaloy-2. With respect to corrosion resistance, Ni is beneficial and Fe is harmful. In the Zirconium Alloy Design Program, the Zr plus 0.3 at. % Fe alloy was the only alloy tested which disintegrated in less than 375 hours at 500°C in steam. All of the other 31 compositions including Zircaloy-2 showed reasonable behavior after 3000 hours at 500°C. (All alloys were given the beta solution plus alpha anneal heat treatment.)

---

\*Zircaloy-4 is a licensed alloy with the nominal composition: 1.5 at. % Sn, 0.15 wt. % Cr, 0.18 to 0.24 wt. % Fe, and less than 70 ppm Ni.

Resistance to over-temperature is not a major advantage anticipated with Zircaloy-4. No other minor compositional changes in Zircaloy-2 have been studied thoroughly.

c. Major Composition Changes

All Zr alloy development before 1962 for high temperature water and steam service was reviewed in the First Quarterly Progress Report on this Zirconium Alloy Design Program.<sup>6</sup> Recent work was reported in the Proceedings of the USAEC Zirconium Alloy Development Symposium held in November 1962.<sup>30</sup>

The relative performance of other alloys being studied at other sites should be mentioned. The Zr-Nb binary alloys were studied in detail for cladding applications<sup>31</sup> and have higher corrosion rates at all temperatures up to 482°C than those for Zircaloy-2 in the same condition of heat treatment (beta solution + alpha anneal). Rösler<sup>32</sup> reported data indicating the best results at 500°C in 1 atm steam were post-transition rates of 3 to 5 mdd (compare 0.8 mdd for Zr-Cr) and that the best alloys were Zr-Cu, Zr-Cu-Nb, and Zr-Cu-Ca alloys of about 1.5 to 2.0 at. % total alloy content. (Zr-Cu and Zr-Cu-Fe alloys were also included in the Zirconium Alloy Design Studies and showed rates as low as 1.9 mdd at 500°C in 68 atm steam. The Zr-Cu binary alloys, however, were found to corrode faster and pick up more hydrogen than Zircaloy-2 at 300°C in steam). Greenberg<sup>33</sup> tested Zr-Ni-Fe and Zr-Cu-Fe alloys at 540°C in steam and found post-transition rates of 2 mdd. The specimens tested, however, were crystal-bar base, as-cast buttons and no specimens were tested at lower temperatures. Pemsler's important early studies<sup>34</sup> yield post-transition rates at 500°C in the range 2 to 5 mdd. His best alloys were Zr-Cr and Zr-Cr-Ni alloys with about 1.6 at. % as the highest level of alloying tested. Pemsler's alloys were not studied for hydrogen uptake. All of these "best alloys" reported by Rösler, by Greenberg, and by Pemsler were either given beta solution, quench, and alpha anneal treatments or just beta solution and quench treatments as in Greenberg's alloys.

### C. ANALYSIS OF RESULTS FOR OPTIMUM ALLOY FOR WATER REACTOR CLADDING

The alloy design experimental results (Section II-D-G) were analyzed in response to the need for increased resistance to local and general over-temperature with the alloy target criteria originally established (Section II-A). The alloy of interest had to show excellent performance at 300 and 400°C (bracketing the normal clad operating temperature) and good performance at 500°C (for resistance to over-temperature).

The results of the first experiments eliminated Nb additions from interest and prompted a detailed analysis of the Zr-Cu-Fe and Zr-Cr-Fe alloys by using the summary equations for corrosion rate and hydriding rate.<sup>35</sup> These results plus the observation of the adverse effect of Cu on 300°C hydrogen up-take, and the additional experimental results which showed excellent performance by Zr + 2.3 at. % Cr, narrowed the analysis to the Zr-Cr-Fe system.

Limits of interest for chromium content were established by considering the criteria of neutron economy, fabricability, resistance to high hydrogen content, strength, and ductility. The limits are:

<u>Lower Cr Content</u>	<u>Upper Cr Content</u>
Strength ( $>1.8$ at. % $\geq$ Zircaloy-2, see Figure 1a)	Fabricability ( $\leq 2.0$ at. %, see Section II)
	Neutron economy ( $<2.1$ at. %, see Klepfer et al. <sup>6</sup> )
	Resistance to H <sub>2</sub> ( $<2.6$ at. %, see Section II)
	Ductility ( $<2.6$ at. % $\geq$ Zircaloy-2, see Figure 1b)

In a similar manner, limits of interest for iron were reviewed:

Lower Fe Content

(Strength)

Upper Fe ContentResistance to H<sub>2</sub> (<0.3 at. %, see Section II)

Fabricability (&lt;2.0 at. %, see Section II)

Neutron economy (<2.5 at. %, see Klepfer, et al,<sup>6</sup>)

The summary equations for corrosion rate and hydriding rate were solved for compositions meeting the following requirements (which considerably better the corresponding values for Zircaloy-2):

	<u>Corrosion Rate</u> (mdd)	<u>Hydriding Rate</u> (ppm/day)
At 500°C	< 2.5	< 2.5
At 400°C	< 0.35	< 0.025
At 300°C	< 0.075	-

The regions of composition meeting these requirement are cross hatched in Figures 6a, b, and c. If the cross-hatched regions for each of the three test temperatures are superimposed, there is no common region of intersection (Figure 6d). The regions approach one another at about 2.0 to 2.3 at. % Cr and 0.1 to 0.2 at. % Fe. A point of intersection can be found if the arbitrary rates required are adjusted slightly. This point is estimated at 2.0 at. % Cr (1.15 wt. %) and 0.16 at. % Fe (0.1 wt. %).

This composition, Zr + 2.0 Cr + 0.16 Fe, is optimum with respect to corrosion resistance and hydriding rate over the entire temperature range 300 to 500°C and has over-temperature resistance superior to that of Zircaloy-2. The alloy is also within the limits of interest with respect to neutron economy, fabricability, resistance to high hydrogen content, strength, and ductility.

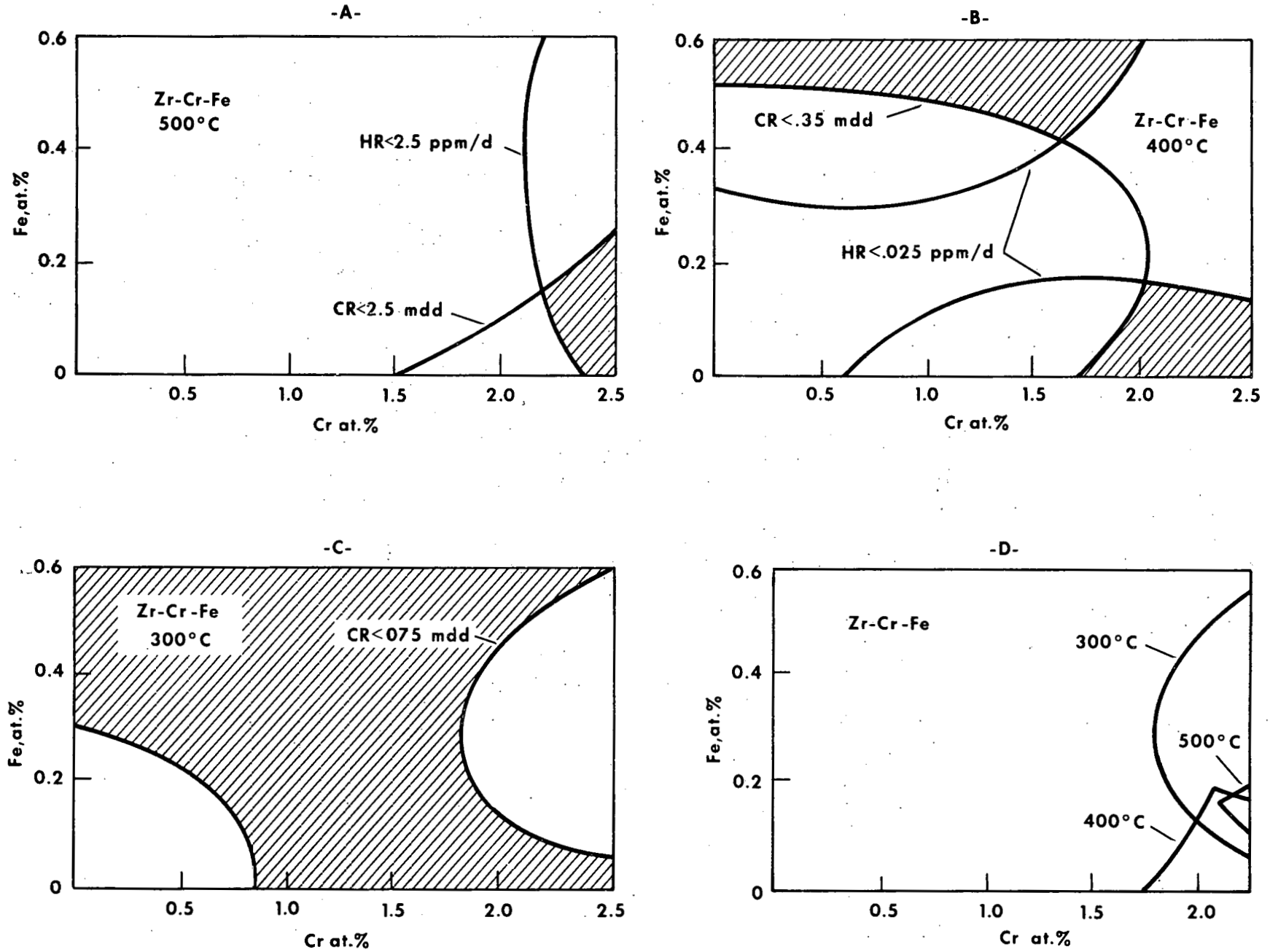


FIGURE 6. REGIONS OF COMPOSITION FOR AN ARBITRARY LEVEL OF PERFORMANCE AT VARIOUS TEMPERATURES

Klepfer<sup>5</sup> had concluded earlier that Zr-Cr binaries containing 1.6 and 2.2 at. % Cr were the only ones among 25 alloys in the Zr-Fe, Zr-V, Zr-Sb, Zr-Cr, and Zr-Nb systems that showed lower hydrogen weight gains than Zircaloy-2 at 360, 400, and 482°C in steam.

The alloy tested under the Alloy Design Study most closely approximating the optimum composition was the Zr + 2.3 at. % Cr alloy tested in the second series of experiments. Corrosion rate and hydrogen contents for this alloy (final anneal at 788°C) are compared to the best data for Zircaloy-2 below:

Long-Term Corrosion Rate, mdd

Alloy	Steam Test Temperature		
	500°C (932°F)	400°C (750°F)	300°C (572°F)
Zircaloy-2	9.6	1.36	0.074
Zr-Cr	0.8	0.28	0.067

Post-Exposure Hydrogen Content, ppm

Alloy	Exposure			
	500°C (932°F)		300°C (572°F)	
	3000 hr	4912 hr	3000 hr	6570 hr
Zircaloy-2	1563	1728	28	34
Zr-Cr	227	<< 450	7	9

From results of the mechanical property tests, it is apparent that this Zr-Cr-Fe alloy will have mechanical property values within about 10% of those for Zircaloy-2, if it receives the same heat treatment. The creep resistance of the Zr-Cr-Fe alloy is expected to be higher than that of Zircaloy-2 because of the greater volume percent second-phase dispersant. This same phase, however, will probably lead to brittle behavior at slightly lower hydrogen concentrations than for Zircaloy-2 (but after much longer times because of the much lower hydriding rates for the Zr-Cr-Fe alloy).



Fuel cladding tubes of the optimum alloy were ordered from a commercial vendor. Practical specifications of composition (in terms of weight percent) were required. Since commercial sponge Zr runs 0.08 to 0.12 wt. % Fe, the final specification for iron content was less than 0.1 wt. % (1000 ppm). By choosing a tolerance of + 10% in corrosion rate, the summary equations gave  $1.15 \pm 0.15$  wt % Cr as the specification for chromium content.

## REFERENCES

1. Douglass, D. L., "Corrosion Mechanism of Zirconium and Its Alloys: III Solute Distribution Between Corrosion Films and Zirconium Alloy Substrates," GEAP-4521 (1964).
2. Douglass, D. L., "Corrosion Mechanism of Zirconium and Its Alloys: I Diffusion of Oxygen in Zirconium Dioxide," GEAP-3999 (1962).
3. Douglass, D. L., "Oxidation Mechanism of Zirconium and Its Alloys: II Oxide Plasticity," GEAP-4473 (1964).
4. Armijo, J. S., "Hydrogen Overvoltage and Electrochemical Potentials of Zirconium and Zirconium Intermetallics," GEAP-4192 (1963).
5. Klepfer, H. H., "Hydrogen Takeup in Zirconium Binary Alloys," Corrosion, 19 (August 1963).
6. Klepfer, H. H., Douglass, D. L. and Armijo, J. S., "Specific Zirconium Alloy Design Program. First Quarterly Progress Report," GEAP-3979 (1962).
7. Klepfer, H. H., "Zirconium Alloy Design for Steam Service," GEAP-4089 (1962).
8. Gaylor, D. W., Klepfer, H. H., Antony, K. C., Nelson, W. B., Douglass, D. L., and Armijo, J. S., "Specific Zirconium Alloy Design Program. Third Quarterly Progress Report," October-December 1962, GEAP-4139.
9. Jaech, J. L., "Statistical Techniques Used in the Specific Zirconium Alloy Design Program," GEAP-4453 (1963).
10. Antony, K. C. and Jones, L. T., "Fabrication of Zirconium Alloys for Specific Zirconium Alloy Design Program," GEAP-4115 (1962).
11. Klepfer, H. H., "Zirconium-Columbium Binary Alloys for Boiling Water Reactor Use. Part I. Corrosion Resistance," J. Nucl. Matl., Vol. 9, (June 1963).
12. Klepfer, H. H., Jaech, J. L., Blood, R. E., Perrine, H. E. and Urata, M. E., "Specific Zirconium Alloy Design Program. Seventh Quarterly Progress Report," GEAP-4484 (1964).
13. Klepfer, H. H., Antony, K. C., Nelson, W. B., Douglass, D. L., and Armijo, J. S., "Specific Zirconium Alloy Design Program. Second Quarterly Progress Report," GEAP-4076 (1962).
14. Nelson, W. B., "A Controlled-Environment Steam Corrosion Facility," GEAP-4393 (1963).

15. Douglass, D. L., "The Contributions of Dispersion and Solution Strengthening in Zr-Sn-Nb Alloys," J. Nucl. Matl., 9, 222 (1963).
16. Keeler, J. H., "Tensile Characteristics of Particle-Strengthened Alloys of Zirconium with Iron," Trans. Amer. Inst. Min. Engrs., 206, 486 (1956).
17. Keeler, J. H., "Tensile Properties of Zr-Cr Alloys-Particle-Strengthening Effects," Trans. Amer. Soc. Metals, 48, 825 (1956).
18. Sawatsky, A., "The Diffusion and Solubility of Hydrogen in Alpha-Phase Zirconium-2," J. Nucl. Matl., 2, 62 (1960).
19. Klepfer, H. H., Jaech, J. L., Blood, R. E. and Douglass, D. L., "Specific Zirconium Alloy Design Program. Fifth Quarterly Progress Report," April-June 1963, GEAP-4284.
20. Marshall, R. P. and Louthan, M. R. Jr., "Tensile Properties of Zircaloy with Oriented Hydrides," in GEAP-4089 (1962).
21. Klepfer, H. H., Dunn, E. L., Blood, R. E. Douglass, D. L. and Armijo, J. S., "Specific Zirconium Alloy Design Program. Fourth Quarterly Progress Report," GEAP-4211 (1963).
22. Klepfer, H. H. and Douglass, D. L., "Factors Limiting the Use of Zirconium Alloys in Superheated Steam," ANS-ASTM Zirconium Seminar, New York, 1963.
23. Naymark, S., "Materials for Dresden and Other Boiling Water Reactors," AIME Nuclear Metallurgy Symposium, 1962.
24. Klepfer, H. H. and Spalaris, C. N., "Mechanical Behavior of Cold-Worked Nuclear Grade Zircaloy-2 Tubing," Nuclear Metallurgy, Vol. VII, AIME, New York, October 1960.
25. Nelson, R. E., "The Corrosion of Zircaloy-2 Fuel Element Cladding in a Boiling Water Reactor Environment," Proceedings of the USAEC Symposium on Zirconium Alloy Development, GEAP-4089, November 1962.
26. Pemsler, J. P., "The Corrosion of Zirconium Alloys in 900<sup>o</sup>F Steam," NMI-1208 (1958). See also NMI-1235 (1960).
27. Kass, S., "The Development of the Zircaloys," Proceedings of the USAEC Symposium on Zirconium Alloy Development, GEAP-4089, November 1962.
28. Klepfer, H. H., "Zirconium-Columbium Binary Alloys for Boiling Water Reactor Use. Part I. Corrosion Resistance," J. Nucl. Matl., 9, 1 (June 1963).
29. Kass, S. and Kirk, W. W., "The Development of Zircaloy-2," Trans. Quarterly, 55, 77 (1962).

30. Klepfer, H. H. (editor), "Proceedings of the USAEC Symposium on Zirconium Alloy Development," GEAP-4089, November 1962.
31. Klepfer, H. H., "Zirconium-Niobium Alloys for Boiling Water Reactor Service. Part I. Corrosion Resistance," J. Nucl. Matl., 9, 1 (June 1963).
32. Rösler, U., "Corrosion Resistance of Improved Zirconium Alloys in High Temperature Steam," Proceedings of the USAEC Symposium on Zirconium Alloy Development, GEAP 4089, November 1962
33. Greenberg, S., "Zirconium Alloys for Use in Superheated Steam," J. Nucl. Matl., 4, 334 (1961).
34. Pemsler, J. P., "The Corrosion of Zirconium Alloys in 900<sup>o</sup>F Steam," NMI-1208 (1958). See also NMI-1235 (1960).
35. Klepfer, H. H., Jaech, J. L., Douglass, D. L., Blood, R. E., and Perrine, H. E., "Specific Zirconium Alloy Design Program, Quarterly Progress Report No. 6," GEAP-4368 (1963).



## APPENDIX

<u>Table No.</u>	<u>Title</u>	<u>Page</u>
A-1	Corrosion Weight Gains ( $\text{mg}/\text{dm}^2$ ) . . . . .	63
A-2	Corrosion Weight Gains ( $\text{mg}/\text{dm}^2$ ) . . . . .	64
A-3	Corrosion Weight Gains ( $\text{mg}/\text{dm}^2$ ) . . . . .	65
A-4	Hydrogen Content (ppm) for Coupons . . . . .	66
A-5	Hydrogen Content (ppm) . . . . .	67
A-6	Hydrogen Content (ppm) . . . . .	68
A-7	Mechanical Test Values at Room Temperature Unexposed . . . . .	69
A-8	Mechanical Test Values at 300°C Unexposed . . . . .	70
A-9	Mechanical Test Values at 400°C Unexposed . . . . .	71
A-10	Mechanical Test Values at 500°C Unexposed . . . . .	72
A-11a	0.2% Offset Yield Strength ( $\text{kg}/\text{mm}^2$ ) and Ultimate Tensile Strength ( $\text{kg}/\text{mm}^2$ ) at 300°C . . . . .	73
A-11b	Percent Total Elongation and Percent Reduction in Area at 300°C . . . . .	74
A-12a	0.2% Offset Yield Strength ( $\text{kg}/\text{mm}^2$ ) and Ultimate Tensile Strength ( $\text{kg}/\text{mm}^2$ ) at 500°C . . . . .	75
A-12b	Percent Total Elongation and Percent Reduction in Area at 500°C . . . . .	76
A-13	Impact Energy Absorption (ft/lb) at 300°C . . . . .	77
A-14a	0.2% Offset Yield Strength ( $\text{kg}/\text{mm}^2$ ) and Ultimate Tensile Strength ( $\text{kg}/\text{mm}^2$ ) at Room Temperature . . . . .	78
A-14b	Percent Total Elongation and Percent Reduction in Area at Room Temperature . . . . .	79
A-15a	0.2% Offset Yield Strength ( $\text{kg}/\text{mm}^2$ ) and Ultimate Tensile Strength ( $\text{kg}/\text{mm}^2$ ) at Room Temperature . . . . .	80
A-15b	Percent Total Elongation and Percent Reduction in Area at Room Temperature . . . . .	81
A-16a	0.2% Offset Yield Strength ( $\text{kg}/\text{mm}^2$ ) and Ultimate Tensile Strength ( $\text{kg}/\text{mm}^2$ ) at Room Temperature . . . . .	82
A-16b	Percent Total Elongation and Percent Reduction in Area at Room Temperature . . . . .	83
A-17	Impact Energy Absorption (ft/lb) at 300°C . . . . .	84

<u>Table No.</u>	<u>Title</u>	<u>Page</u>
A-18	Impact Energy Absorption (ft/lb) at 300°C . . . . .	85
A-19	Mechanical Property Data for Zr-Cr Base Alloys. . . . .	86
A-20	Mechanical Property Data for Zr-Cu Base Alloys. . . . .	87
A-21	Steam Corrosion Weight Gain Data for Zr-Cu Base Alloys (Weight Gain, mg/dm <sup>2</sup> ). . . . .	88
A-22	Steam Corrosion Weight Gain Data for Zr-Cu Base Alloys (Weight Gain, mg/dm <sup>2</sup> ). . . . .	89
A-23	Corrosion Hydrogen Data for Zr-Cr Base Alloys . . . . .	90
A-24	Corrosion Hydrogen Data for Zr-Cu Base Alloys . . . . .	91
A-25	Effect of Fabrication Schedule on Mechanical Properties . . . . .	92

TABLE A-1. Corrosion Weight Gains (mg/dm<sup>2</sup>)

Alloy	Exposed at 300°C*																									
	375 hr	$\sigma^a$	750 hr	$\sigma^b$	1125 hr	$\sigma^c$	1500 hr	$\sigma^d$	2250 hr	$\sigma^e$	2625 hr	$\sigma^f$	3000 hr	$\sigma^g$	3570 hr	$\sigma^h$	4320 hr	$\sigma^i$	4695 hr	$\sigma^j$	5820 hr	$\sigma^k$	6570 hr	$\sigma^l$	7812 hr	$\sigma^m$
001	11.9	2.3	13.4	0.5	15.5	0.7	16.7	0.9	18.7	0.8	20.1	0.5	20.1	0.7	22.1	1.3	21.9	1.3	23.1	1.2	23.7	1.6	24.9	1.6	28.4	3.1
002	11.1	0.9	12.1	0.5	13.5	0.4	14.5	0.5	16.5	0.5	17.8	0.4	18.4	0.3	19.8	0.7	19.4	0.4	21.5	2.6	22.3	2.6	24.0	1.3	26.3	1.2
003	11.8	2.8	12.8	1.1	13.3	0.5	15.0	0.4	16.5	0.5	17.9	0.7	18.8	0.6	19.6	0.5	19.6	0.8	21.9	2.6	22.7	2.6	24.2	1.6	26.1	3.4
004	10.2	2.5	11.3	0.6	12.8	0.6	14.2	0.9	16.3	0.7	17.5	1.2	17.9	1.1	19.7	1.9	19.8	2.6	21.3	5.2	22.6	4.5	23.3	3.9	24.9	2.5
005	9.0	1.7	12.7	0.7	18.3	0.7	21.2	0.7	24.8	0.8	25.7	0.9	27.3	1.1	28.7	0.7	29.8	0.4	30.4	0.4	32.3	1.2	34.8	0.8	37.8	3.7
006	9.2	1.8	11.8	0.7	14.1	0.8	16.6	0.9	19.8	1.3	20.9	1.5	22.8	1.7	24.1	1.9	25.3	2.6	27.0	3.9	29.2	3.2	31.8	5.2	31.6	3.7
007	8.7	1.3	10.0	0.4	12.0	0.6	13.4	0.6	16.0	0.9	17.8	1.1	18.5	1.1	20.7	2.6	20.7	3.2	21.4	3.2	23.5	3.2	26.5	3.9	27.9	1.1
008	10.0	1.4	12.7	0.4	14.9	0.5	16.8	0.8	18.6	0.7	20.0	0.8	19.9	1.1	21.7	1.9	21.8	1.9	21.8	1.9	23.9	0.6	26.0	1.9	28.1	0.6
009	8.1	2.2	10.0	0.9	12.0	1.1	13.8	1.4	16.9	1.5	17.6	2.6	19.9	2.0	21.0	2.6	21.4	2.0	23.7	0.6	24.0	1.0	25.9	1.3	28.7	4.8
010	11.9	16.7	14.0	6.2	16.9	7.3	19.1	8.8	16.9	0.7	17.9	2.6	19.5	2.4	21.3	0.7	21.9	0.6	23.1	0.4	24.2	0.6	26.8	1.3	29.1	0.8
011	9.3	1.8	10.5	0.6	11.8	0.7	12.4	0.8	13.9	0.9	16.2	0.6	16.9	0.6	18.6	1.3	19.4	1.3	20.3	0.6	20.3	0.6	22.6	0.8	25.5	3.4
012	9.2	0.9	11.3	0.4	13.3	0.5	14.0	0.6	15.7	0.3	17.0	0.3	18.4	1.1	19.4	1.2	20.3	0.6	20.9	0.6	25.3	1.2	23.4	0.8	25.4	1.7
013	10.2	1.8	11.3	0.4	12.2	0.7	13.3	0.6	14.6	0.7	16.0	0.5	17.5	0.6	18.1	0.8	18.5	2.9	19.4	1.9	19.8	1.3	21.3	1.3	23.1	0.5
014	12.1	1.8	15.9	0.6	20.0	1.3	23.6	0.7	28.9	1.1	30.6	0.7	31.0	1.8	32.4	1.6	32.6	0.8	35.3	1.9	39.5	3.2	43.7	4.5	47.4	5.8
015	10.1	1.4	11.6	0.5	13.6	0.8	14.9	0.6	17.1	0.8	17.9	0.3	18.7	0.5	19.7	0.3	19.8	0.6	20.7	1.9	21.8	1.9	23.1	2.6	24.0	1.1
016	8.2	0.4	8.6	0.6	10.4	0.3	11.5	0.6	13.3	0.4	15.6	0.6	17.2	0.5	17.8	0.5	18.2	4.8	20.2	1.3	21.0	1.3	24.1	1.3	25.9	3.4
017	11.1	1.4	12.3	0.4	13.8	0.5	14.9	0.4	17.2	0.4	18.6	0.5	19.6	0.6	21.0	0.6	21.5	1.0	21.5	1.0	22.6	0.8	27.9	4.5	27.3	2.8
018	9.0	2.2	10.8	0.4	12.3	0.4	13.5	0.5	14.7	0.5	15.3	0.5	16.4	0.5	17.3	1.2	17.4	2.0	19.0	2.6	19.4	2.6	22.7	4.5	22.1	1.8
019	10.2	1.1	10.9	0.6	12.9	0.9	14.6	0.8	16.8	0.8	18.2	0.6	18.6	0.6	20.0	1.9	19.7	1.9	19.7	1.9	20.1	1.9	21.6	1.2	23.6	1.1
020	11.2	0.9	13.0	0.3	16.3	0.7	19.3	0.4	24.0	1.1	25.1	0.5	27.3	0.8	28.5	1.0	29.5	0.8	31.3	0.6	33.5	1.6	35.9	1.2	40.5	2.8
021	14.3	5.0	17.0	0.5	21.0	0.7	24.7	0.7	30.3	0.5	33.7	0.7	34.9	1.2	37.6	1.9	40.4	2.6	43.1	2.4	48.8	3.9	54.1	3.2	60.9	6.4
022	10.3	1.4	11.2	0.4	12.8	0.7	15.0	0.8	17.8	1.4	20.6	0.9	23.8	2.7	27.5	4.1	31.5	6.4	33.2	7.3	38.0	10.1	42.2	11.6	53.1	22.7
023	15.2	1.4	20.2	0.4	30.5	0.9	39.4	1.6	53.7	1.8	61.0	1.8	61.4	8.1	65.2	10.6	69.6	8.1	75.8	9.7	88.7	15.7	99.6	17.3	112.8	43.0
024	7.5	1.2	8.5	0.3	10.8	0.5	13.2	0.9	15.4	1.1	15.5	1.1	16.0	1.4	17.0	1.3	17.3	1.6	17.3	1.6	17.6	1.9	19.2	2.6	21.1	0.1
025	5.6	1.8	5.9	0.5	7.4	0.7	8.3	0.7	9.6	0.5	11.3	0.6	12.6	0.9	13.7	1.2	14.1	1.6	14.5	1.6	15.4	1.3	17.9	1.3	20.3	1.5
026	13.7	1.4	15.5	0.5	19.1	1.1	21.4	1.0	25.0	1.3	26.5	1.5	27.0	1.2	29.5	3.2	30.3	3.2	30.9	3.2	31.8	2.8	33.3	3.2	36.9	3.4
027	6.8	1.7	7.7	0.2	8.9	0.5	9.9	0.3	11.7	0.4	13.9	1.0	14.3	0.8	14.9	0.6	14.9	0.6	16.2	3.2	18.4	1.9	20.3	1.9	23.0	3.4
028	4.6	1.4	5.0	0.5	6.1	0.4	6.4	0.3	7.6	0.4	8.6	0.3	9.6	0.3	10.4	0.6	11.2	0.8	11.5	0.8	12.1	0.4	14.0	1.6	17.2	2.9
029	9.2	2.7	11.1	0.3	13.1	0.4	14.3	0.4	16.7	0.5	18.1	0.4	19.0	0.5	19.9	1.2	20.4	0.5	22.2	1.9	22.2	1.9	23.6	0.8	26.8	4.2
030	10.7	1.8	11.9	0.3	13.7	0.4	15.1	0.4	16.4	0.5	17.7	0.3	19.2	0.5	20.7	0.7	21.2	0.6	22.5	1.9	23.1	1.9	24.2	0.8	27.7	5.7
031	9.1	0.9	10.8	0.5	12.6	0.6	14.3	0.7	16.8	0.8	17.8	1.1	18.4	0.8	19.7	1.3	19.5	1.3	21.1	3.9	21.8	3.2	24.0	1.3	26.1	1.2
032	10.5	0.9	11.3	0.5	13.0	0.6	14.1	0.5	15.8	0.6	17.7	0.8	18.5	1.1	18.9	0.9	19.2	1.2	19.9	1.9	21.1	1.3	22.8	1.9	24.6	1.9

\* All values represent the average value of: a = 16 specimens; b = 15 specimens; c = 14 specimens; d = 13 specimens; e = 10 specimens; f = 7 specimens; g = 8 specimens; h = 5 specimens; i = 4 specimens; j = 4 specimens; k = 4 specimens; l = 4 specimens; m = 3 specimens.



TABLE A-2. Corrosion Weight Gains (mg/dm<sup>2</sup>)

Alloy	Exposed at 400°C*															
	175 hr	$\sigma^a$	375 hr	$\sigma^b$	750 hr	$\sigma^c$	1125 hr	$\sigma^d$	1500 hr	$\sigma^e$	2250 hr	$\sigma^f$	3000 hr	$\sigma^g$	3578 hr	$\sigma^h$
001	20.8	1.8	28.8	1.4	49.0	2.9	78.2	6.6	96.0	10.1	110.9	8.7	109.8	17.2	105.8	16.1
002	20.3	1.8	26.4	0.3	33.8	0.6	40.5	0.9	46.2	2.8	57.8	5.2	73.3	6.8	87.8	8.9
003	20.1	2.3	25.5	0.6	31.4	0.6	37.3	0.7	42.6	1.2	52.0	1.7	63.3	1.3	70.3	2.6
004	20.7	1.7	27.4	0.7	36.2	0.9	43.2	1.3	50.6	1.8	63.7	4.1	80.0	3.9	101.2	5.2
005	27.1	2.2	34.5	0.7	44.2	0.9	52.2	1.8	63.0	2.5	80.6	2.5	90.8	2.9	102.3	2.1
006	30.9	2.7	42.6	0.9	60.6	0.9	73.2	1.3	84.1	1.3	100.6	3.6	118.7	3.2	133.8	1.9
007	26.3	2.2	33.8	0.6	46.3	1.1	57.1	1.5	67.2	2.3	83.9	2.8	104.8	2.9	123.0	2.6
008	26.2	2.9	35.3	0.7	48.3	2.2	59.4	2.0	71.0	4.8	100.0	4.7	118.6	12.2	141.1	15.8
009	27.6	1.4	37.8	0.6	54.1	1.6	64.7	1.2	75.6	1.3	100.7	4.6	129.4	8.9	160.4	14.8
010	24.3	1.3	30.4	0.4	38.5	1.1	48.1	1.4	56.9	1.8	71.2	1.8	83.7	1.4	94.9	1.9
011	25.6	8.1	33.3	4.1	44.4	5.1	51.8	4.6	60.0	5.4	72.8	7.3	76.1	1.9	89.2	1.3
012	21.0	2.6	27.4	0.5	36.0	1.1	52.1	1.0	89.2	2.1	159.6	4.9	194.2	34.6	205.7	45.8
013	19.9	1.2	26.5	0.5	32.1	0.8	36.7	0.6	39.8	0.5	46.0	1.0	52.6	1.5	58.0	0.6
014	39.1	3.4	53.3	1.5	76.9	1.7	92.8	2.4	107.9	2.3	132.7	3.3	148.2	5.9	162.9	11.1
015	22.8	1.3	28.9	0.5	35.9	0.6	43.3	0.8	50.3	2.1	61.6	1.9	73.3	2.1	85.9	3.9
016	25.2	1.7	35.5	0.7	52.5	0.7	69.9	1.7	90.8	2.0	129.1	4.8	163.4	8.0	194.6	3.4
017	18.5	3.9	25.1	1.5	31.9	0.8	36.4	1.8	40.3	2.9	49.6	2.4	55.5	2.9	59.3	3.0
018	21.8	1.4	27.0	0.4	32.1	0.6	36.6	1.0	40.8	1.4	48.5	3.3	51.6	1.4	56.4	0.8
019	16.9	1.4	23.3	0.4	30.3	0.8	35.3	0.7	39.5	0.8	47.2	0.9	54.5	2.5	60.2	2.7
020	26.5	1.8	35.7	0.6	50.7	1.6	62.4	1.1	72.8	3.3	96.6	4.9	121.6	5.3	137.3	8.8
021	40.0	3.2	57.6	1.4	83.7	1.7	100.7	3.0	121.2	4.9	166.1	4.8	225.0	13.3	260.1	13.6
022	24.1	2.3	33.0	0.4	52.1	0.6	67.9	1.6	83.9	2.3	119.6	4.2	183.2	37.8	229.5	48.2
023	37.1	3.1	56.7	1.1	88.5	1.4	110.5	2.4	128.2	1.3	158.4	2.0	174.4	8.1	191.1	11.5
024	18.0	1.4	25.0	0.5	31.7	0.9	38.2	1.0	43.2	0.9	51.9	1.2	60.2	1.1	66.3	1.3
025	31.7	2.2	38.8	0.8	46.6	0.8	52.3	0.7	56.8	0.7	66.2	1.1	73.4	3.5	78.9	5.1
026	52.6	5.9	59.0	1.8	65.3	1.9	68.7	1.5	72.5	0.6	76.8	1.4	84.5	2.6	87.4	3.2
027	23.2	5.9	31.2	0.6	43.6	1.7	53.2	0.9	61.8	1.1	78.0	1.9	103.7	4.8	120.3	4.8
028	14.4	4.3	21.2	1.3	29.4	1.3	37.3	1.5	45.2	2.8	66.9	4.5	91.2	7.5	111.7	3.6
029	22.1	1.8	28.4	0.7	36.4	0.7	43.0	1.1	47.7	1.6	57.7	0.7	67.5	1.7	73.8	2.2
030	21.4	0.9	27.1	0.4	34.1	1.4	40.2	1.6	44.1	1.0	54.7	1.6	58.9	3.6	62.7	5.3
031	22.2	5.5	27.9	1.8	36.0	1.7	43.7	1.9	52.3	1.9	67.4	3.6	99.7	24.6	117.4	27.4
032	25.3	2.7	33.6	0.8	41.8	0.5	61.1	2.6	82.3	1.9	126.7	5.1	161.7	11.2	195.5	9.7

\*All values represent the average value of: a = 16 specimens; b = 15 specimens;  
c = 14 specimens; d = 13 specimens; e = 12 specimens; f = 9 specimens;  
g = 8 specimens; h = 5 specimens.

TABLE A-3. Corrosion Weight Gains (mg/dm<sup>2</sup>)

Alloy	Exposed at 500°C*																							
	75 hr	$\sigma_a$	175 hr	$\sigma_b$	375 hr	$\sigma_c$	750 hr	$\sigma_d$	1125 hr	$\sigma_e$	1500 hr	$\sigma_f$	3000 hr	$\sigma_g$	3792 hr	$\sigma_h$	4542 hr	$\sigma_i$	4917 hr	$\sigma_j$	5667 hr	$\sigma_k$	6792 hr	$\sigma_l$
001	53.2	2.8	79.4	1.7	138.1	3.8	236.7	9.0	304.2	6.7	367.7	10.8	682.4	21.7	821.3	8.4	943.5	3.2	1015.4	23.7	1135.7	37.9	1318.0	16.9
002	52.1	7.3	74.0	2.4	138.3	3.7	246.8	5.2	352.6	9.0	429.3	16.8	774.5	41.1	971.0	10.3	-	-	-	-	-	-	-	-
003	46.2	3.7	68.1	2.0	126.1	10.0	233.7	11.9	327.4	11.4	395.1	16.7	746.1	35.6	917.5	10.3	-	-	-	-	-	-	-	-
004	50.0	4.1	74.3	1.6	143.3	5.5	263.7	8.2	357.1	10.0	442.6	14.2	961.6	20.8	974.8	24.2	-	-	-	-	-	-	-	-
005	64.7	3.7	91.0	1.6	148.2	2.9	216.4	2.9	256.6	5.2	297.9	4.9	508.6	12.0	584.2	13.6	641.7	4.5	670.5	2.6	757.4	17.1	836.0	44.1
006	66.8	25.4	105.2	2.2	197.1	7.0	302.7	10.4	366.8	10.0	442.0	8.4	731.6	10.6	861.4	12.3	-	-	-	-	-	-	-	-
007	63.9	4.5	93.4	2.2	191.4	10.8	306.5	14.1	396.0	12.1	475.2	13.3	885.7	23.9	1077.4	45.8	-	-	-	-	-	-	-	-
008	60.1	4.3	99.4	4.0	223.6	11.5	372.9	13.1	478.3	19.5	582.1	22.5	1056.6	42.7	1285.0	112.3	-	-	-	-	-	-	-	-
009	71.1	9.1	114.6	6.6	258.0	12.9	411.0	17.1	516.4	21.7	627.1	24.6	1061.9	59.7	1264.8	45.2	-	-	-	-	-	-	-	-
010	58.9	6.8	82.9	2.6	168.3	5.4	254.2	5.0	371.5	7.8	434.9	11.5	784.2	26.2	963.8	38.1	-	-	-	-	-	-	-	-
011	56.2	3.7	80.6	2.9	146.7	5.9	251.8	7.1	332.6	9.4	408.9	11.2	741.4	30.7	862.5	62.0	-	-	-	-	-	-	-	-
012	55.2	4.5	71.3	6.7	147.8	6.7	251.3	21.7	360.6	21.8	438.0	31.8	806.6	55.6	1018.8	16.8	-	-	-	-	-	-	-	-
013	46.7	1.8	60.7	9.6	96.6	2.8	175.4	4.7	226.3	3.2	276.0	6.2	496.4	11.7	585.0	14.2	640.7	14.8	689.7	13.6	764.9	0.9	875.0	1.4
014	84.2	25.5	123.2	8.7	214.5	13.3	323.1	21.8	369.9	28.6	422.0	15.3	724.8	18.2	866.2	12.3	961.6	15.5	1018.2	11.6	1144.5	212.2	1289.6	214.5
015	57.2	3.2	82.3	1.6	175.9	3.8	305.1	4.3	390.4	6.7	458.8	11.6	855.4	21.4	1038.5	20.0	-	-	-	-	-	-	-	-
016	70.5	9.5	134.9	5.7	296.6	24.2	502.5	26.0	630.6	30.3	773.9	29.8	1440.0	39.9	1709.7	70.4	-	-	-	-	-	-	-	-
017	51.0	5.0	64.7	4.0	90.8	3.5	137.9	3.0	180.1	6.4	206.5	8.7	377.5	18.7	450.7	15.5	525.2	22.6	558.2	12.3	635.3	89.4	724.2	112.6
018	47.2	3.4	61.0	4.6	85.0	3.5	113.8	2.5	145.5	9.0	176.8	17.6	318.4	45.4	430.5	38.1	481.3	43.9	520.1	42.6	585.4	45.0	679.8	31.0
019	48.7	9.5	67.8	2.1	100.2	2.6	146.6	3.4	203.1	7.2	261.3	14.1	523.7	31.3	602.4	6.5	670.9	4.5	732.1	14.8	818.9	142.3	932.9	154.4
020	64.7	5.4	94.5	3.0	162.5	5.3	256.7	5.4	321.8	7.7	382.0	9.0	661.7	33.7	818.3	53.6	950.0	112.9	998.2	121.3	1100.7	104.4	1263.4	93.0
021	88.8	5.9	143.0	3.9	274.9	7.0	435.7	11.9	544.1	13.5	661.3	15.2	1106.3	29.3	1308.4	40.0	-	-	-	-	-	-	-	-
022	65.8	6.8	116.7	3.4	242.9	11.5	403.7	20.8	515.9	26.7	605.2	30.7	1093.0	34.2	1261.7	18.7	-	-	-	-	-	-	-	-
023	84.0	5.0	136.0	3.7	240.5	5.8	370.3	7.8	459.6	9.5	547.0	9.1	942.9	16.7	1105.3	32.3	-	-	-	-	-	-	-	-
024	56.0	4.6	74.2	2.3	106.8	5.2	147.7	14.8	195.6	19.0	253.4	6.1	499.6	54.3	633.5	9.0	707.9	3.2	774.8	2.6	852.5	205.8	951.0	234.8
025	-	-	-	-	-	-	-	-	-	-	-	-	-	-	-	-	-	-	-	-	-	-	-	-
026	111.0	7.7	128.9	2.5	157.3	3.2	189.4	4.5	217.3	5.3	243.8	4.9	377.2	9.9	414.6	43.6	476.0	14.8	504.5	9.0	537.2	41.1	623.9	31.8
027	64.9	7.7	97.2	2.7	184.2	15.0	320.2	15.6	424.2	19.9	523.5	28.8	1000.6	33.8	1236.3	21.3	1409.7	183.9	1487.2	188.5	1661.1	152.5	1871.2	89.2
028	43.7	4.3	67.9	2.9	140.8	12.0	248.6	17.5	333.3	11.5	409.4	23.0	748.1	78.2	806.6	57.3	898.6	3.2	959.5	75.4	1055.0	77.8	1185.4	84.8
029	49.7	3.2	68.0	1.6	109.0	4.0	189.7	6.1	262.7	6.3	310.3	11.3	589.9	9.3	738.7	9.7	822.1	7.7	912.8	48.5	1009.4	44.1	1173.6	27.9
030	51.6	4.8	72.7	1.9	115.6	4.4	201.5	3.1	263.2	6.0	321.2	12.2	584.6	9.6	706.8	7.1	782.1	16.8	857.9	116.9	938.9	130.4	1087.8	138.7
031	54.4	5.9	78.1	2.2	151.7	3.3	255.9	5.0	330.0	6.6	397.0	8.3	698.4	22.6	841.7	14.2	-	-	-	-	-	-	-	-
032	87.5	5.7	135.7	6.3	252.8	6.0	367.1	7.3	471.2	9.0	581.7	12.9	1406.3	37.8	1793.8	43.9	-	-	-	-	-	-	-	-

\* All values represent the average value of: a = 16 specimens; b = 15 specimens; c = 14 specimens; d = 13 specimens; e = 12 specimens; f = 9 specimens; g = 6 specimens; h = 3 specimens; i = 2 specimens; j = 2 specimens; k = 2 specimens; l = 2 specimens.

TABLE A-4. Hydrogen Content (ppm) for Coupons

Alloy	Exposed at 300°C*					
	0 hr	2250 hr	2625 hr	3000 hr	3570 hr	6570 hr
001	3	29	27	25	25	32
002	13	50	49	44	37	23
003	9	42	44	43	42	41
004	13	30	28	29	31	43
005	5	40	13	37	39	34
006	24	28	8	25	29	33
007	34	50	54	53	57	38
008	34	24	25	30	35	22
009	20	35	41	46	54	47
010	2	40	38	39	40	26
011	12	31	38	46	50	19
012	25	46	48	47	44	64
013	8	51	52	42	34	52
014	12	22	21	22	21	30
015	14	46	41	36	36	59
016	8	15	14	14	14	22
017	9	28	30	32	36	26
018	9	29	33	34	35	49
019	7	27	28	26	27	43
020	24	51	55	55	53	74
021	10	24	26	24	25	29
022	6	27	29	27	25	42
023	10	47	46	48	46	32
024	13	30	33	32	31	42
025	13	19	14	15	16	18
026	12	63	70	60	56	80
027	23	21	22	20	21	19
028	12	34	29	25	23	33
029	5	22	22	18	19	20
030	16	39	42	40	38	31
031	7	40	35	29	27	31
032	27	31	34	28	24	34

\* In each case, the value reported is the average of at least two duplicate analyses on the same coupon.

TABLE A-5. Hydrogen Content (ppm)

Alloy	Exposed at 400°C*								
	0 hr	175 hr	375 hr	750 hr	1125 hr	1500 hr	2250 hr	3000 hr	3578 hr
001	3	36	41	46	57	72	69	71	67
002	13	48	45	48	57	61	71	54	47
003	0	54	64	62	61	61	60	64	66
004	13	47	43	47	46	50	66	67	77
005	5	54	93	59	70	68	65	84	81
006	24	37	42	50	50	55	61	62	59
007	34	78	81	79	74	77	89	100	107
008	34	40	42	44	47	61	73	96	125
009	20	72	64	77	77	82	92	101	104
010	2	48	53	54	56	60	75	84	75
011	12	56	57	62	60	52	44	37	34
012	25	61	60	68	84	261	462	559	574
013	8	40	47	56	65	68	69	70	63
014	12	32	36	45	47	53	68	79	87
015	14	51	57	57	57	58	63	71	80
016	8	30	34	38	45	63	89	93	113
017	9	51	50	37	33	28	32	33	41
018	9	34	48	46	53	53	78	52	56
019	7	32	36	34	36	40	37	42	44
020	24	65	72	83	96	117	114	173	203
021	10	38	40	45	50	59	69	87	101
022	6	48	54	58	60	62	78	85	107
023	10	51	52	56	71	86	104	120	151
024	13	31	25	27	28	30	30	31	31
025	13	31	31	31	31	30	29	30	31
026	12	94	102	117	116	124	126	138	140
027	23	19	21	21	23	23	32	32	34
028	12	23	27	35	43	46	51	46	47
029	5	35	35	39	45	45	42	38	39
030	16	43	44	36	40	39	39	42	46
031	7	42	51	47	53	55	62	62	62
032	27	22	28	27	34	46	69	75	91

\* In each case, the value reported is the average of at least two duplicate analyses on the same coupon.

TABLE A-6. Hydrogen Content (ppm)

Alloy	Exposed at 500°C*											
	0 hr	75 hr	175 hr	375 hr	750 hr	1125 hr	1500 hr	3000 hr	3792 hr	4542 hr	4917 hr	6792 hr
001	3	109	136	186	237	379	392	752	-	1064	-	1476
002	13	73	101	161	212	324	327	601	671	-	-	-
003	9	108	125	203	275	433	440	910	852	-	-	-
004	13	88	113	221	285	396	444	780	791	-	-	-
005	5	99	136	165	196	246	235	420	-	-	360	572
006	24	48	59	137	162	231	247	429	440	-	-	-
007	34	56	85	176	221	316	350	524	557	-	-	-
008	34	83	138	327	406	395	458	591	660	-	-	-
009	20	68	98	212	256	345	382	567	681	-	-	-
010	2	70	102	247	324	393	410	660	875	-	-	-
011	12	64	68	116	171	256	271	501	513	-	-	-
012	25	97	122	221	261	406	433	734	853	-	-	-
013	8	77	81	122	179	250	281	496	-	-	637	632
014	12	77	92	165	166	181	150	284	-	-	522	-
015	14	105	134	272	348	453	463	691	830	-	-	-
016	8	83	154	355	511	646	499	1042	1233	-	-	-
017	9	46	52	64	75	114	77	244	-	-	575	-
018	9	67	76	85	109	153	200	439	-	-	497	703
019	7	67	74	81	114	162	165	351	-	-	415	-
020	24	92	126	194	258	441	468	626	969	-	-	1069
021	10	77	97	176	227	349	526	963	1051	-	-	-
022	6	105	145	259	368	490	500	818	841	-	-	-
023	10	101	146	316	453	566	623	1051	1196	-	-	-
024	13	48	48	58	74	128	174	470	-	-	627	-
025	13	-	-	-	-	-	-	-	-	-	-	-
026	12	181	201	200	240	293	319	494	-	-	844	-
027	23	41	46	84	152	233	206	607	1159	-	-	1348
028	12	35	49	121	109	227	232	506	-	744	-	-
029	5	73	89	121	151	237	213	453	-	632	-	-
030	16	93	107	144	230	245	267	512	-	791	-	-
031	7	88	116	193	231	413	413	647	791	-	-	-
032	27	119	183	352	422	591	644	1563	1726	-	-	-

\* In each case, the value reported is the average of at least two duplicate analyses on the same coupon.

TABLE A-7. Mechanical test Values at Room Temperature Unexposed\*

<u>Alloy</u>	<u>0.2% Offset Yield Strength, kg/mm<sup>2</sup></u>	<u>Ultimate Tensile Strength, kg/mm<sup>2</sup></u>	<u>Percent Total Elongation</u>	<u>Percent Reduction in Area</u>
001	46.2	60.0	12.3	32.3
002	55.4	73.2	13.7	27.0
003	58.8	79.8	12.5	34.5
004	51.1	70.7	15.0	38.6
005	70.4	95.3	3.8	11.7
006	71.3	96.0	7.3	22.7
007	67.0	89.8	10.1	30.5
008	73.2	96.3	7.8	31.0
009	89.5	116.6	0.9	10.8
010	66.8	93.1	6.7	34.2
011	59.0	79.8	10.1	29.4
012	64.6	91.8	9.1	16.0
013	50.5	66.2	14.6	34.0
014	41.2	59.9	12.0	38.7
015	59.7	84.0	9.6	25.3
016	65.3	85.0	11.7	35.1
017	34.5	47.2	20.7	43.4
018	47.8	65.8	14.4	31.0
019	49.8	64.2	13.3	39.1
020	48.3	63.2	13.8	42.9
021	45.4	59.5	16.7	47.1
022	62.8	82.4	13.8	47.8
023	44.9	53.1	19.9	60.2
024	42.0	55.4	15.4	37.0
025	31.4	39.5	29.3	50.4
026	38.9	51.3	19.1	41.1
027	35.1	43.2	25.9	51.5
028	50.1	67.0	13.0	43.0
029	46.2	64.0	10.1	31.3
030	53.5	70.2	13.0	28.1
031	56.4	71.5	11.5	27.3
032	38.9	49.0	17.2	30.1

\* Values reported represent the average of two tests.

TABLE A-8. Mechanical Test Values at 300°C Unexposed\*

<u>Alloy</u>	<u>0.2% Offset Yield Strength, kg/mm<sup>2</sup></u>	<u>Ultimate Tensile Strength, kg/mm<sup>2</sup></u>	<u>Percent Total Elongation</u>	<u>Percent Reduction in Area</u>
001	31.2	36.6	18.7	61.1
002	32.8	40.5	19.5	47.2
003	38.7	50.2	16.6	65.0
004	31.8	41.0	17.6	61.6
005	43.5	59.6	10.2	38.1
006	57.7	71.1	10.5	43.3
007	46.8	59.5	17.7	46.6
008	54.7	71.1	12.5	51.1
009	75.9	94.2	5.1	12.0
010	61.7	78.2	8.5	43.8
011	42.3	53.5	15.4	53.3
012	53.3	64.9	9.6	22.4
013	29.1	35.6	18.2	50.6
014	30.3	35.9	18.8	57.6
015	45.0	58.1	14.9	62.0
016	43.1	49.8	20.2	64.3
017	21.7	25.9	27.8	63.1
018	33.8	39.4	18.0	55.4
019	28.2	33.1	24.0	71.0
020	31.7	37.4	16.6	58.9
021	31.3	35.2	21.7	75.1
022	44.1	50.9	17.2	63.6
023	27.9	31.9	21.1	77.5
024	27.9	31.8	21.2	65.5
025	19.0	20.2	27.3	76.5
026	23.3	27.0	22.8	54.5
027	23.0	25.2	26.0	73.1
028	32.6	36.8	16.4	55.4
029	32.4	38.1	10.9	48.6
030	31.5	38.4	19.6	54.9
031	43.9	51.4	12.7	36.8
032	25.5	28.4	22.6	52.2

\* Values reported represent the average of two tests.

TABLE A-9. Mechanical Test Values at 400°C Unexposed\*

Alloy	0.2% Offset Yield Strength, kg/mm <sup>2</sup>	Ultimate Tensile Strength, kg/mm <sup>2</sup>	Percent Total Elongation	Percent Reduction in Area
001	27.9	32.6	19.4	63.7
002	28.7	35.2	20.3	57.7
003	34.1	43.1	18.2	60.7
004	31.1	35.7	20.4	63.4
005	44.4	54.9	10.7	40.8
006	44.9	58.6	13.6	33.1
007	44.9	53.2	17.5	52.1
008	47.5	62.2	11.0	48.5
009	64.7	84.6	10.6	27.7
010	47.3	64.9	10.5	43.9
011	43.1	51.7	17.5	56.2
012	45.2	53.2	12.9	39.4
013	28.0	51.3	21.1	58.7
014	29.5	33.4	18.0	59.9
015	40.2	48.3	16.6	48.3
016	32.8	38.6	20.9	64.2
017	20.5	23.1	28.0	71.6
018	31.1	34.9	24.1	62.6
019	26.3	29.3	23.1	70.6
020	29.3	33.0	17.0	52.4
021	29.1	31.1	21.3	65.8
022	43.8	51.9	11.3	37.2
023	27.7	29.5	20.4	71.1
024	25.5	28.3	24.2	72.0
025	18.8	18.9	25.7	73.6
026	22.1	23.7	22.4	55.3
027	22.2	23.9	21.4	68.4
028	29.9	33.8	16.4	48.2
029	27.2	30.0	16.6	62.3
030	29.5	35.0	20.6	53.8
031	42.7	49.7	12.9	50.2
032	24.6	26.9	21.5	56.8

\* Values reported represent the average of two tests.



TABLE A-10. Mechanical Test Values at 500°C Unexposed\*

<u>Alloy</u>	<u>0.2% Offset Yield Strength, kg/mm<sup>2</sup></u>	<u>Ultimate Tensile Strength, kg/mm<sup>2</sup></u>	<u>Percent Total Elongation</u>	<u>Percent Reduction in Area</u>
001	24.1	26.4	27.3	75.8
002	24.8	28.4	32.7	74.8
003	29.9	35.2	25.4	80.3
004	25.3	29.1	34.1	81.7
005	32.9	40.0	23.5	97.2
006	31.3	38.0	32.6	97.9
007	35.2	42.1	27.7	87.4
008	41.0	52.7	20.6	90.4
009	43.1	59.0	14.0	96.4
010	33.9	42.4	26.2	90.1
011	31.1	38.9	34.6	97.9
012	35.2	42.3	36.2	70.7
013	22.4	25.1	39.0	77.0
014	23.5	27.7	42.7	74.9
015	30.5	35.4	36.2	72.8
016	26.2	30.7	31.0	81.1
017	16.1	18.1	47.1	87.0
018	25.2	28.0	24.3	60.1
019	20.6	25.1	33.9	85.6
020	24.3	28.0	30.0	69.6
021	24.4	27.8	33.1	83.2
022	35.7	42.6	17.9	76.2
023	24.0	25.8	23.8	74.9
024	20.3	22.7	31.2	79.3
025	13.8	15.0	47.2	89.6
026	16.4	18.3	28.4	65.5
027	17.1	19.0	40.8	83.3
028	26.0	28.9	34.5	59.2
029	20.5	24.6	41.7	83.3
030	24.6	28.4	33.5	78.2
031	33.2	40.0	24.6	62.9
032	20.9	22.2	35.6	75.5

\*Values reported represent the average of two tests.

TABLE A-11a. 0.2% Offset Yield Strength (YS) ( $\text{kg}/\text{mm}^2$ ) and Ultimate Tensile Strength (UTS) ( $\text{kg}/\text{mm}^2$ ) at  $300^\circ\text{C}$

Alloy	Exposed at $300^\circ\text{C}^*$							
	0 hr		1500 hr		2250 hr		3000 hr	
	YS	UTS	YS	UTS	YS	UTS	YS	UTS
001	31.2	36.6	31.0	37.6	31.2	38.9	33.2	40.7
002	32.8	40.5	31.5	38.5	29.3	37.6	28.6	37.4
003	38.7	50.2	40.8	51.7	38.9	54.1	36.6	54.6
004	31.8	41.0	31.9	39.4	30.9	39.0	30.9	40.0
005	43.5	59.6	48.6	62.6	43.9	62.2	47.6	62.4
006	57.7	71.1	53.7	71.1	57.0	80.8	53.5	66.7
007	46.8	59.5	42.9	55.9	46.6	57.9	50.2	63.2
008	54.7	71.1	55.4	76.3	52.2	69.9	56.9	71.5
009	75.9	94.2	67.2	88.5	75.3	96.4	68.9	82.8
010	61.7	78.2	51.7	66.3	46.3	64.6	42.0	62.6
011	42.3	53.5	49.1	59.8	49.3	62.1	56.6	16.6
012	53.3	64.9	46.8	61.5	50.7	63.2	48.8	60.5
013	29.1	35.6	28.1	35.1	27.8	34.8	27.6	34.5
014	30.3	35.9	26.7	37.2	32.1	38.4	31.5	41.6
015	45.0	58.1	35.8	46.8	38.9	48.5	40.9	52.0
016	43.1	49.8	36.0	43.4	36.4	46.0	34.6	43.0
017	21.7	25.9	21.1	25.3	19.8	25.8	21.1	25.4
018	33.8	39.4	31.1	37.5	31.0	37.0	29.8	36.3
019	28.2	33.1	27.2	31.2	28.1	31.9	27.7	32.1
020	31.7	37.4	30.7	35.4	30.6	35.6	30.2	35.9
021	31.3	35.2	28.7	34.8	26.9	34.5	29.9	35.6
022	44.1	50.9	42.5	54.8	42.2	53.1	42.0	48.0
023	27.9	31.9	27.7	31.2	27.2	30.7	26.6	31.0
024	27.9	31.8	27.6	31.6	27.5	31.9	28.1	32.2
025	19.0	20.2	18.6	21.5	18.0	20.4	17.6	20.2
026	23.3	27.0	21.4	26.0	21.9	25.4	22.4	26.0
027	23.0	25.2	22.1	25.4	21.6	25.1	21.5	25.4
028	32.6	36.8	33.1	37.6	31.1	36.6	30.1	34.5
029	32.4	38.1	25.0	31.5	23.8	29.0	23.8	28.5
030	31.5	38.4	30.9	40.1	31.7	40.1	33.8	40.1
031	43.9	51.4	50.6	58.5	46.6	55.0	41.8	53.7
032	25.5	28.4	25.3	28.5	24.9	29.2	25.2	29.3

\* Values reported for 0 hr represent the average of two tests. All other values reported are based on one test.

TABLE A-11b. Percent Total Elongation (Elong) and Percent Reduction in Area (RA) at 300°C

Alloy	Exposed at 300°C*							
	0 hr		1500 hr		2250 hr		3000 hr	
	Elong	RA	Elong	RA	Elong	RA	Elong	RA
001	18.7	61.1	14.7	50.8	15.9	55.1	17.8	59.9
002	19.5	47.2	16.6	46.0	18.3	92.5	15.9	50.9
003	16.6	65.0	14.2	58.8	15.6	58.7	14.2	49.4
004	17.6	61.6	18.1	59.9	18.1	59.8	19.7	54.6
005	10.2	38.1	9.3	31.3	8.8	31.0	6.8	29.7
006	10.5	43.3	11.2	46.5	5.7	23.2	11.8	58.2
007	17.7	46.6	18.0	55.7	18.1	55.4	17.2	58.6
008	12.5	51.1	10.4	55.0	11.5	48.6	9.1	54.3
009	5.1	12.0	3.3	14.0	5.2	23.2	1.7	8.9
010	8.5	43.8	9.0	48.1	12.5	51.5	10.9	53.4
011	15.4	53.3	12.8	52.2	15.3	59.8	6.6	34.1
012	9.6	22.4	9.3	26.0	10.7	38.0	10.3	34.1
013	18.2	50.6	19.1	46.8	18.8	43.1	15.9	39.8
014	18.8	57.6	16.7	54.3	14.0	52.1	13.6	58.7
015	14.9	62.0	16.7	51.2	15.6	56.3	14.2	52.5
016	20.2	64.3	20.0	61.5	21.8	68.5	18.6	62.7
017	27.8	63.1	26.7	56.3	27.9	65.7	26.2	67.7
018	18.0	55.4	14.2	43.6	19.4	54.7	15.3	45.9
019	24.0	71.0	22.1	69.5	20.0	64.9	23.0	64.4
020	16.6	58.9	23.0	53.5	17.2	62.4	21.3	60.2
021	21.7	75.1	19.9	74.2	22.1	74.7	22.6	73.4
022	17.2	63.6	17.0	58.7	17.2	65.3	12.8	67.5
023	21.1	77.5	21.6	75.1	19.4	71.4	21.5	71.4
024	21.2	65.5	20.2	68.3	22.4	67.6	20.3	67.5
025	27.3	76.5	29.7	75.6	28.9	79.1	29.8	76.9
026	22.8	54.5	20.7	56.4	23.0	56.3	27.0	59.4
027	26.0	73.1	26.0	66.4	24.8	70.2	23.0	72.9
028	16.4	55.4	16.9	53.0	18.3	63.6	16.9	69.3
029	10.9	48.6	21.5	59.1	22.4	59.7	25.9	64.9
030	19.6	54.9	18.5	54.0	16.6	57.6	17.5	52.4
031	12.7	36.8	9.0	37.8	6.5	19.9	9.6	35.5
032	22.6	52.2	19.9	56.3	21.3	59.3	27.3	61.1

\* Values reported for 0 hr represent the average of two tests.  
All other values reported are based on one test.

TABLE A. 0.2% Offset Yield Strength (YS) (kg/mm<sup>2</sup>) and Ultimate Tensile Strength (UTS) (kg/mm<sup>2</sup>) at 500°C

Alloy	Exposed at 500°C*									
	0 hr		1125 hr		1500 hr		3000 hr		3792 hr	
	YS	UTS	YS	UTS	YS	UTS	YS	UTS	YS	UTS
001	24.1	26.4	19.5	24.3	19.5	24.9	19.5	23.8	-	-
002	24.8	28.4	20.7	27.4	21.0	27.7	19.3	24.6	18.7	24.3
003	29.9	35.2	22.7	30.6	24.6	32.3	21.5	23.0	19.3	28.1
004	25.3	29.1	23.2	28.8	21.2	27.0	20.2	25.1	18.0	23.5
005	32.9	40.0	25.2	35.0	25.0	36.0	22.1	32.5	-	-
006	31.3	38.0	25.6	35.3	23.7	32.6	21.1	23.7	19.8	26.0
007	35.2	42.1	26.5	35.7	27.3	35.1	20.2	30.6	22.6	28.3
008	41.0	52.7	13.9	18.8	26.3	35.8	24.1	31.3	+	+
009	43.1	59.0	31.5	45.4	29.5	41.1	29.0	42.1	29.2	39.1
010	33.9	42.4	22.0	31.0	22.4	28.9	23.5	30.2	22.7**	30.4**
011	31.1	38.9	22.4	29.1	23.7	33.6	25.8	31.7	22.1	29.0
012	35.2	42.3	28.1	34.1	25.2	33.5	24.3	30.8	23.0	27.6
013	22.4	25.1	21.9	26.1	19.3	25.5	18.4	23.6	-	-
014	23.5	27.7	21.2	27.6	18.9	25.9	15.7**	22.7**	-	-
015	30.5	35.4	23.6	31.1	26.5	34.6	20.8	28.1	21.6	27.9
016	26.2	30.7	22.2**	26.9**	21.3	27.8	+	+	18.3**	20.5**
017	16.1	18.1	12.3	16.3	13.6	17.6	14.2	17.4	-	-
018	25.2	28.0	21.0	25.3	20.9	26.5	18.9	25.9	-	-
019	20.6	25.1	18.5	23.6	18.9	23.5	18.5	22.8	-	-
020	24.3	28.0	18.5	23.7	17.2	20.2	16.6	20.2	-	-
021	24.4	27.8	15.9	21.1	14.3	19.4	15.8	19.8	13.3**	17.8**
022	35.7	42.6	24.1	31.5	22.8**	29.8**	20.4	26.7	18.3**	24.1**
023	24.0	25.8	15.6	20.5	14.5	19.7	14.3	19.0	13.6**	17.6**
024	20.3	22.7	16.8	20.2	15.0	19.2	15.9	22.3	-	-
025	13.8	15.0	-	-	-	-	-	-	-	-
026	16.4	18.3	12.6	15.9	16.2	15.2	12.2	15.1	-	-
027	17.1	19.0	12.4	15.0	9.4	13.3	10.7	13.2	-	-
028	26.0	28.9	22.7	33.3	20.2	30.3	18.9	24.8	-	-
029	20.5	24.6	14.3	18.5	13.4	19.3	13.6	18.0	-	-
030	24.6	28.4	19.1	24.8	18.7	24.0	16.5	22.2	-	-
031	33.2	40.0	24.6	30.2	19.8	28.4	19.3	27.0	20.6	28.0
032	20.9	22.2	16.2	20.9	14.6	21.0	14.9	18.9	14.0**	16.7**

\* Values reported for 0 hr represent the average of two tests. All other values reported are based on one test.

\*\* Specimen broke at or outside of gauge mark.

+ All or part of test unsuccessful.

TABLE A-12b. Percent Total Elongation (Elong) and Percent Reduction in Area (RA) at 500°C

Alloy	Exposed at 500°C*									
	0 hr		1125 hr		1500 hr		3000 hr		3792 hr	
	Elong	RA	Elong	RA	Elong	RA	Elong	RA	Elong	RA
001	27.3	75.8	22.4	81.5	20.3	72.8	18.3	64.7	-	-
002	32.7	74.8	22.7	72.2	23.8	69.9	21.0	58.0	16.6	70.6
003	25.4	80.3	20.7	76.4	23.8	80.3	22.6	76.7	15.9	78.0
004	34.1	81.7	25.9	79.0	23.0	76.9	15.5	80.1	15.1	76.9
005	23.5	97.2	15.3	87.0	15.1	90.6	15.9	85.6	-	-
006	32.6	97.9	18.9	85.7	16.9	84.2	19.9	85.2	18.3	83.0
007	27.7	87.4	22.2	85.1	22.1	74.1	14.4	65.8	12.0	76.9
008	20.6	90.4	24.6	89.9	24.9	93.8	21.9	90.5	+	+
009	14.0	96.4	10.7	67.7	24.4	93.5	9.6	35.9	9.3	53.2
010	26.2	90.1	26.0	80.0	22.9	88.0	12.8	67.8	9.6**	64.6**
011	34.6	97.9	24.6	78.6	28.9	95.6	17.5	87.6	16.7	76.5
012	36.2	70.7	27.8	92.8	24.6	82.4	27.0	72.3	28.2	84.6
013	39.0	77.0	27.0	84.8	24.9	65.7	25.4	71.1	-	-
014	42.7	74.9	27.0	86.7	22.4	89.0	21.5**	74.8**	-	-
015	36.2	72.8	27.0	67.9	29.5	76.1	15.1	67.3	12.8	69.7
016	31.0	81.1	4.9**	76.1**	19.4	75.2	+	+	0.0**	0.0**
017	47.1	87.0	56.9	81.0	34.4	88.0	31.8	83.2	-	-
018	24.3	60.1	18.1	65.0	19.4	69.0	15.9	63.3	-	-
019	33.9	85.6	27.9	83.6	31.7	83.5	27.0	83.1	-	-
020	30.0	69.6	15.0	66.8	18.1	68.4	10.4	84.1	-	-
021	33.1	83.2	19.1	73.9	29.8	75.1	18.3	83.0	7.3**	45.6**
022	17.9	76.2	11.8	62.0	7.6**	61.1**	5.7	62.8	8.8**	50.6**
023	23.8	74.9	19.1	69.8	16.7	65.0	17.5	71.0	8.8**	58.2**
024	31.2	79.3	34.9	83.0	22.2	75.6	12.8	62.8	-	-
025	47.2	89.6	-	-	-	-	-	-	-	-
026	28.4	65.5	38.2	76.6	30.1	81.4	10.7	78.3	-	-
027	40.8	83.3	33.9	85.5	38.0	78.7	25.4	75.0	-	-
028	34.5	59.2	11.2	59.5	15.9	77.8	12.8	65.8	-	-
029	41.7	83.3	34.9	87.9	24.6	68.2	20.7	77.1	-	-
030	33.5	78.2	28.2	87.2	28.5	82.5	19.9	74.7	-	-
031	24.6	62.9	25.2	68.8	19.1	54.5	13.6	61.6	14.4	55.6
032	35.6	75.5	18.1	67.1	20.7	72.5	22.2	84.3	8.0**	62.8**

\* Values reported for 0 hr represent the average of two tests. All other values reported are based on one test.

\*\* Specimen broke at or outside of gauge mark.

+ All or part of test unsuccessful.

TABLE A-13. Impact Energy Absorption (ft/lb) at 300°C

Alloy	Exposed at 300°C*								
	0 hr	375 hr	750 hr	1125 hr	1500 hr	2250 hr	2625 hr	3000 hr	3570 hr
001	6.4	5.2	4.8	5.0	4.7	4.9	4.2	4.5	4.4
002	3.2	2.6	2.8	2.0	2.8	3.0	3.0	2.9	2.8
003	2.9	2.7	2.8	2.6	2.2	3.0	3.1	3.5	3.4
004	3.1	3.1	2.8	3.0	3.2	3.0	2.9	2.9	2.9
005	4.5	3.9	3.0	3.5	3.9	3.5	4.2	4.0	3.4
006	2.3	4.4	4.2	4.1	4.0	4.2	4.6	4.3	3.9
007	3.6	3.1	2.9	3.0	3.2	3.0	3.2	3.8	3.2
008	1.9	1.3	1.0	0.9	1.0	0.7	1.1	2.2	2.0
009	1.0	1.2	1.2	1.1	1.2	1.0	1.1	1.2	1.4
010	3.4	2.6	2.5	2.7	2.7	3.5	3.4	3.0	2.8
011	1.6	3.8	3.8	4.2	3.4	3.0	4.3	3.6	3.8
012	2.4	2.6	2.4	2.2	2.1	2.4	2.3	2.8	2.6
013	4.2	3.4	2.9	2.9	3.0	3.0	2.9	3.1	3.0
014	5.5	5.6	4.5	4.3	4.7	5.2	4.9	5.3	4.9
015	3.7	2.5	2.5	2.4	2.8	3.2	2.9	2.9	3.2
016	5.3	5.8	4.7	4.8	4.7	5.3	5.4	**	6.2
017	7.6	6.1	6.2	6.2	5.7	5.7	5.6	6.2	5.7
018	5.3	4.4	3.9	4.5	5.3	4.5	4.4	4.5	4.5
019	10.0	+	6.3	6.0	6.5	5.7	5.9	5.6	5.9
020	7.0	7.1	6.6	7.5	7.8	6.5	6.8	8.0	7.8
021	5.5	8.8	8.6	8.0	7.2	6.6	7.7	7.1	**
022	5.7	5.0	3.4	3.3	3.2	3.3	5.4	5.0	5.1
023	**	**	13.0	**	**	**	**	**	**
024	9.6	8.6	7.8	**	9.0	6.2	7.2	**	9.2
025	**	**	**	**	**	10.2	**	**	**
026	7.4	**	**	**	7.5	**	7.8	**	**
027	**	**	**	**	**	**	10.6	**	**
028	8.3	5.5	**	+	**	8.5	6.9	7.6	7.8
029	6.8	5.5	5.5	5.7	5.0	5.7	4.7	5.0	5.4
030	5.9	3.7	3.8	4.1	4.8	4.6	4.7	3.9	4.2
031	3.8	4.1	3.7	3.8	+	4.0	4.0	4.5	3.7
032	**	**	**	**	**	**	**	**	**

\* In each case, the value reported is that obtained from one impact test.

\*\* Specimen too ductile for sheet impact test.

+ Test unsuccessful.

TABLE A-14a. 0.2% Offset Yield Strength (YS) ( $\text{kg}/\text{mm}^2$ ) and Ultimate Tensile Strength (UTS) ( $\text{kg}/\text{mm}^2$ ) at Room Temperature

Alloy	Exposed at 300°C*									
	0 hr		1500 hr		2250 hr		3000 hr		6570 hr	
	YS	UTS	YS	UTS	YS	UTS	YS	UTS	YS	UTS
001	46.2	60.0	48.4	61.1	47.7	59.9	50.7	62.3	48.9	65.5
002	55.4	73.2	45.9	64.4	48.0	63.9	50.9	62.6	49.8	64.0
003	58.8	79.8	58.5	78.7	62.3	81.4	60.5	82.4	58.0	79.5
004	51.1	70.7	48.3	65.9	49.9	65.3	49.8	65.2	50.5	64.8
005	70.4	95.3	62.8	84.3	63.4	83.7	71.1	89.2	58.5	85.3
006	71.3	96.0	66.3	86.1	81.8	108.6	69.3	95.6	67.3	91.8
007	67.0	89.8	62.4	87.0	62.4	82.3	69.3	87.3	70.9	87.0
008	73.2	96.3	82.5	107.5	83.0	113.9	81.5	107.1	81.3	107.1
009	89.5	116.6	85.4	85.4	82.0	82.0	45.4	45.4	60.6**	60.6**
010	66.8	93.1	67.9	89.6	68.5	91.5	61.8	86.7	63.2	89.7
011	59.0	79.8	67.6	90.3	68.9	86.2	72.4	93.3	77.1	89.2
012	64.6	91.8	66.3	85.9	70.8	91.5	66.9	89.0	71.5	89.8
013	50.5	66.2	48.2	61.5	42.0	61.1	44.3	60.4	42.2	59.7
014	41.2	59.9	54.4	58.0	44.2	63.4	49.4	60.6	49.3	62.2
015	59.7	84.0	55.9	73.5	56.7	74.6	58.5	76.5	64.4	83.4
016	65.3	85.0	52.0	66.8	57.0	70.4	52.4	68.3	51.0	68.2
017	34.5	47.2	31.6	45.0	35.4	45.2	33.6	44.4	31.3	68.2
018	47.8	65.8	45.4	58.5	45.4	57.9	43.1	56.7	44.4	44.6
019	49.8	64.2	42.9	54.2	43.6	55.0	45.2	56.1	43.5	57.3
020	48.3	63.2	45.0	56.4	43.3	55.4	44.4	57.1	48.1	52.9
021	45.4	59.5	40.2	52.3	40.4	52.4	44.4	55.9	40.6	58.8
022	62.8	82.4	65.7	81.8	59.8	78.9	64.1	91.3	54.1	72.2
023	44.9	53.1	40.5	49.1	42.1	48.3	41.8	48.3	40.5	48.5
024	42.0	55.4	42.6	55.6	42.0	55.8	46.7	56.0	42.9	54.4
025	31.4	39.5	31.2	40.0	31.8	39.3	33.0	39.2	33.2	39.2
026	38.9	51.3	36.3	46.3	34.1	46.0	36.9	46.3	36.4	46.7
027	35.1	43.2	35.5	43.5	34.6	43.1	36.3	43.5	33.3	43.6
028	50.1	67.0	51.1	64.2	45.4	56.7	45.4	54.6	44.1	53.7
029	46.2	64.0	44.1	56.0	37.9	49.3	39.5	48.3	38.2	47.9
030	53.5	70.2	49.9	65.4	49.1	64.4	47.7	60.9	45.9	61.0
031	56.4	71.5	60.6	78.7	60.4	75.0	58.2	77.1	57.5	72.2
032	38.9	49.0	37.3	46.7	39.0	47.2	40.9	48.0	39.2	48.2

\* Values reported for 0 hr represent the average of three tests. All other values reported are based on one test.

\*\* Extremely brittle specimen, no plastic deformation observable.

TABLE A-14b. Percent Total Elongation (Elong) and Percent Reduction in Area (RA) at Room Temperature

Alloy	Exposed at 300°C*									
	0 hr		1500 hr		2250 hr		3000 hr		6570 hr	
	Elong	RA	Elong	RA	Elong	RA	Elong	RA	Elong	RA
001	12.3	32.3	12.6	34.1	9.3	40.5	11.5	36.0	12.5	35.2
002	12.3	27.0	27.9	27.6	10.7	30.6	10.3	32.4	10.9	26.4
003	12.5	34.5	10.6	42.1	11.4	40.7	12.8	37.1	12.0	39.2
004	15.0	38.6	16.9	43.5	13.4	38.2	16.6	42.6	12.9	39.4
005	3.8	11.7	5.2	19.5	4.4	17.4	3.3	13.0	4.7	17.0
006	7.3	22.7	9.3	40.7	4.1	10.0	6.3	25.1	7.3	28.4
007	10.1	30.5	11.2	46.6	15.6	46.2	15.5	41.0	13.2	35.5
008	7.8	31.0	5.2	22.8	4.4	18.9	9.1	36.7	6.62	26.0
009	0.9	10.8	0.0	9.5	0.0	11.0	2.5	4.8	1.6**	6.9**
010	6.7	34.2	6.6	33.2	6.5	40.9	7.7	39.2	8.0	33.7
011	10.1	29.4	8.8	34.2	6.6	27.8	11.2	26.9	9.3	31.5
012	9.1	16.0	5.5	21.3	2.1	12.0	7.4	24.1	5.0	6.9
013	14.6	34.0	12.6	23.8	10.7	26.2	12.9	31.5	11.4	22.9
014	12.0	28.7	9.3	37.3	6.0	36.3	9.9	38.7	9.6	32.2
015	9.6	25.3	11.8	40.5	8.4	37.1	10.9	26.2	11.4	29.8
016	11.7	35.1	11.4	42.3	13.9	44.8	16.2	43.6	15.5	34.8
017	20.7	43.4	22.2	42.0	21.6	44.2	21.3	43.1	21.0	31.3
018	14.4	31.0	12.9	37.3	12.1	37.3	12.5	29.6	13.7	30.6
019	13.3	39.1	17.5	46.8	14.0	46.8	13.6	37.8	15.9	37.6
020	13.8	42.9	14.0	35.8	13.4	42.7	15.3	37.8	14.0	31.3
021	16.7	47.1	18.6	55.4	17.2	58.1	17.8	50.6	19.9	50.9
022	13.8	47.8	13.4	53.7	9.9	47.7	6.9	38.8	13.4	50.4
023	19.9	60.2	20.7	59.5	24.6	64.8	23.5	58.4	24.0	49.6
024	15.4	37.0	18.8	47.3	18.5	49.5	17.5	44.5	15.3	35.4
025	29.3	50.4	29.1	54.7	29.8	58.6	29.8	54.7	30.0	46.8
026	19.1	41.1	15.9	37.3	17.0	44.8	18.0	40.5	18.3	30.4
027	25.9	51.5	23.3	47.8	24.9	53.5	26.5	53.4	26.0	46.8
028	13.0	43.0	11.7	43.2	13.7	43.8	13.1	39.1	14.8	36.6
029	10.1	31.3	18.1	40.5	16.2	43.3	20.2	39.1	19.1	33.6
030	13.0	28.1	13.9	34.4	11.7	34.3	9.9	36.0	11.8	28.6
031	11.5	27.3	7.6	25.1	5.2	26.9	7.9	26.9	9.1	21.8
032	17.2	30.1	17.0	37.8	18.9	44.5	17.4	39.3	19.1	37.3

\* Values reported for 0 hr represent the average of three tests. All other values reported are based on one test.

\*\* Extremely brittle specimen, no plastic deformation observable.



TABLE A-15a. 0.2% Offset Yield Strength (YS) ( $\text{kg}/\text{mm}^2$ ) and Ultimate Tensile Strength (UTS) ( $\text{kg}/\text{mm}^2$ ) at Room Temperature

Alloy	Exposed at 400°C*									
	0 hr		1500 hr		2250 hr		3000 hr		3578 hr	
	YS	UTS	YS	UTS	YS	UTS	YS	UTS	YS	UTS
001	46.2	60.0	74.6	105.9	46.7	61.9	50.2	61.3	41.1 <sup>+</sup>	59.8 <sup>+</sup>
002	55.4	73.2	47.0	67.2	45.4	62.8	50.2	62.4	46.3	62.4
003	58.8	79.8	56.6	80.4	61.1	85.4	47.2	79.3	58.0	76.6
004	51.1	70.7	45.9	64.2	47.8	65.5	54.1	69.7	49.5	69.5
005	70.4	95.3	60.3	84.0	58.5	82.4	63.8	83.3	66.6	81.0
006	71.3	96.0	61.0	84.8	61.9	82.9	64.6	80.6	69.3	89.4
007	67.0	89.8	65.1	88.5	72.0	95.0	70.1	89.2	61.9	84.0
008	73.2	96.3	69.3	99.9	69.3	89.6	67.2	90.6	59.5	87.5
009	89.5	116.6	64.4	64.4	98.5	101.9	79.9	106.7	64.9 <sup>**</sup>	64.9 <sup>**</sup>
010	66.8	93.1	57.1	81.8	71.5	105.2	59.5	87.6	59.5	76.7
011	59.0	79.8	56.1	73.1	57.9	69.8	60.0	76.3	56.3	75.7
012	64.6	91.8	70.7	90.2	54.8	74.6	52.8	61.9	62.4 <sup>**</sup>	80.2 <sup>**</sup>
013	50.5	66.2	45.5	59.6	40.9	60.4	44.8	62.9	43.7	58.4
014	41.2	59.9	43.3	61.1	50.9	64.6	52.2	73.1	58.5	73.3
015	59.7	84.0	67.2	91.9	54.8	75.0	50.6	68.9	51.8	68.9
016	65.3	85.0	51.1	68.4	52.2	68.7	53.7	69.3	52.2	68.0
017	34.5	47.2	31.2	44.5	34.6	44.7	37.7	51.1	36.7	45.5
018	47.8	65.8	42.8	57.2	42.9	55.7	45.4	56.0	45.9	59.3
019	49.8	64.2	41.5	55.2	46.4	58.4	39.9	55.9	46.7	56.8
020	48.3	63.2	42.6	56.6	45.7	56.4	44.1	56.1	45.9	56.9
021	45.4	59.5	33.6	52.4	42.4	52.5	45.2	55.9	43.4	52.2
022	62.8	82.4	61.9	80.6	59.3	75.4	57.4	70.2	59.9	70.3
023	44.9	53.1	39.5	49.3	40.1	49.4	37.3	20.1	37.8	48.0
024	42.0	55.4	36.3	53.1	40.8	52.8	42.0	52.6	39.2	50.3
025	31.4	39.5	28.9	38.7	33.7	39.0	33.0	38.9	33.7	38.7
026	38.9	51.3	34.1	45.9	36.1	45.4	35.0	45.0	33.7	46.1
027	35.1	43.2	35.6	43.1	35.0	43.1	38.0	43.8	36.3	44.0
028	50.1	67.0	41.3	54.1	++	55.3	47.6	56.7	59.9	83.7
029	46.2	64.0	38.5	47.5	37.7	47.5	38.2	47.9	38.0	47.6
030	53.5	70.2	47.8	65.2	48.8	62.9	56.3	67.1	55.2	67.8
031	56.4	71.5	50.6	65.9	56.4	66.7	58.7	73.5	58.0	69.7
032	38.9	49.0	37.5	46.4	36.3	45.9	37.6	45.4	37.4	45.4

\* Values reported for 0 hr represent the average of three tests. All other values reported are based on one test.

<sup>+</sup> Specimen split due to internal corrosion.

<sup>\*\*</sup> Specimen broke at or outside of gauge mark.

<sup>++</sup> All or part of test unsuccessful.

TABLE A-15b. Percent Total Elongation (Elong) and Percent Reduction in Area (RA) at Room Temperature

Alloy	Exposed at 400°C*									
	0 hr		1500 hr		2250 hr		3000 hr		3578 hr	
	Elong	RA	Elong	RA	Elong	RA	Elong	RA	Elong	RA
001	12.3	32.3	4.3	3.8	10.9	41.8	11.5	39.9	4.1 <sup>+</sup>	0.5 <sup>+</sup>
002	12.3	27.0	12.3	22.7	7.9	25.1	10.9	24.7	9.1	14.1
003	12.5	34.5	14.7	42.1	11.2	37.5	8.5	34.5	11.5	32.5
004	15.0	38.6	16.1	43.8	14.0	47.7	12.3	36.3	11.4	32.4
005	3.8	11.7	3.8	21.1	1.3	18.1	4.6	14.5	2.7	1.6
006	7.3	22.7	10.4	30.6	7.3	33.7	9.5	36.7	3.6	8.4
007	10.1	30.5	10.1	38.0	6.0	27.8	11.2	35.0	12.0	29.8
008	7.8	31.0	6.8	28.7	7.4	25.1	8.8	31.5	10.7	22.8
009	0.9	10.8	3.0	12.6	0.0	2.1	1.3	4.3	0.6 <sup>**</sup>	0.0 <sup>**</sup>
010	6.7	34.2	11.2	47.7	6.0	19.9	7.1	32.4	9.0	38.8
011	10.1	29.4	7.9	33.3	0.9	0.0	12.0	38.2	9.6	26.4
012	9.1	16.0	5.8	14.0	7.7	21.3	1.4	7.4	3.3 <sup>**</sup>	2.7 <sup>**</sup>
013	14.6	34.0	13.9	24.2	10.4	24.4	11.8	28.1	9.9	25.9
014	12.0	38.7	9.3	37.6	9.8	30.6	9.1	26.7	9.6	25.2
015	9.6	25.3	6.8	23.3	12.1	21.8	11.7	30.6	14.7	22.9
016	11.7	35.1	13.9	44.6	9.6	34.6	12.9	35.7	9.8	15.7
017	20.7	43.4	21.6	45.2	27.0	45.2	15.5	39.1	22.4	35.4
018	14.4	31.0	12.8	37.3	9.0	31.1	12.5	36.2	12.1	21.4
019	13.3	39.1	15.1	46.7	18.5	45.0	16.4	39.4	17.5	35.4
020	13.8	42.9	12.1	28.7	10.1	24.7	13.2	29.4	14.2	25.4
021	16.7	47.1	18.6	60.8	18.0	58.0	16.7	48.4	18.0	51.4
022	13.8	47.8	10.9	47.1	3.0	29.3	9.9	44.6	9.5	35.4
023	19.9	60.2	20.2	66.0	17.8	62.6	18.3	60.3	19.1	55.1
024	15.4	37.0	13.6	48.7	16.2	46.3	17.8	44.5	16.6	40.7
025	29.3	50.4	30.8	55.0	40.4	55.4	25.7	49.1	26.2	35.0
026	19.1	41.1	17.5	37.3	14.2	40.5	17.5	30.9	17.0	36.5
027	25.9	51.5	24.0	49.5	23.3	53.0	24.9	52.5	22.7	49.0
028	13.0	43.0	12.1	40.9	12.0	37.3	13.1	40.7	3.2	8.4
029	10.1	31.3	19.1	47.1	18.3	38.7	18.8	40.8	19.2	40.8
030	13.0	28.1	12.9	35.9	14.0	32.0	13.1	41.4	7.9	30.8
031	11.5	27.3	11.4	50.4	5.4	25.5	4.6	12.1	6.5	10.6
032	17.2	30.1	19.6	42.7	18.3	34.9	18.8	35.5	20.7	37.8

\* Values reported for 0 hr represent the average of three tests. All other values reported are based on one test.

\*\* Specimen broke at or outside of gauge mark.

<sup>+</sup> Specimen split due to internal corrosion.

TABLE A-16a. 0.2% Offset Yield Strength (YS) (kg/mm<sup>2</sup>) and Ultimate Tensile Strength (kg/mm<sup>2</sup>) at Room Temperature

Alloy	Exposed at 500°C*													
	0 hr		1125 hr		1500 hr		3000 hr		3792 hr		4542 hr		4917 hr	
	YS	UTS	YS	UTS	YS	UTS	YS	UTS	YS	UTS	YS	UTS	YS	UTS
001	46.2	60.0	49.8	61.5	49.3	61.5	45.7	59.7	-	-	39.5	51.0	-	-
002	55.4	73.2	46.3	60.3	42.8	60.2	45.5	58.1	39.8	53.7	-	-	-	-
003	58.8	79.8	57.1	74.0	49.4	72.0	54.0	67.3	42.5 <sup>+</sup>	47.1 <sup>+</sup>	-	-	-	-
004	51.1	70.7	47.3	63.5	44.4	62.0	43.9	59.3	37.9	53.5	-	-	-	-
005	70.4	95.3	61.0 <sup>+</sup>	74.4 <sup>+</sup>	46.0 <sup>+</sup>	56.2 <sup>+</sup>	58.4 <sup>**</sup>	58.4 <sup>**</sup>	-	-	-	-	56.3 <sup>+</sup>	70.3 <sup>+</sup>
006	71.3	96.0	57.1	76.6	54.8	75.3	50.5	64.6	45.9	62.3	-	-	-	-
007	67.0	89.8	58.0	75.3	54.8	79.3	53.3	69.0	47.8 <sup>+</sup>	53.7 <sup>+</sup>	-	-	-	-
008	73.2	96.3	52.4	68.1	54.3	81.6	46.7 <sup>**</sup>	46.7 <sup>**</sup>	15.1 <sup>+</sup>	15.1 <sup>+</sup>	-	-	-	-
009	89.5	116.6	61.5 <sup>**</sup>	61.5 <sup>**</sup>	61.7 <sup>+</sup>	68.3 <sup>+</sup>	36.1 <sup>**</sup>	36.1 <sup>**</sup>	32.4 <sup>+</sup>	32.4 <sup>+</sup>	-	-	-	-
010	66.8	93.1	48.5	65.5	45.0	65.0	48.1	63.0	43.4 <sup>+</sup>	44.6 <sup>+</sup>	-	-	-	-
011	59.0	79.8	48.8	61.5	66.8 <sup>+</sup>	74.6 <sup>+</sup>	51.6 <sup>+</sup>	67.2 <sup>+</sup>	50.3	73.3	-	-	-	-
012	64.6	91.8	56.3	78.0	60.5	67.2	52.7	60.9	39.8 <sup>+</sup>	39.8 <sup>+</sup>	-	-	-	-
013	50.5	66.2	45.4	64.6	42.7	60.0	45.4	57.7	-	-	-	-	38.1	51.5
014	41.2	59.9	45.9	56.3	41.1	54.0	39.5	49.0	-	-	-	-	32.8	43.1
015	59.7	84.0	50.2	70.1	55.2	72.1	51.0	68.0	44.9 <sup>+</sup>	45.9 <sup>+</sup>	-	-	-	-
016	65.3	85.0	51.0	65.9	45.9 <sup>**</sup>	45.9 <sup>**</sup>	23.9 <sup>**</sup>	23.9 <sup>**</sup>	16.8 <sup>+</sup>	16.8 <sup>+</sup>	-	-	-	-
017	34.5	47.2	31.2	44.2	35.1	45.9	35.8 <sup>+</sup>	46.9 <sup>+</sup>	-	-	-	-	32.5	45.6
018	47.8	65.8	41.5	54.3	40.8	55.0	40.3	55.9	-	-	-	-	36.9	48.8
019	49.8	64.2	45.9	57.6	45.5	57.6	42.4	53.6	-	-	-	-	40.0	51.7
020	48.3	63.2	41.5	53.7	43.3	55.0	39.4	50.4	33.9 <sup>+</sup>	42.5 <sup>+</sup>	-	-	-	-
021	45.4	59.5	41.4	53.0	38.2	53.3	35.7 <sup>+</sup>	48.4 <sup>+</sup>	29.2 <sup>+</sup>	30.6 <sup>+</sup>	-	-	-	-
022	62.8	82.4	52.8	66.7	50.6 <sup>+</sup>	66.6 <sup>+</sup>	39.8 <sup>+</sup>	46.7 <sup>+</sup>	31.0 <sup>+</sup>	31.0 <sup>+</sup>	-	-	-	-
023	44.9	53.1	33.4	49.8	37.2	52.4	32.8 <sup>+</sup>	38.4 <sup>+</sup>	29.3	36.9	-	-	-	-
024	42.0	55.4	48.1	50.9	39.7	50.3	40.3	50.3	-	-	-	-	42.1	53.0
025	31.4	39.5	-	-	-	-	-	-	-	-	-	-	-	-
026	38.9	51.3	35.3	45.4	35.4	46.0	34.4	44.6	-	-	-	-	30.6	42.3
027	35.1	43.2	31.2	41.8	31.1	42.2	28.5	41.1	28.0	38.0	-	-	-	-
028	50.1	67.0	44.6 <sup>+</sup>	60.2 <sup>+</sup>	51.5	66.5	43.4 <sup>+</sup>	55.4 <sup>+</sup>	-	-	37.6	49.5	-	-
029	46.2	64.0	34.9	45.4	36.3	49.3	33.0	47.6	-	-	31.5	42.3	-	-
030	53.5	70.2	46.5	60.0	45.5	58.0	42.2	54.5	-	-	40.8	54.1	-	-
031	56.4	71.5	53.1	71.5	43.6 <sup>+</sup>	49.9 <sup>+</sup>	42.8 <sup>**</sup>	42.8 <sup>**</sup>	35.9 <sup>++</sup>	35.9 <sup>++</sup>	-	-	-	-
032	38.9	49.0	31.0	45.8	35.1	47.3	32.8	37.6	29.2 <sup>+</sup>	29.2 <sup>+</sup>	-	-	-	-

\* Values reported for 0 hr represent the average of three tests. All other values reported are based on one test.

\*\* Extremely brittle specimen, no plastic deformation observable.

<sup>+</sup> Specimen broke at or outside of gauge mark.

<sup>++</sup> Specimen split due to internal corrosion.

TABLE A-16b. Percent Total Elongation (Elong) and Percent Reduction in Area (RA) at Room Temperature

Alloy	Exposed at 500°C*													
	0 hr		1125 hr		1500 hr		3000 hr		3792 hr		4542 hr		4917 hr	
	Elong	RA	Elong	RA	Elong	RA	Elong	RA	Elong	RA	Elong	RA	Elong	RA
001	12.3	32.3	10.4	24.9	10.4	28.9	5.7	13.5	-	-	2.2	5.3	-	-
002	12.3	27.0	7.3	11.5	6.9	15.5	2.5	4.3	2.2	4.8	-	-	-	-
003	12.5	34.5	6.9	16.0	6.9	14.1	3.6	0.5	0.0 <sup>+</sup>	2.7 <sup>+</sup>	-	-	-	-
004	15.0	38.6	9.1	18.0	11.2	22.8	9.8	16.5	7.6	27.8	-	-	-	-
005	3.8	11.7	1.9 <sup>+</sup>	0.0 <sup>+</sup>	2.4 <sup>+</sup>	1.1 <sup>+</sup>	1.4 <sup>**</sup>	1.6 <sup>**</sup>	-	-	-	-	0.8 <sup>+</sup>	5.8 <sup>+</sup>
006	7.3	22.7	7.1	13.0	4.6	3.7	6.8	9.4	3.0	12.0	-	-	-	-
007	10.1	30.5	11.0	27.0	7.4	14.7	9.6	18.0	0.8 <sup>+</sup>	0.0 <sup>+</sup>	-	-	-	-
008	7.8	31.0	10.4	26.5	5.0	12.5	1.1 <sup>**</sup>	0.0 <sup>**</sup>	0.5 <sup>+</sup>	0.0 <sup>+</sup>	-	-	-	-
009	0.9	10.8	2.5 <sup>**</sup>	0.0 <sup>**</sup>	0.9 <sup>+</sup>	1.1 <sup>+</sup>	0.0 <sup>**</sup>	0.0 <sup>**</sup>	0.8 <sup>+</sup>	0.0 <sup>+</sup>	-	-	-	-
010	6.7	34.2	8.8	29.7	8.2	21.9	4.1	13.0	0.2 <sup>+</sup>	0.0 <sup>+</sup>	-	-	-	-
011	10.1	29.4	4.9	14.0	1.7 <sup>+</sup>	0.0 <sup>+</sup>	0.0 <sup>+</sup>	0.0 <sup>+</sup>	4.1	15.5	-	-	-	-
012	9.1	16.0	6.5	6.4	2.1	1.1	0.2	1.1	1.4 <sup>+</sup>	0.5 <sup>+</sup>	-	-	-	-
013	14.6	34.0	14.2	19.0	7.6	9.0	7.4	8.0	-	-	-	-	10.3	18.9
014	12.0	38.7	12.5	27.0	7.7	15.0	5.5	13.5	-	-	-	-	6.6	26.5
015	9.6	25.3	9.9	13.8	6.6	6.0	0.6	0.0	0.8 <sup>+</sup>	0.5 <sup>+</sup>	-	-	-	-
016	11.7	35.1	4.1	1.6	1.6 <sup>**</sup>	0.0 <sup>**</sup>	0.0 <sup>**</sup>	0.0 <sup>**</sup>	0.0 <sup>+</sup>	0.0 <sup>+</sup>	-	-	-	-
017	20.7	43.4	17.7	36.6	23.7	38.0	19.2 <sup>+</sup>	38.0 <sup>+</sup>	-	-	-	-	12.5	28.1
018	14.4	31.0	14.0	24.7	12.1	19.3	5.8	13.0	-	-	-	-	9.5	19.9
019	13.3	39.1	16.7	31.4	17.0	33.9	15.9	38.5	-	-	-	-	14.8	26.5
020	13.8	42.9	9.9	18.8	8.0	11.5	7.7	11.0	1.1 <sup>+</sup>	2.1 <sup>+</sup>	-	-	-	-
021	16.7	47.1	10.7	25.4	10.3	26.7	1.3 <sup>+</sup>	1.6 <sup>+</sup>	0.6 <sup>+</sup>	0.0 <sup>+</sup>	-	-	-	-
022	13.8	47.8	4.3	15.5	1.6 <sup>+</sup>	0.0 <sup>+</sup>	0.0 <sup>+</sup>	0.0 <sup>+</sup>	0.5 <sup>+</sup>	2.1 <sup>+</sup>	-	-	-	-
023	19.9	60.2	19.9	39.1	13.4	19.9	1.3 <sup>+</sup>	0.0 <sup>+</sup>	0.3	2.1	-	-	-	-
024	15.4	37.0	15.6	36.2	16.7	35.0	14.4	25.4	-	-	-	-	7.3	24.7
025	29.3	50.4	-	-	-	-	-	-	-	-	-	-	-	-
026	19.1	41.1	17.2	23.0	19.7	26.7	20.3	26.2	-	-	-	-	13.1	36.4
027	25.9	51.5	19.9	42.4	18.0	27.6	8.8	21.8	11.0	37.1	-	-	-	-
028	13.0	43.0	1.4 <sup>+</sup>	0.0 <sup>+</sup>	2.8	8.4	1.6 <sup>+</sup>	4.3 <sup>+</sup>	-	-	4.3	20.8	-	-
029	10.1	31.3	21.6	35.5	14.0	23.7	16.7	22.9	-	-	13.7	28.8	-	-
030	13.0	28.1	13.2	27.4	13.4	29.8	10.6	25.2	-	-	7.1	20.8	-	-
031	11.5	27.3	4.1	0.0	1.1 <sup>+</sup>	0.0 <sup>+</sup>	0.6 <sup>**</sup>	0.0 <sup>**</sup>	1.7 <sup>++</sup>	7.4 <sup>++</sup>	-	-	-	-
032	17.2	30.1	15.1	24.7	12.0	20.9	0.6	16.6	0.2 <sup>+</sup>	1.6 <sup>+</sup>	-	-	-	-

\* Values reported for 0 hr represent the average of three tests. All other values reported are based on one test.

\*\* Extremely brittle specimen, no plastic deformation observable.

<sup>+</sup> Specimen broke at or outside of gauge mark.

<sup>++</sup> Specimen split due to internal corrosion.

TABLE A-17. Impact Energy Absorption (ft/lb) at 300°C

Alloy	Exposed at 400°C*								
	0 hr	175 hr	375 hr	750 hr	1125 hr	1500 hr	2250 hr	3000 hr	3578 hr
001	6.4	4.2	4.3	5.0	5.0	4.7	5.1	5.5	4.5
002	3.2	2.6	2.8	2.5	2.1	2.7	2.8	2.9	3.3
003	2.9	3.0	3.2	3.2	2.7	2.5	2.2	1.9	2.1
004	3.1	2.7	3.2	3.0	2.8	3.0	+	2.7	2.8
005	4.5	2.1	2.4	3.2	3.2	3.7	3.6	3.1	3.0
006	2.3	4.0	3.7	3.5	3.5	3.7	3.5	2.7	2.1
007	3.6	2.9	3.3	2.5	3.2	2.6	2.6	3.2	2.8
008	1.9	2.0	2.0	1.8	2.1	2.2	1.9	1.5	1.4
009	1.0	1.3	0.9	0.9	0.8	0.9	0.7	1.0	1.4
010	3.4	3.3	2.7	2.5	2.4	3.0	2.4	2.5	2.5
011	1.6	3.7	3.6	3.5	3.2	2.7	2.4	2.2	2.7
012	2.4	2.8	2.5	2.4	2.2	1.7	0.7	0.3	0.6
013	4.2	2.8	3.0	3.0	2.7	2.9	2.2	3.0	2.9
014	5.5	5.6	4.5	4.6	4.3	4.5	4.5	4.5	4.9
015	3.7	3.0	3.2	2.9	2.8	3.0	2.5	2.8	2.7
016	5.3	5.2	5.1	5.5	5.0	6.0	5.2	5.6	5.4
017	7.6	5.9	5.7	6.0	6.2	6.5	6.0	5.9	5.9
018	5.3	5.5	5.0	4.6	4.7	4.5	4.0	4.7	5.2
019	10.0	6.6	6.7	7.6	7.0	7.3	6.1	6.2	5.9
020	7.0	8.4	7.2	8.2	7.1	7.8	7.8	9.0	**
021	5.5	7.7	7.7	**	7.3	7.9	6.5	8.0	8.5
022	5.7	4.4	5.4	4.9	4.1	3.8	3.5	3.0	2.8
023	**	**	**	**	11.0	**	**	12.0	**
024	9.6	8.4	7.6	6.4	6.7	7.2	6.3	7.4	6.9
025	**	**	**	**	**	9.4	**	9.0	9.1
026	7.4	7.6	**	**	**	8.5	8.2	**	**
027	**	**	11.1	**	9.5	9.7	10.0	**	**
028	8.3	7.9	5.7	5.5	6.5	5.4	**	6.8	5.5
029	6.8	5.3	5.4	5.5	5.7	5.9	5.4	5.2	**
030	5.9	3.9	3.7	3.6	3.7	3.7	3.8	4.1	4.4
031	3.8	3.8	3.4	3.5	2.8	3.0	2.7	2.9	4.2
032	**	**	**	**	**	**	**	**	**

\* In each case, the value reported is that obtained from one impact test.

\*\* Specimen too ductile for sheet impact test.

+ Test unsuccessful.

TABLE A-18. Impact Energy Absorption (ft/lb) at 300°C

Alloy	Exposed at 500°C*								
	0 hr	175 hr	375 hr	750 hr	1125 hr	1500 hr	3000 hr	3792 hr	6792 hr
001	6.4	4.7	5.1	4.7	4.7	4.1	3.7	--	0.1
002	3.2	2.9	2.4	2.3	2.3	2.1	0.7	0.2	--
003	2.9	2.3	2.1	1.9	1.9	1.5	0.2	0.2	--
004	3.1	3.1	2.4	2.0	1.8	1.4	0.3	0.2	--
005	4.5	2.7	2.2	2.3	2.1	1.9	1.7	--	0.3
006	2.3	2.1	2.1	1.5	1.7	1.5	0.3	0.4	--
007	3.6	3.0	2.4	0.7	0.3	0.4	0.3	0.2	--
008	1.9	1.2	0.2	0.2	0.2	0.2	0.2	0.2	--
009	1.0	1.2	0.2	0.1	0.1	0.3	0.1	0.2	--
010	3.4	2.8	1.6	0.3	0.3	0.8	0.3	0.1	--
011	1.6	2.4	2.2	1.5	0.9	1.2	1.7	0.3	--
012	2.4	2.4	1.8	2.0	1.8	1.4	0.2	0.2	--
013	4.2	3.1	3.5	2.9	3.0	2.7	3.0	--	3.4
014	5.5	4.0	4.8	3.8	4.3	3.3	4.4	--	--
015	3.7	1.7	2.2	1.7	1.2	0.4	0.5	0.2	--
016	5.3	4.5	1.0	0.7	0.5	0.7	0.2	0.1	--
017	7.6	6.2	5.9	5.6	5.8	5.2	5.0	--	--
018	5.3	4.7	5.1	4.9	4.8	4.8	4.4	--	5.7
019	10.0	6.2	6.0	5.7	6.2	5.3	5.4	--	--
020	7.0	7.6	7.1	7.9	6.9	5.7	6.8	--	0.1
021	5.5	6.7	6.8	5.5	4.8	2.6	0.3	0.2	--
022	5.7	2.5	2.4	2.3	1.9	1.2	2.2	0.6	--
023	**	**	**	**	10.0	10.0	**	1.5	--
024	9.6	7.1	7.7	7.6	8.5	7.5	7.9	--	--
025	**	--	--	--	--	--	--	--	--
026	7.4	**	**	**	**	**	6.7	--	--
027	**	**	7.4	7.4	6.8	6.7	**	--	0.4
028	8.3	5.7	6.3	5.8	5.2	5.5	3.9	--	--
029	6.8	4.7	5.3	5.0	5.0	**	4.0	--	--
030	5.9	4.6	4.9	5.0	2.7	2.6	2.4	--	--
031	3.8	4.1	3.2	3.3	2.9	2.9	0.2	0.1	--
032	**	**	**	**	**	11.3	0.2	0.1	--

\* In each case, the value reported is that obtained from one impact test.

\*\* Specimen too ductile for sheet impact test.

TABLE A-19. Mechanical Property Data  
for Zr-Cr Base Alloys

Alloy Addition* (at.%)	0.2% Offset Yield Strength, kg/mm <sup>2</sup>	Ultimate Tensile Strength, kg/mm <sup>2</sup>	Percent Total Elongation	Percent Reduction in Area
<u>25°C</u>				
2.3 Cr	40	56	13	43
1.9 Cr	49	63	11	41
1.5 Cr + 0.2 Fe**	42	55	15	37
1.3 Cr + 0.5 Fe**	50	64	13	39
1.9 Cr + 0.1 Ni	45	58	17	45
1.9 Cr + 0.4 Ni	47	59	14	44
1.9 Cr + 0.4 Be	42	52	16	42
1.9 Cr + 0.8 Fe	36	46	20	48
Zircaloy-2**	39	49	17	30
<u>300°C</u>				
2.3 Cr	31	36	11	62
1.9 Cr	36	45	12	66
1.5 Cr + 0.2 Fe**	26	28	24	72
1.3 Cr + 0.5 Fe**	26	29	23	71
1.9 Cr + 0.1 Ni	33	39	17	59
1.9 Cr + 0.4 Ni	32	39	17	66
1.9 Cr + 0.4 Be	28	33	22	73
1.9 Cr + 0.8 Be	22	26	26	52
Zircaloy-2**	26	28	23	52
<u>500°C</u>				
2.3 Cr	24	27	13	71
1.9 Cr	25	32	16	78
1.5 Cr + 0.2 Fe**	20	23	31	79
1.3 Cr + 0.5 Fe**	21	25	34	86
1.9 Cr + 0.1 Ni	25	28	25	89
1.9 Cr + 0.4 Ni	22	24	27	91
1.9 Cr + 0.4 Be	19	24	32	86
1.9 Cr + 0.8 Be	16	19	35	87
Zircaloy-2**	21	22	36	76

\* Sponge Zr contained 0.05 at.% Fe.

\*\* First experiment data, all alloys fabricated by the same schedule: beta treated, 565°C alpha anneal.

TABLE A-20. Mechanical Property Data  
for Zr-Cu Base Alloys

Alloy Addition (at.%)	0.2% Offset Yield Strength, kg/mm <sup>2</sup>	Ultimate	Percent Total Elongation	Percent Reduction in Area
		Tensile Strength, kg/mm <sup>2</sup>		
<u>25°C</u>				
1.2 Cu + 0.05 Fe	36	47	20	38
1.6 Cu + 0.2 Fe	43	56	20	38
1.2 Cu + 0.05 Fe*	39	51	19	41
1.1 Cu + 0.3 Fe*	34	47	21	43
1.2 Cu + 0.4 Ni + 0.2 Fe	44	57	16	38
1.2 Cu + 0.4 Be + 0.2 Fe	46	58	21	44
Zircaloy-2*	39	49	17	30
<u>300°C</u>				
1.2 Cu + 0.05 Fe	23	28	19	60
1.6 Cu + 0.2 Fe	25	31	24	61
1.2 Cu + 0.5 Fe*	23	27	23	54
1.1 Cu + 0.3 Fe*	22	26	28	63
1.2 Cu + 0.4 Ni + 0.2 Fe	25	31	17	62
1.2 Cu + 0.4 Be + 0.2 Fe	24	30	23	69
Zircaloy-2*	26	28	23	52
<u>500°C</u>				
1.2 Cu + 0.05 Fe	17	20	40	87
1.6 Cu + 0.2 Fe	17	22	45	84
1.2 Cu + 0.5 Fe*	16	18	28	65
1.1 Cu + 0.3 Fe*	16	18	47	87
1.2 Cu + 0.4 Ni + 0.2 Fe	19	22	36	91
1.2 Cu + 0.4 Be + 0.2 Fe	17	20	33	85
Zircaloy-2*	21	22	36	76

\* First experiment data, all alloys fabricated by the same schedule: beta treated, 565°C alpha anneal.



TABLE A-21. Steam Corrosion Weight Gain Data for Zr-Cr Base Alloys  
(Weight Gain, mg/dm<sup>2</sup>)

Alloy Addition (at. %)*	175 hr	750 hr	1125 hr	1875 hr	2250 hr	3000 hr
<u>300°C Exposure</u>						
2.3 Cr	-	13.8	15.0	-	16.9	19.3
1.9 Cr	-	12.9	13.2	-	15.9	18.5
1.5 Cr + 0.2 Fe*	-	9.6	12.6	-	17.1	16.7
1.3 Cr + 0.5 Fe	-	10.4	11.8	-	18.5	19.1
1.9 Cr + 0.1 Ni	-	12.9	13.4	-	15.3	17.5
1.9 Cr + 0.4 Ni	-	12.5	12.9	-	15.1	17.5
1.9 Cr + 0.4 Be	-	12.6	13.2	-	14.7	16.7
1.9 Cr + 0.8 Be	-	11.8	12.1	-	13.7	15.3
Zircaloy-2**	-	12.3	14.0	-	17.1	18.3

(2σ limit ≈ ± 0.6 for each coupon group average)

500°C Exposure

2.3 Cr	51	123	188	313	-	439
1.9 Cr	56	131	198	303	-	423
1.5 Cr + 0.2 Fe*	72	134	183	-	-	456
1.3 Cr + 0.5 Fe	68	161	228	-	-	564
1.9 Cr + 0.1 Ni	51	102	122	187	-	290
1.9 Cr + 0.4 Ni	53	102	124	180	-	301
1.9 Cr + 0.4 Be	44	132	181	287	-	407
1.9 Cr + 0.8 Be	41	89	123	228	-	345
Zircaloy-2**	128	324	411	-	-	1115

(2σ ≈ ± 2) (2σ ≈ ± 4) (2σ ≈ ± 7) (2σ ≈ ± 7) (2σ ≈ ± 9)

\* Sponge Zr contained 0.05 at.% Fe.

\*\* First experiment data, all alloys fabricated by the same schedule: Beta treated, 565°C alpha anneal.

TABLE A-22. Steam Corrosion Weight Gain Data for Zr-Cu Base Alloys  
(Weight Gain, mg/dm<sup>2</sup>)

Alloy Addition (at. %)	<u>175 hr</u>	<u>750 hr</u>	<u>1125 hr</u>	<u>1875 hr</u>	<u>2250 hr</u>	<u>3000 hr</u>
<u>300°C Exposure</u>						
1.2 Cu + 0.05 Fe	-	17.4	18.3	-	20.1	22.5
1.6 Cu + 0.2 Fe	-	17.1	17.3	-	19.1	20.0
1.2 Cu + 0.05 Fe*	-	15.7	18.8	-	25.4	26.9
1.1 Cu + 0.3 Fe*	-	11.6	13.2	-	17.1	18.5
1.2 Cu + 0.4 Ni + 0.2 Fe	-	18.8	19.7	-	20.9	22.6
1.2 Cu + 0.4 Be + 0.2 Fe	-	16.3	16.9	-	17.7	20.1
Zircaloy-2*	-	12.3	14.0	-	17.1	18.3
(2σ ≈ ± 0.6)						
<u>500°C Exposure</u>						
1.2 Cu + 0.05 Fe	86	195	213	257	-	323
1.6 Cu + 0.2 Fe	72	123	151	210	-	338
1.2 Cu + 0.5 Fe*	125	187	214	-	-	360
1.1 Cu + 0.3 Fe*	67	130	169	-	-	344
1.2 Cu + 0.4 Ni + 0.2 Fe	62	110	128	167	-	223
1.2 Cu + 0.4 Be + 0.2 Fe	50	118	158	265	-	395
Zircaloy-2*	128	324	411	-	-	1115
(2σ ≈ ± 2) (2σ ≈ ± 4) (2σ ≈ ± 7) (2σ ≈ ± 7) (2σ ≈ ± 9)						

\* First experiment data, all alloys fabricated by the same schedule: Beta treated, 565°C alpha anneal.

TABLE A-23. Corrosion Hydrogen Data for Zr-Cr Base Alloys

Alloy Addition (at. %)	Hydrogen Content (ppm)				
	0 hr	750 hr	1125 hr	2250 hr	3000 hr
<u>300°C Exposure</u>					
2.3 Cr	11	-	16	21	21
1.9 Cr	12	-	24	28	29
1.5 Cr + 0.2 Fe*	(13)	-	-	30	32
1.3 Cr + 0.5 Fe*	(13)	-	-	27	26
1.9 Cr + 0.1 Ni	14	-	43	41	36
1.9 Cr + 0.4 Ni	10	-	40	39	37
1.9 Cr + 0.4 Be	9	-	34	33	28
1.9 Cr + 0.8 Be	12	-	16	16	15
Zircaloy-2**	(13)	-	-	31	28
<u>500°C Exposure</u>					
2.3 Cr	11	150	251	-	961
1.9 Cr	12	90	133	-	663
1.5 Cr + 0.2 Fe*	(13)	-	128	-	470
1.3 Cr + 0.5 Fe*	(13)	-	162	-	451
1.9 Cr + 0.1 Ni	14	72	70	-	384
1.9 Cr + 0.4 Ni	10	72	80	-	388
1.9 Cr + 0.4 Be	9	208	334	-	1004
1.9 Cr + 0.08 Be	12	121	180	-	805
Zircaloy-2**	(13)	-	591	-	1563

\* Sponge Zr contained 0.05 at.% Fe.

\*\* First experiment data, all alloys fabricated by same schedule: Beta treated, 565°C alpha anneal.

TABLE A-24. Corrosion Hydrogen Data for  
Zr-Cu Base Alloys

Alloy Addition (at. %)	0 hr	750 hr	1125 hr	2250 hr	3000 hr
<u>300°C Exposure</u>					
1.2 Cu + 0.05 Fe	14	-	67	64	65
1.6 Cu + 0.2 Fe	19	-	64	49	46
1.2 Cu + 0.05 Fe*	(13)	-	-	63	60
1.1 Cu + 0.3 Fe*	(13)	-	-	28	32
1.2 Cu + 0.4 Ni + 0.2 Fe	8	-	35	40	37
1.2 Cu + 0.4 Be + 0.2 Fe	7	-	38	37	36
Zircaloy-2*	(13)	-	-	31	28
<u>500°C Exposure</u>					
1.2 Cu + 0.05 Fe	14	291	319	-	490
1.6 Cu + 0.2 Fe	19	121	152	-	407
1.2 Cu + 0.05 Fe*	(13)	-	293	-	294
1.1 Cu + 0.3 Fe*	(13)	-	114	-	244
1.2 Cu + 0.4 Ni + 0.2 Fe	8	78	80	-	165
1.2 Cu + 0.4 Be + 0.2 Fe	7	165	207	-	703
Zircaloy-2*	(13)	-	591	-	1563

\* First experiment data, all alloys fabricated  
by the same schedule: Beta treated, 565°C  
alpha anneal.

TABLE A-25. Effect of Fabrication Schedule on Mechanical Properties

<u>Alloy Composition</u>	<u>Fabrication Schedule</u>	<u>0.2% Offset Yield Strength, kg/mm<sup>2</sup></u>	<u>Ultimate Tensile Strength, kg/mm<sup>2</sup></u>	<u>Percent Total Elongation</u>	<u>Percent Reduction in Area</u>
		<u>25°C</u>			
Zr + 2.3 at.% Cr	A	40	56	13	43
	B	27	37	16	33
	C	30	39	30	67
		<u>300°C</u>			
	A	31	36	11	62
	B	12	16	30	68
	C	13	19	37	83
		<u>500°C</u>			
	A	24	27	13	71
	B	8	11	30	81
	C	9	13	44	90
		<u>25°C</u>			
Zr + 1.2 at.% Cu	A**	39	51	19	41
	A	36	47	20	38
	B	29	40	24	39
	C	27	36	35	62
		<u>300°C</u>			
	A**	23	27	23	54
	A	23	28	19	60
	B	13	18	30	67
	C	12	17	42	82
		<u>500°C</u>			
	A**	16	18	28	66
	A	17	20	40	87
	B	11	14	33	81
	C	9	13	42	91

\* See text for complete description. A and B were beta treated. Final anneal: A = 565°C, B and C = 788°C.

\*\* First experiment data for alloy 026 which is also Zr + 1.2 at.% Cr.

Sponge Zr contained 0.05 at.% Fe.

## P. A. 24 - DISTRIBUTION LIST

	<u>No. of Copies</u>
USAEC San Francisco Operations Office 2111 Bancroft Way Berkeley 4, California ATTN: W. H. Brummett, Jr.	24
USAEC Division of Reactor Development Washington 25, D. C. ATTN: Office Foreign Activities	1
Office of Naval Reactors	1
Water Reactor Branch Civilian Reactors	1
Fuels & Materials Development Branch, Nuclear Technology	2
Reports & Statistics Branch	1
USAEC Chicago Operations Office 9700 South Cass Avenue Argonne, Illinois ATTN: Director, Reactor Programs Division	1
Argonne National Laboratory 9700 South Cass Avenue Argonne, Illinois ATTN: J. E. Draley	1
S. Greenberg	1
Oak Ridge National Laboratory P. O. Box X Oak Ridge, Tennessee ATTN: M. L. Picklesimer	1
Westinghouse Electric Corporation Bettis Atomic Power Laboratory P. O. Box 1468 Pittsburgh 30, Pennsylvania ATTN: S. Kass	1
B. Lustman	1

## Distribution List

No. of Copies

Knolls Atomic Power Laboratory  
 P. O. Box 1072  
 Schenectady, New York  
 ATTN: William M. Cashin

1

Hanford Atomic Products Operation  
 General Electric Company  
 Richland, Washington  
 ATTN: F. W. Albaugh

1

General Nuclear Engineering  
 P. O. Box 245  
 Dunedin, Florida  
 ATTN: J. M. West

1

Armour Research Foundation of  
 Illinois Institute of Technology  
 Joint U.S.-Euratom Program  
 "Improved Zirconium Alloys"  
 10 West 35th Street  
 Chicago 16, Illinois  
 ATTN: R. VanThyne

1

Siemens-Schuckertwerke, A. G.  
 Joint U.S.-Euratom Program  
 "Zirconium Hydride in Zircaloy-2 and Zr-Nb Alloys"  
 Erlangen 2, Germany  
 ATTN: Program Manager

1

Pechiney  
 Joint U.S.-Euratom Program  
 "Zirconium and Alloys"  
 23 Rue Balzac  
 Paris 8, France  
 ATTN: Program Manager

1

Metallgesellschaft, A. G.  
 Director of Laboratory  
 Reuterweg 14  
 Frankfurt/Main  
 Germany

1

Atomic Energy of Canada, Ltd.  
 Chemistry & Metallurgy Division  
 Chalk River, Ontario  
 ATTN: Dr. W. R. Thomas, Head  
 General Metallurgy Branch

1

## Distribution List

No. of Copies

Battelle Memorial Institute  
 505 King Avenue  
 Columbus 1, Ohio  
 ATTN: S. W. Porembka

1

University of Florida  
 Engineering & Industrial Experiment Station  
 Gainesville, Florida  
 ATTN: R. E. Reed-Hill

1

U. S. Bureau of Mines  
 Region 1  
 P. O. Box 492  
 Albany, Oregon  
 ATTN: Mark Wright

1

E. I. DePont de Nemours & Company  
 Atomic Energy Division  
 2430 Nemours Building  
 Wilmington, Delaware  
 ATTN: E. E. Hayes

1

Babcock & Wilcox Company  
 Atomic Energy Division  
 1201 Kemper Street  
 Lynchburg, Virginia

1